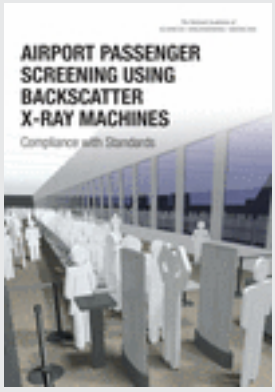

Airport Passenger Screening Using Backscatter X-Ray Machines: Compliance with Standards

DETAILS

148 pages | 7 x 10 | PAPERBACK
ISBN 978-0-309-37133-9 | DOI: 10.17226/21710

AUTHORS

Committee on Airport Passenger Screening: Backscatter X-Ray Machines; National Materials and Manufacturing Board; Division on Engineering and Physical Sciences; Nuclear and Radiation Studies Board; Division on Earth and Life Studies; National Academies of Sciences, Engineering, and Medicine

AIRPORT PASSENGER SCREENING USING BACKSCATTER X-RAY MACHINES

Compliance with Standards

Committee on Airport Passenger Screening: Backscatter X-Ray Machines

National Materials and Manufacturing Board

Division on Engineering and Physical Sciences

and

Nuclear and Radiation Studies Board

Division on Earth and Life Sciences

The National Academies of
SCIENCES • ENGINEERING • MEDICINE

THE NATIONAL ACADEMIES PRESS
Washington, DC
www.nap.edu

THE NATIONAL ACADEMIES PRESS 500 Fifth Street, NW Washington, DC 20001

This study was supported by Contract/Grant No. HSHQDC-11-D-00009 between the National Academy of Sciences and the Department of Homeland Security. Any opinions, findings, conclusions, or recommendations expressed in this publication do not necessarily reflect the views of any organization or agency that provided support for the project.

International Standard Book Number-13: 978-0-309-37133-9
International Standard Book Number-10: 0-309-37133-3

Cover Image: A common scene at a fictional airport employing passenger screening using a backscatter X-ray machine. Artist: Erik Svedberg. Image created by ray tracing, where computational rays of light backscatter, reflect, or are transmitted throughout the geometry of the scene to paint the full picture.

This report is available in limited quantities from

National Materials and Manufacturing Board
500 Fifth Street, NW
Washington, DC 20001
nmmb@nas.edu
http://www.nationalacademies.edu/nmmb

Additional copies of this report are available for sale from the National Academies Press, 500 Fifth Street, NW, Keck 360, Washington, DC 20001; (800) 624-6242 or (202) 334-3313; http://www.nap.edu.

Printed in the United States of America

Suggested citation: National Academies of Sciences, Engineering, and Medicine. 2015. *Airport Passenger Screening Using Backscatter X-Ray Machines: Compliance with Standards.* Washington, DC: The National Academies Press.

The National Academies of
SCIENCES • ENGINEERING • MEDICINE

The **National Academy of Sciences** was established in 1863 by an Act of Congress, signed by President Lincoln, as a private, nongovernmental institution to advise the nation on issues related to science and technology. Members are elected by their peers for outstanding contributions to research. Dr. Ralph J. Cicerone is president.

The **National Academy of Engineering** was established in 1964 under the charter of the National Academy of Sciences to bring the practices of engineering to advising the nation. Members are elected by their peers for extraordinary contributions to engineering. Dr. C. D. Mote, Jr., is president.

The **National Academy of Medicine** (formerly the Institute of Medicine) was established in 1970 under the charter of the National Academy of Sciences to advise the nation on medical and health issues. Members are elected by their peers for distinguished contributions to medicine and health. Dr. Victor J. Dzau is president.

The three Academies work together as the **National Academies of Sciences, Engineering, and Medicine** to provide independent, objective analysis and advice to the nation and conduct other activities to solve complex problems and inform public policy decisions. The Academies also encourage education and research, recognize outstanding contributions to knowledge, and increase public understanding in matters of science, engineering, and medicine.

Learn more about the **National Academies of Sciences, Engineering, and Medicine** at **www.national-academies.org**.

COMMITTEE ON AIRPORT PASSENGER SCREENING: BACKSCATTER X-RAY MACHINES

HARRY E. MARTZ, JR., Lawrence Livermore National Laboratory, *Chair*
BARBARA J. McNEIL, Harvard Medical School, *Vice Chair*
SALLY A. AMUNDSON, Columbia University Medical Center
DAVID E. ASPNES, North Carolina State University
ARNOLD BARNETT, Massachusetts Institute of Technology
THOMAS B. BORAK, Colorado State University
LESLIE A. BRABY, Texas A&M University, College Station
MATS P.E. HEIMDAHL, University of Minnesota, Minneapolis
SANDRA L. HYLAND, Consultant, Falls Church, Virginia
SHELDON H. JACOBSON, University of Illinois, Urbana-Champaign
JAY S. LOEFFLER, Massachusetts General Hospital
C. KUMAR N. PATEL, Pranalytica, Inc.
MAURO SARDELA, University of Illinois, Urbana-Champaign
ZHI-MIN YUAN, Harvard School of Public Health

Staff

JAMES LANCASTER, Acting Director, National Materials and Manufacturing Board
ERIK B. SVEDBERG, Senior Program Officer, Study Director
OURANIA KOSTI, Senior Program Officer
HYEKYUNG (CLARISSE) KIM, Christine Mirzayan Science and Technology Policy Graduate Fellow
HEATHER LOZOWSKI, Financial Associate
NEERAJ P. GORKHALY, Research Associate
JOSEPH PALMER, Senior Project Assistant

NUCLEAR AND RADIATION STUDIES BOARD

Staff

[1] Deceased on July 28, 2014.

Preface

The Department of Homeland Security (DHS) requested that the National Research Council (NRC) provide an independent study of the radiation exposures resulting from X-ray backscatter advanced imaging technology (AIT) systems used in screening travelers in U.S. airports. According to the Transportation Security Administration (TSA), a component of DHS responsible for the security of the transportation systems in the United States, AIT systems provide enhanced security benefits by detecting both metallic and non-metallic threat items, including weapons, explosives, and other concealed objects on passengers, some of which would not be detected by walk-through metal detectors.[1] X-ray backscatter AITs were deployed in U.S airports in 2008 and subsequently removed from all airports by June 2013 due to privacy concerns. This removal was an effect of Congress stipulating in the FAA Modernization and Reform Act of 2012[2] that all TSA body scanners should have automatic target recognition, thus eliminating the need for a screener to view the image of the person being scanned, something manufacturers

[1] General Accountability Office, *Transportation Security Administration: Progress and Challenges Faced in Strengthening Three Key Security Programs*, Statement of Stephen M. Lord, Director, Homeland Security and Justice Issues, Testimony Before the Committee on Oversight and Government Reform and Committee on Transportation and Infrastructure, U.S. House of Representatives, GAO-12-541T, March 26, 2012, http://oversight.house.gov/wp-content/uploads/2012/03/3-26-12-Joint-TI-Lord-Testimony.pdf.

[2] U.S. House of Representatives, FAA Modernization and Reform Act of 2012 Conference Report to Accompany H.R. 658, 11th Congress, Report 112-381, February 1, 2012, http://www.gpo.gov/fdsys/pkg/CRPT-112hrpt381/pdf/CRPT-112hrpt381.pdf.

failed to implement. TSA is looking to deploy a second-generation X-ray backscatter AIT equipped with privacy software to eliminate production of an image of the person being screened.

This study aims to address concerns about exposure to radiation from X-ray backscatter AITs raised by Congress, individuals within the scientific community, and others. It was carried out by a committee of experts appointed by the NRC. The Committee on Airport Passenger Screening: Backscatter X-Ray Machines consisted of 14 members with expertise that spans the disciplines relevant to the study task: radiation physics and dosimetry, radiation biology, diagnostic and therapeutic radiology, materials science, systems and electrical engineering, manufacturing testing and evaluation, aviation safety, software safety, and statistics.

Three factors made the committee's task challenging:

1. There were no X-ray backscatter AIT systems deployed in U.S. airports at the time the committee started and completed its examination. In fact, the committee did not have access to any machines until about 8 months after it was convened, and after that it had limited access to the AITs and limited time to complete its work.
2. The X-ray backscatter AIT systems available to the committee for examination were located in facilities belonging to government agencies and either under preliminary testing or used as a reference. Therefore, no destructive testing could be done; the committee was thus unable to perform a complete examination of the systems' safety interlocks, which prevent overexposures of the people being screened. Such an examination would have potentially involved damaging the machines while they were in operation to document whether the machines safely terminated operations in response to the destructive testing.
3. Much of the information related to the design and operation of the AITs is excluded from public domain for reasons of national security or because of its proprietary and confidential nature.

Despite the above-mentioned factors, the committee was able to complete its radiation dose study of two X-ray backscatter AIT systems representing past and possibly future screening of travelers in U.S. airports. The committee hopes that its findings and recommendations will be useful to the general public and TSA, the sponsor, and others in evaluating the radiation exposure of any future X-ray backscatter AIT and examining the adequacy of the system design, including safety interlocks to avoid overexposures.

In closing, we thank the committee members for their exceptional efforts in carrying out this investigation and preparing this report. We and the committee

also thank the NRC staff for facilitating this study. Senior program officers Erik Svedberg and Ourania Kosti organized the committee meetings and the committee's work and assisted the committee with report writing and review. Program assistant Joe Palmer and research associate Neeraj Gorkhaly managed the logistics of the meetings and all the daily tasks.

The committee also thanks those who were guest speakers at its meetings and who added to the committee members' understanding of X-ray backscatter and the issues surrounding it:

Domenic Bianchini, Transportation Security Administration,
Wesley E. Bolch, University of Florida,
John Boone, University of California, Davis Medical Center,
Richard Burdette, Transportation Security Administration,
Frank Cartwright, Transportation Security Administration,
Jack Glover, National Institute of Standards and Technology,
David E. Hintenlang, University of Florida,
Larry T. Hudson, National Institute of Standards and Technology,
Daniel Kassiday, Food and Drug Administration,
Ronnie Minniti, National Institute of Standards and Technology,
Jill M. Segraves, Transportation Security Administration, and
Steve Smith, Tech84.

We also wish to thank Wesley E. Bolch, Shannon E. O'Reilly, Matthew R. Maynard, and Elliott J. Stepusin of the computation team and David E. Hintenlang and Sadije Redzovic of the physical dosimetry team in the Department of Biomedical Engineering at the University of Florida, Gainesville.

Harry Martz, *Chair,* and Barbara McNeil, *Vice Chair*
Committee on Airport Passenger Screening:
Backscatter X-Ray Machines

Acknowledgment of Reviewers

This report has been reviewed in draft form by individuals chosen for their diverse perspectives and technical expertise, in accordance with procedures approved by the Report Review Committee. The purpose of this independent review is to provide candid and critical comments that will assist the institution in making its published report as sound as possible and to ensure that the report meets institutional standards for objectivity, evidence, and responsiveness to the study charge. The review comments and draft manuscript remain confidential to protect the integrity of the deliberative process. We wish to thank the following individuals for their review of this report:

William Brinkman, Princeton University,
John Boone, University of California, Davis,
Carl Crawford, Csuptwo, LLC,
Ward Plummer, Louisiana State University,
David Schauer, International Commission on Radiation Units and Measurements,
Steven Simon, National Institutes of Health, and
Richard Toohey, M.H. Chew & Associates.

Although the reviewers listed above have provided many constructive comments and suggestions, they were not asked to endorse the views presented in the report, nor did they see the final draft of the report before its release. The review of this report was overseen by Etta D. Pisano, Medical University of South Carolina,

and Robert A. Frosch, Harvard University, who were responsible for making certain that an independent examination of this report was carried out in accordance with institutional procedures and that all review comments were carefully considered. Responsibility for the final content of this summary rests entirely with the committee and the institution.

Contents

SUMMARY 1

1 INTRODUCTION 9
Advanced Imaging Technology in U.S. Airports, 9
Safety Concerns Related to X-Ray Backscatter AIT, 16
The Study Request, 21
Strategy to Address the Study Charge, 22
Information Gathering and Challenges, 25
Report Organization, 25

2 RADIATION PHYSICS RELEVANT TO ADVANCED IMAGING TECHNOLOGY 27
The Physics of X-Ray Absorption, 27
Beam Attenuation and Deposited Energy, 30

3 X-RAY BACKSCATTER ADVANCED IMAGING TECHNOLOGY 33
Rapiscan Secure 1000, 34
AS&E SmartCheck, 37
Tek84 Ait84, 38

4 DOSIMETRY FOR X-RAY BACKSCATTER ADVANCED IMAGING TECHNOLOGY 40
X-Ray Spectra, 41
Kerma, 41
Absorbed Dose, 43
Effective Dose, 43
Reference Effective Dose, 46
Relationship Between Kerma and Absorbed Dose, 46

5 RADIATION PROTECTION STANDARDS 48
Dose, 48
Radiation Health Effects and Risks at Low Doses, 51
System Design, Interlocks, and Operating Procedures, 52
Indicators and Safety Interlocks, 52
Operational Procedures, 54

6 REVIEW OF X-RAY BACKSCATTER ADVANCED IMAGING TECHNOLOGY STUDIES 56
Comparing Radiation Measurements, 57
The JHU/APL Report, 60
The NIST Report, 63
The AAPM Report, 66
The USAPHC Report, 69
The FDA Report, 71
Summary of Measurements from Reviewed Studies, 73
Summary of the Interlock Topic from Reviewed Studies, 74
Other Studies and Considerations, 75
The Dose from Compton Backscatter Screening, 75
Letter to the Presidential Science and Technology Advisor, 78
Estimation of Organ and Effective Dose Due to Compton Backscatter Security Scans, 81
Security Analysis of a Full-Body Scanner, 81
Findings and Recommendations on Exposure and Dose, 82
Individual Being Screened, 82
Kerma Measurements, 83
Half-Value Layer Measurements, 83
Depth Dose Distribution Measurements, 83
Dose Outside Inspection Area Potentially Affecting Bystanders, 84

7 MEASUREMENTS, DOSE CALCULATIONS, AND SYSTEM DESIGN FOR X-RAY BACKSCATTER ADVANCED IMAGING TECHNOLOGY SYSTEMS 86
Measurement Procedures, 87
Measuring Half-Value Layer, 87
Measuring Percent Depth Dose, 90
Measuring Air Kerma, 92
Determination of the Kerma per Screening Outside the Inspection Area, 93
AS&E SmartCheck System Measurement Results and System Design, 95
Half-Value Layer Results, 95
Percent Depth Dose Measurements, 96
Air Kerma Results, 100
Committee Review of the AS&E SmartCheck System Design, 103
The Rapiscan Secure 1000 System Measurement Results and System Design, 103
Half-Value Layer Results, 105
Percent Depth Dose Results, 107
Air Kerma Results, 113
Committee Review of the Rapiscan Secure 1000 System Design, 114
Summary of Key Findings for Both Measured Systems, 122
Dose Computations, 123
Objectives, 123
Introduction, 123
X-Ray Source Term, 126
Summary, 148
Results, 149
Findings and Recommendations, 151
Measurements, 151
System Design, 151
Dose Computations, 152

APPENDIXES

A Statement of Task 157
B Glossary, Acronyms, and Abbreviations 158
C Organ Absorbed Doses 163
D Summary of Statistics from Previous Studies 170
E Biographies of Committee Members and Contractors 176

Summary

The Transportation Security Administration (TSA), a component of the Department of Homeland Security (DHS) responsible for the security of the transportation systems in the United States, has deployed security systems of advanced imaging technology (AIT) to screen passengers at airports. According to TSA, AIT systems provide enhanced security benefits by detecting both metallic and nonmetallic threat items, including weapons, explosives, and other concealed objects on passengers that would not be detected by walk-through metal detectors. To date (December 2014) TSA has deployed AITs in U.S. airports of two different technologies: millimeter wave and X-ray backscatter AIT systems. These technologies use different types of radiation to penetrate through clothing and create a reflected image of the body. Millimeter wave AIT systems use radio waves, a type of nonionizing radiation, while X-ray backscatter AIT systems use X-rays, a type of ionizing radiation. This report focuses on the X-ray backscatter AIT used by TSA for screening passengers.

DHS requested that the National Research Council (NRC)[1] provide an examination of the radiation exposures resulting from X-ray backscatter AIT used in screening travelers. This examination would include an analysis of whether

[1] Effective July 1, 2015, the institution is called the National Academies of Sciences, Engineering, and Medicine. References in this report to the National Research Council are used in a historical context identifying programs prior to July 1.

1. The X-ray backscatter AIT system that uses ionizing radiation complies with applicable health and safety standards for public and occupational exposures to ionizing radiation, and
2. AIT system design, operating procedures, and maintenance procedures are appropriate to prevent over exposures of travelers and operators to radiation.

The complete statement of task for the NRC Committee on Airport Passenger Screening: Backscatter X-Ray Machines is shown in Appendix A.

In 2008, TSA deployed the X-ray backscatter AIT systems in airports, specifically Rapiscan Secure 1000 units manufactured by Rapiscan Systems. TSA subsequently removed the Rapiscan Secure 1000 units from all airports by June 2013 because of the manufacturer's inability to develop privacy software (known as automatic target recognition, or ATR), which enabled the display of anomalies on a generic figure instead of an image of the individual's body, by the deadline mandated by Congress. At the time the committee started its examination, there were no X-ray backscatter AIT systems deployed in airports in the United States. The only AIT systems deployed at airports for passenger screening at the time of the committee examination were the millimeter wave units. TSA is currently evaluating second-generation X-ray backscatter AITs manufactured by American Science and Engineering, Inc. (AS&E).

Despite removing the Rapiscan Secure 1000 units from all airports, DHS expressed its interest in the NRC performing an examination of the Rapiscan Secure 1000 that was previously deployed in U.S. airports. Because there is a possibility that TSA could deploy second-generation X-ray backscatter AITs manufactured by AS&E, DHS asked NRC to also examine an AS&E AIT system. The AIT systems available to the NRC committee for this examination were a Rapiscan Secure 1000 unit located at the National Institute of Standards and Technology and an AS&E SmartCheck prototype located at TSA's Transportation Systems Integration Facility. The two AIT systems available to the committee represent past (Rapiscan Secure 1000) and possible future (AS&E SmartCheck) X-ray backscatter AIT systems for airport passenger screening. The committee did not examine other X-ray backscatter AIT systems available today, such as Tek84's Ait84. The Ait84 system is not equipped with ATR and, therefore, is not a candidate for deployment at U.S. airports.

In its examination of the Rapiscan Secure 1000 and AS&E SmartCheck systems, the committee was specifically asked not to evaluate the *justification* of the use of X-ray backscatter AIT systems, although an alternative technology that does not use ionizing radiation exists. The committee was also asked not to evaluate whether the standard with which this technology needs to comply is appropriate and/or

adequate to protect human health. The committee was asked if the AITs conform to applicable standards.

X-ray backscatter AITs must conform to the American National Standards Institute/Health Physics Society (ANSI/HPS) Accredited Standards Committee N43 (Equipment for non-medical radiation applications) N.43.17-2009 standard.[2] The ANSI/HPS N43.17-2009 standard provides guidelines for both manufacturers and users of AIT systems and covers dose to subject, interlocks, operational procedures, and information to be provided to the travelers by the operators. The standard limits the dose per screening to 250 nanosievert (nSv) (0.25 μSv), called the *reference effective dose*. Similarly, the annual dose received by an individual from one facility shall not exceed 250,000 nSv (250 μSv). The reference effective dose, a simplified version of the effective dose, is easier to calculate but considered sufficiently accurate to ensure radiation safety. The standard does not issue different limits for subgroups of the general population, such as pregnant women and children, implying that the dose limit offers sufficient protection to them also.

To address its statement of task, the committee performed a comprehensive analysis of previous investigations of the AITs (see Chapter 6). In addition, the committee directed the work performed by an NRC-contracted team (see Chapter 7) tasked with making dosimetry and beam characteristics measurements for both the Rapiscan Secure 1000 and AS&E SmartCheck AITs. A second NRC-contracted team performed detailed computations to screened passengers using Monte Carlo methods with a suite of digitized human phantoms (see Chapter 7).

Results of the subcontractors' work were used by the committee to draw its findings and recommendations for the first part of the statement of task related to whether exposures from the AIT systems comply with the applicable health and safety standard. The committee was unable to carry out AIT system design reliability analyses because this material is proprietary and is protected from public release. Therefore, to respond to the second part of the statement of task, the committee inspected and tested some AIT safety systems and, through the NRC subcontractors, performed a detailed failure mode analysis of the dose received by the person being screened in situations where safety interlocks fail and overexposure may be possible.

Overall, the committee found that both the Rapiscan Secure 1000 and AS&E SmartCheck X-ray backscatter AIT systems complied with the applicable standard. This finding was in agreement with previous investigations of the doses received under routine operation of the X-ray backscatter AITs. The committee also found that the dose received under worst-case scenarios of AIT system failure, those

[2] The ANSI/HPS N43.17-2009 standard, "Radiation Safety for Personnel Security Screening Systems Using X-Ray or Gamma Radiation," is available at the Health Physics Society website at http://hps.org/hpssc/index.html.

failures that result in the beam becoming *stuck* while still producing X rays, does not exceed the applicable standard and therefore cannot result in overexposure.

The key findings and recommendations that emerged from the committee's examination are presented and discussed below. Additional technical details to support these key findings and recommendations are presented in Chapters 6 and 7 of the report.

KEY FINDINGS AND RECOMMENDATIONS

Dose Reported in Previous Investigations

Individual Being Screened

Key Finding: Previous radiation dose studies employed different methodologies and instrumentation to estimate the dose delivered by Rapiscan Secure 1000 X-ray backscatter AITs. These studies generally agreed that the radiation exposure dose per screening to an average passenger is about a factor of 10 below the limit of 250 nSv per screening, the dose set by the ANSI/HPS N43.17 2009 standard.

Individual Outside the Screening Area

Key Finding: Measurements of radiation outside the inspection area have generally been made with detectors that are calibrated for X-ray energies higher than those scattered from a passenger being scanned by the Rapiscan Secure 1000 system. As a result, the detectors may indicate a lower dose than is actually present. The detectors have sometimes failed to distinguish a signal from the background radiation.

Key Recommendation: To estimate X-ray radiation exposure outside the inspection area, measurements should be made with detectors calibrated for X-ray energies below the maximum for the AIT system's X-ray tube and for the radiation levels expected. Use of detectors that are appropriate for other applications but not ideal for measuring dose in a X-ray backscatter AIT system may result in inaccurate measurements.

Dose Reported in the NRC-Contracted Study

Individual Being Screened

The committee's approach in examining dose to the individual being screened differs from that of previous investigations in two ways:

- It made use of sensitive detectors with tissue-equivalent phantoms to verify beam intensity, X-ray quality, and penetration; and
- It performed computations using estimates of beam intensity, scanning geometry, and digitized (high-fidelity) human phantoms that have realistic dimensions and morphology.

Based on these improvements in approach, the committee has the following key finding:

Key Finding: For either the Rapiscan Secure 1000 or the AS&E SmartCheck systems, as determined by the committee for adults and children,

- The effective doses are about the same as those calculated following the simplified formula for the reference effective dose identified by the ANSI/HPS N43.17-2009 standard;
- The effective doses are lower than those in previous reports using plane-parallel X-ray beams with stylized geometrical (low-fidelity) human phantoms; and
- Sensitivity analysis showed that under a range of different conditions, including passenger position in the AIT system and increases in the energy (i.e., by increasing the tube high voltage) of the X-ray beam, the computed effective dose would not increase by more than a factor of 3 and, even so, would remain below the limit specified in the ANSI/HPS N43.17-2009 standard.

The committee can also make the following more specific statements:

Key Finding:

- No person, regardless of age and weight modeled, would exceed the effective dose limit per screen (i.e., 250 nSv/screen), as defined by the ANSI/HPS N43.17-2009 standard.

- The absorbed dose per screen to the developing fetus at any of the three stages post-conception is less than 0.0002 percent of the recommended limit for radiation protection of the fetus during the entire gestation period.
- The absorbed dose to the epithelial layer of radiosensitive cells in the skin is not significantly elevated (~1.6 percent) compared to the average absorbed dose to the skin.
- The dose received by the lens of the eye, skin, or female breast during a stationary beam of X rays for the duration of the scan were at least 2 orders of magnitude below thresholds where tissue injury might occur.

In general, the committee found the following:

Key Finding: Under routine operations, the computed effective doses using computational X-ray sources and scanning geometries, coupled with the digitized hybrid phantoms, are similar to the ANSI reference effective dose and an order of magnitude below the limit of 250 nSv/screen, as set forth in the applicable ANSI/HPS N43.17-2009 standard.

Key Finding: The agreement between the estimated dose results from the NRC subcontractor and the results from earlier studies confirms that the reference effective dose calculations performed in the previous studies were adequate to establish compliance with effective dose limits recommended in the ANSI/HPS N43.17-2009 standard.

Individual Outside the Screening Area

Key Finding: Using appropriate detectors, the estimated values of the radiation outside the inspection area that might affect a bystander are so low as to be statistically indistinguishable from background radiation.

AIT System Design Evaluated in the NRC-Contracted Study

Although the NRC subcontractors performed detailed radiation measurements and dose computations, the committee was unable to unequivocally determine whether the X-ray backscatter AIT systems studied have adequate operating safety interlocks that would prevent the AIT system from exceeding the ANSI/HPS N43.17-2009 standard under every imaginable situation. This is because

- The committee was not given an opportunity to independently verify how all of the interlocks perform in different situations, with the exception of

simple functions such as termination of operation if a door was opened. Such testing would need engineering support from the manufacturer and require unique testing tools as well as dismantling portions of the AIT systems, which would potentially cause damage.
- The committee was not given a demonstration of how interlocks are checked at the manufacturer level from either Rapiscan or AS&E.
- Detailed electrical and mechanical drawings and computer code descriptions and documents describing internal functions at the most fundamental level of the AIT systems are either restricted from public access or were not made available by manufacturers to either the committee or the sponsor.

However, the committee was able to inspect the interior of both the Rapiscan Secure 1000 and AS&E SmartCheck AIT systems. AS&E representatives also described to the committee how many of the interlocks are intended to perform on their second-generation prototype.

With the above limitations noted, having evaluated as many aspects of the AIT systems' safety interlocks as possible, both mechanical and electrical, and combining that knowledge with the measurements and computations performed, the committee can make the following statements:

Key Finding: It appears that the X-ray backscatter AIT systems adhere to the recommended safety mechanisms described in the ANSI/HPS N43.17-2009 standard.

Key Finding: Acceptance tests and periodic inspection tests guided by the safety inspection forms previously used during deployment are sufficient to meet the indicators, controls, and safety interlocks requirements of the ANSI/HPS N43.17-2009 standard.

Key Finding: Equipment manufacturers recommend that a test piece be scanned daily to evaluate proper operation of the AIT system, because this ensures that many of the needed safety system requirements in ANSI/HPS N43.17-2009 standard work properly. The committee agrees with this recommendation but was unable to determine if this was done, because the X-ray backscatter AIT systems are not currently deployed in the field at commercial airports.

Key Recommendation: Any future testing procedures should at a minimum continue to follow the indicators, controls, and safety interlocks requirements of the ANSI/HPS N43.17-2009 standard, or similar testing procedures, and include daily verification of safety parameters by a test piece.

Key Finding: Based on the committee's review and test of the Rapiscan Secure 1000 system's interlocks, the committee was unable to identify any circumstances where an accidental failure or deliberate reconfiguration of the AIT system could result in either a person being screened or the operator receiving an effective dose larger than that from a normal screening.

Key Finding: Based on the committee's inspection of the AS&E SmartCheck AIT system, with the AS&E representative present, the committee was unable to identify any circumstances where an accidental failure or deliberate reconfiguration of the AIT system could result in either a person being screened or the operator receiving a larger X-ray dose than the intended screening dose.

Key Finding: Given the results obtained by the committee on radiation measurements and computations for the X-ray AIT systems investigated, the screening of an individual would need to extend for more than 60 seconds for an individual to be exposed to radiation that exceeds the ANSI/HPS N43.17-2009 standard limit. In comparison, a typical screen takes about 6 seconds.

Key Recommendation: Future X-ray AITs should have some independent mechanism to ensure that the AIT does not screen any person for longer than the time needed to acquire the appropriate image while keeping radiation exposure compliant with the safety principle of as low as (is) reasonably achievable.

1

Introduction

ADVANCED IMAGING TECHNOLOGY IN U.S. AIRPORTS

Passenger screening at commercial airports in the United States has gone through significant changes since the events of September 11, 2001. In response to increased concern over terrorist attacks on aircrafts, the Transportation Security Administration (TSA), a component of the Department of Homeland Security (DHS) responsible for the security of the transportation systems in the United States, has deployed security scanners of advanced imaging technology (AIT) to screen passengers at airports. According to TSA, AIT systems provide enhanced security benefits by detecting both metallic and non-metallic threat items, including weapons, explosives, and other concealed objects, on passengers that would not be detected by walk-through metal detectors.[1] This report does not address the benefits of AIT systems. The committee was not asked to address such issues.

TSA started deploying AITs in 2008 for use as a secondary[2] screening of airport

[1] Government Accountability Office, *Transportation Security Administration: Progress and Challenges Faced in Strengthening Three Key Security Programs, Statement of Stephen M. Lord, Director, Homeland Security and Justice Issues,* Testimony Before the Committee on Oversight and Government Reform and Committee on Transportation and Infrastructure, House of Representatives, released March 26, 2012, http://oversight.house.gov/wp-content/uploads/2012/03/3-26-12-Joint-TI-Lord-Testimony.pdf.

[2] *Primary screening* is screening to which all passengers are subject. *Secondary screening* is additional screening that may be used based on the response to the primary screening, randomization, or other metrics that suggest that further information is needed about a passenger (e.g., to possibly resolve an alarm during primary screening).

BOX 1.1
Ionizing Radiation

Radiation consists of elementary particles that are capable of interacting with material and transferring energy to this material. Ionizing radiation is a category of particles that deposit energy which is sufficiently concentrated to eject electrons from individual atoms. Although the amount of energy is quite small, the patterns of ionization create localized damage that can cause malfunctions in inanimate objects such as microelectronics or injury to biological systems.

For purposes of radiation protection in humans, the exposure to ionizing radiation is measured in terms of effective dose termed a sievert (Sv). A single large exposure to ionizing radiation of greater than 6 Sv (6,000,000,000 nSv) could result in fatality soon after the exposure; whereas low doses of radiation around 100 mSv (100,000,000 nSv) might result in excess risk of carcinogenesis many years following the exposure.

Continuous exposure of the general population to ionizing radiation originates from ubiquitous natural background and utilization of man-made sources. Sources of natural background, that are located outside of the body, consist of penetrating cosmic rays (muons and neutrons), and gamma rays originating from radioactivity in terrestrial minerals containing uranium (^{238}U), Thorium (^{230}Th), and potassium (^{40}K). There are also sources of natural radioactivity that accumulate within the body through ingestion of food and liquids, such as potassium (^{40}K), carbon (^{14}C) and through inhalation (radon). The magnitude of these sources varies considerably with geographical location, elevation above sea level and lifestyle. Man-made activities include voluntary medical procedures and exposure from other sources such as consumer products, commercial aviation and nuclear power generation.

The National Council on Radiation Protection and Measurements (NCRP) has published a comprehensive report summarizing the exposure to radiation of the U.S. population. The average effective dose in 2006 was 6 mSv per year (6,000,000 nSv per year). Figure 1.1.1 illustrates the relative contributions to the average annual exposure from the various sources. It is interesting that radon is the largest contributor to natural background (solid colors) whereas the largest contribution to the overall average comes from diagnostic imaging procedures such as conventional X-rays, CT examinations, and nuclear medicine.

security. Their deployment was accelerated, and usage was switched to primary[3] screening after the December 25, 2009, event when Northwest Airlines Flight 253 was the target of a failed attempt by a passenger to set off plastic explosives hidden in his underwear.

Current procedures require that all passengers be screened using an AIT system deployed at the airport.[4] Passengers can choose to opt out of such screening and be subjected to a patdown search by a TSA security officer. In some cases, passen-

[3] S. Mahoney, Laying down the law, *Security Today*, April 01, 2010, http://security-today.com/articles/2010/04/01/laying-down-the-law.aspx?admgarea=ht.airport.

[4] With certain exceptions, as noted on www.tsa.gov, such as travelers over the age of 75, travelers with certain types of disabilities, and those approved for the TSA Pre✓™ program.

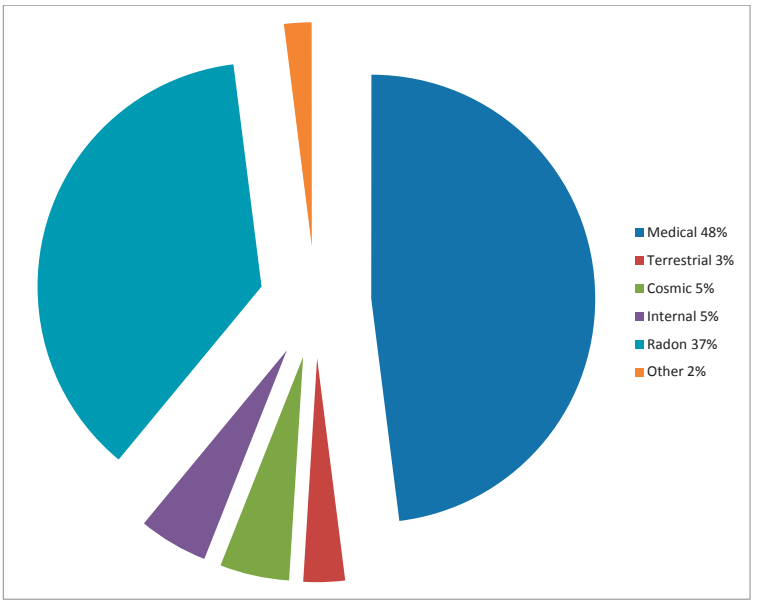

FIGURE 1.1.1 Average annual exposure to radiation of the U.S. population. SOURCE: Data from National Council on Radiation Protection and Measurements, *NCRP Report No. 160: Ionizing Radiation Exposure of the Population of the United States,* Bethesda, Md., 2009.

gers opting for an AIT screening during primary screening may subsequently be required to undergo a patdown search if anomalies[5] are detected.

To date (December 2014), TSA has deployed in U.S. airports two different types of AIT systems that use different types of radiation to detect threats:[6] the first technology (see Figure 1.1a) deployed by TSA, is based on the X-ray Compton scattering effect of X rays, a type of ionizing radiation (see Box 1.1 for a short de-

[5] *Anomalies* in this context indicates some type of object(s) that will require further screening to resolve.

[6] There are two types of radiation: ionizing radiation and nonionizing radiation. Ionizing radiation has enough energy to remove electrons from atoms and create ions. Nonionizing radiation does not have enough energy to remove electrons from atoms but can cause them to move or vibrate. Ionizing radiation and nonionizing radiation have different biological effects.

scription of ionizing radiation). The deployed equipment, a Rapiscan Secure 1000 manufactured by Rapiscan Systems, projects a fast-moving, narrow, low-energy X-ray beam[7] over the body surface to detect the radiation reflected (or backscattered) from the person being screened as well as any objects on that person. These X rays are of lower energy and intensity than medical X rays are and do not penetrate the body as deeply. Objects on the surface and shallow subsurface of the body can be detected with this technology.

The second technology (see Figure 1.1b), and the only one currently deployed at airports by TSA, uses millimeter-length radio waves, a type of nonionizing radiation, and the equipment deployed is the L-3 ProVision manufactured by L-3 Security and Detection Systems. Millimeter wave technology measures the electromagnetic waves backscattered from the human body or objects on the human.

X-ray backscatter and millimeter wave AITs have the capacity to create detailed images of those being screened and reveal genitalia, breasts, fat creases, and all types of prosthetics and piercings[8] (see Figure 1.2). In the early phases of deployment of AIT, TSA took several steps to protect the privacy of passengers. For example, TSA decided neither to save nor transport the images acquired from screening, and it eventually isolated the operator viewing the images from the individuals being screened. In 2011, in response to ongoing privacy concerns, TSA piloted a program for manufacturers to develop automatic target recognition (ATR) software for AITs to enable display of anomalies on a generic figure (see Figure 1.3) that is identical for all persons being screened, as opposed to a backscatter image of the individual's body, removing the need for a TSA agent to review the images generated.

As part of the Federal Aviation Administration Modernization and Reform Act of 2012 (P.L. 112-95), Congress mandated that all AIT units be equipped with ATR by June 1, 2012, a deadline later extended to June 1, 2013. While all of the millimeter wave units have been equipped with the ATR software, Rapiscan Systems did not develop ATR software for its X-ray backscatter AIT units that passed testing. As a result, TSA canceled its contract with Rapiscan and removed all 250 X-ray backscatter units manufactured by Rapiscan from U.S. airport checkpoints by May 31, 2013.

Currently, there are no X-ray backscatter AIT units deployed in U.S. airports, but 740 AIT millimeter wave units are located at about 160 airports in the United States.[9] In November 2012, TSA issued a contract award to American Science and Engineering, Inc. (AS&E) to deliver next-generation X-ray backscatter AIT systems

[7] In the context of X-ray AIT systems, the operating potential of the X-ray tube is 50 kV.

[8] P. Mehta and R. Smith-Bindman, Airport full-body screening: What is the risk?, *Archives of Internal Medicine* 171(12):1112-1115. 2011.

[9] Transportation Security Administration (TSA), "Advanced Imaging Technology," https://www.tsa.gov/traveler-information/advanced-imaging-technology-ait, accessed December 4, 2014.

(a)

(b)

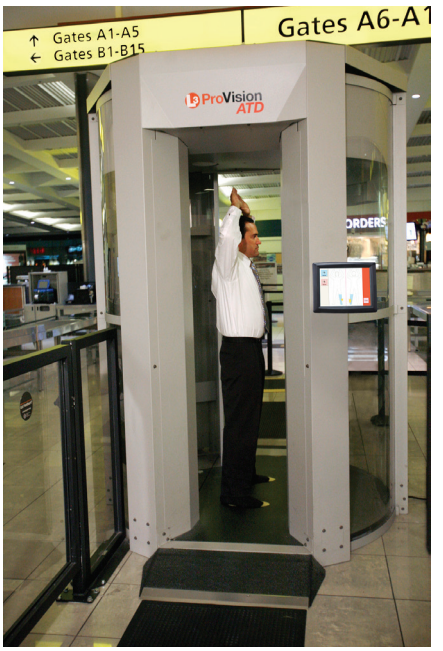

FIGURE 1.1 Advanced imaging technologies deployed by TSA: (a) X-ray-based Rapiscan Secure 1000. (b) Millimeter-wave-based L-3 ProVision ATD. SOURCE: (a) Courtesy of Scott Olson/Getty Images; (b) Courtesy of L-3 Communications.

FIGURE 1.2 Images from AITs not equipped with automatic target recognition: (a) X-ray backscatter AIT (b) millimeter wave AIT. SOURCE: (a) Courtesy of the Transportation Security Administration; (b) Courtesy of L-3 Communications.

(a)

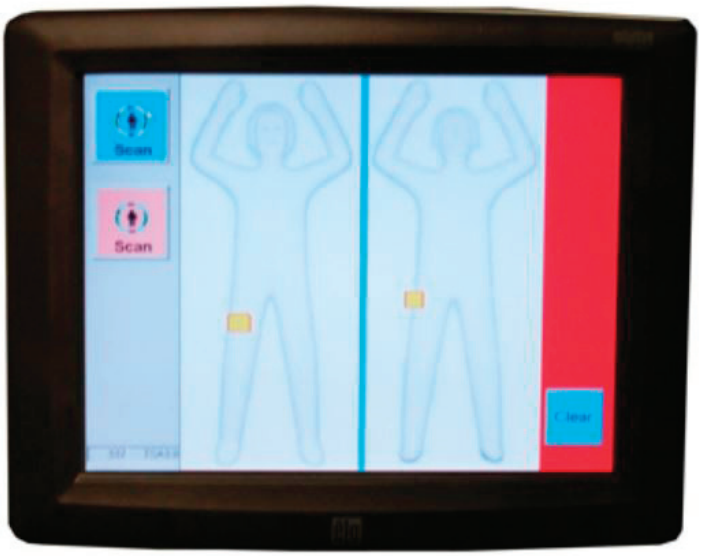

(b)

FIGURE 1.3 Images from a millimeter wave AIT equipped with automatic target recognition. NOTE: If potential threat items are detected on the person being scanned, they are indicated on a generic outline of a person that is identical for all passengers screened (a). Areas identified as containing potential threats will require additional screening. (b) If no potential threat items are detected, an "OK" appears on the monitor with no outline. SOURCE: Courtesy of the Transportation Security Administration.

BOX 1.2
Statement of Task

An ad hoc committee will review previous studies as well as current processes used by the Department of Homeland Security (DHS) and equipment manufacturers to estimate radiation exposures resulting from backscatter X-ray advanced imaging technology (AIT) system use in screening air travelers, and provide a report with findings and recommendations on:

1. Whether exposures comply with applicable health and safety standards for public and occupational exposures to ionizing radiation, and
2. Whether system design (e.g., safety interlocks), operating procedures, and maintenance procedures are appropriate to prevent over exposures of travelers and operators to ionizing radiation.

This study will not address legal, cultural or privacy implications of this technology.

NOTE: The committee's work plan further stipulated that as part of this study, the Academies will subcontract with an appropriate independent testing organization or qualified consultants to conduct field studies measuring the radiation dosage emitted by the machines as they are used.

for testing. TSA also issued a contract award to L-3 Security and Detection Systems to deliver next-generation millimeter wave AIT systems for testing. Both systems are equipped with ATR capabilities. The National Research Council (NRC)[10] has been asked by DHS to evaluate the X-ray backscatter AIT systems as specified in the statement of task (Box 1.2). In response, the NRC appointed the Committee on Airport Passenger Screening: Backscatter X-Ray Machines.

SAFETY CONCERNS RELATED TO X-RAY BACKSCATTER AIT

Although it was privacy concerns and lack of ATR that led to the removal of the Rapiscan X-ray backscatter AITs from the airports, another concern relates to their *safety*. X-ray backscatter systems emit ionizing radiation. While some of the X rays emitted during a scan[11] are reflected back, some are absorbed by the body,

[10] Effective July 1, 2015, the institution is called the National Academies of Sciences, Engineering, and Medicine. References in this report to the National Research Council are used in a historical context identifying programs prior to July 1.

[11] In this report *scan* and *scanning* refers to the AIT system using X-rays to inspect one view of the passenger (front or back) whereas "screening" refers to the complete inspection with a scan of both the front and the back (two scans).

and a very small fraction is transmitted through the body. Ionizing radiation is high-frequency electromagnetic radiation that has enough energy to potentially damage the DNA in cells. This in turn may lead to cancer. Based on the linear-nonthreshold (LNT) dose-response model of radiation effects[12,13] currently used for radiation protection purposes, any dose,[14] no matter how small, is assumed to be linked to an increase in the risk[15] of contracting cancer.

Safety concerns related to the X-ray backscatter AIT systems are often discussed at the individual as well as the societal level. At the individual level, two special populations are suggested to be at higher risk of developing cancer from being screened with the X-ray backscatter AIT systems:

1. Children and the developing fetus are generally believed to be more sensitive to the effects of radiation for a given radiation dose compared to the general population,[16] and
2. Frequent flyers and airline and airport staff whose cumulative dose, and therefore risk, increases because they are screened more frequently compared to the general population.

At the societal level, the concern about risks from exposure[17] to the X-ray backscatter AIT systems is as follows: Even though the dose to an individual from screening with the X-ray backscatter AITs may be small, and therefore the risk of developing cancer for that particular individual is also small, the *collective dose*[18] to the more than 815 million passengers traveling annually within the United States[19] and likely to be screened with this technology may be high. Based on the LNT model currently used for radiation protection purposes, the concept of col-

[12] International Commission on Radiological Protection (ICRP), Recommendations of the ICRP, Publication 26, *Annals of the ICRP* 1(3), 1977.

[13] National Council on Radiation Protection and Measurements (NCRP), *Evaluation of the Linear-Nonthreshold Dose-Response Model for Ionizing Radiation*, Report No. 136, Bethesda, Md., 2001.

[14] Dose is a term used to express how much radiation exposure a person has received. The word *dose* without a modifier (such as *effective* dose or *absorbed* dose) refers to energy deposition in a general sense, rather than a specific amount.

[15] *Risk* is defined as the probability of an adverse health effect to occur.

[16] UNSCEAR, Effects of radiation exposure of children, Annex B in *Sources, Effects and Risks of Ionizing Radiation*, UNSCEAR 2013 Report, Volume II, United Nations, New York, N.Y., 2013.

[17] *Exposure* is here used as a general term indicating that a subject has been exposed to radiation. Unless otherwise stated, it is not intended to imply any relationship to the ICRU (International Commission on Radiation Units) notion of exposure.

[18] *Collective dose* is the sum of all individual effective doses over the time period under consideration.

[19] Department of Transportation, Bureau of Transportation Statistics, "Total Passengers on U.S. Airlines and Foreign Airlines U.S. Flights Increased 1.3% in 2012 from 2011," Press Release BTS 16-13, April 4, 2013, http://www.rita.dot.gov/bts/press_releases/bts016_13.

lective dose does appear to justify this concern. However, the National Council on Radiation Protection and Measurements (NCRP)[20] and the International Commission on Radiological Protection (ICRP)[21] point out that application of collective dose to large populations requires an extrapolation of risk estimates to doses far below values where any data exist (see discussion in Chapter 2) and thus cannot be justified. It is impossible to determine if there is any increase in the number of cancer occurrences in a large population exposed to a low dose, because baseline cancer rates are high (around 40 percent in the United States),[22] and the variation in the risk of developing cancer is considerably high because of individual lifestyle and environmental factors. The baseline cancer rate far exceeds any increase in individual risk that might be induced by the radiation exposure from the X-ray backscatter AIT.

The dose received from the X-ray backscatter AIT was tested in a number of investigations, including those of the Food and Drug Administration (FDA),[23] the Johns Hopkins University/Applied Physics Laboratory (JHU/APL),[24] the U.S. Army Public Health Command (USAPHC),[25] the National Institute of Standards and Technology (NIST),[26] and the American Association of Physicists in Medicine (AAPM).[27] These investigations made measurements of the radiation emitted by the AIT systems and calculated the dose to the whole body, which was then compared to the current standard for usage of X-ray backscatter AIT systems, namely, the American National Standards Institute/Health Physics Society (ANSI/HPS) N43.17-2009 standard,[28] to determine whether the calculated dose complies with that standard. The FDA, JHU/APL, NIST, and AAPM studies made measurements

[20] NCRP, *Principles and Application of Collective Dose in Radiation Protection*, Report No. 121, Bethesda, Md., 1995.

[21] ICRP, The 2007 Recommendations of the International Commission on Radiological Protection, ICRP Publication 103, *Annuls of the ICRP* 37(2-4), 2007.

[22] National Research Council, *Health Risks From Exposure to Low Levels of Ionizing Radiation: BEIR VII—Phase 2*. The National Academies Press. Washington, D.C., 2006.

[23] F. Cerra, *Assessment of the Rapiscan Secure 1000 Body Scanner for Conformance with Radiological Safety Standards*, Food and Drug Administration, Arlington, Va., July 21, 2006.

[24] Johns Hopkins University Applied Physics Laboratory, *Radiation Safety Engineering Assessment Report for the Rapiscan Secure 1000 in Single Pose Configuration*, NSTD-09-1085, Version 2, Laurel, Md., August 2010.

[25] U.S. Army Public Health Command (USAPHC), *Radiation Protection Consultation No. 26-MF-0E7k-11 Rapiscan Secure 1000 Single Pose Dosimetry Study*, Aberdeen Proving Ground, Md., 2012.

[26] Glover et al., *Assessment of the Rapiscan Secure 1000 Single Pose (ATR version) for Conformance with National Radiological Safety Standards*, 2012.

[27] American Association of Physicists in Medicine, *Radiation Dose from Airport Scanners: Report from Task Group 217*, College Park, Md., 2013.

[28] The ANSI/HPS N43.17-2009 standard, "Radiation Safety for Personnel Security Screening Systems Using X-Ray or Gamma Radiation," is available at the Health Physics Society website at http://hps.org/hpssc/index.html.

using portable instruments and calculated eye and skin equivalent doses from computer modeling; the USAPHC study made measurements using commercially available personnel dosimeters. These five studies are discussed in more detail in Chapter 6.

The standard governing radiation exposure from X-ray backscatter AIT systems—from ANSI/HPS N43.17-2009—sets a maximum whole body dose of 250 nanosieverts (nSv) per screening. The five investigations mentioned above showed that a single screening with the Rapiscan Secure 1000 SP (single pose)[29] unit is associated with an effective dose to a person being screened, roughly in the range of one-twenty-fifth to one-eighth of the standard limit (11 to 33 nSv) per screening (see the Table 1.1 column, "Reference Effective Dose to Standard Man Being Screened"). The NIST study also provided estimates of dose to sensitive subpopulations such as young children. The estimated dose to these sensitive subpopulations also was less than one-eighth of the standard (30 nSv, see Table 1.1 column "Effective Dose to Sensitive Populations Considered"). Also, most of the studies investigated dose to bystanders—that is, to persons such as the operators and persons waiting in line to be screened—who may receive some dose because of their proximity to the inspection area. In most studies, the dose to bystanders[30] was found to be about one-tenth of the dose received by the person being scanned, if it could be measured at all with the available equipment.

The studies shown in Table 1.1 were in agreement that the dose to persons being screened is below the standard with which X-ray backscatter AIT systems need to comply. According to NCRP, any dose of 100,000 nSv or less per source or practice is considered *negligible*.[31] Dose from an X-ray backscatter scan, even when considering the highest dose estimate from the previous studies (30 nSv), is less than one-hundredth of what NCRP describes as a negligible level. Cancer risks at effective doses of the order of "100,000 nSv or less" are currently unknown.

Despite the general agreement among the studies reviewed by the committee that doses received from the X-ray backscatter AIT systems are very low, concerns were raised by individuals within the scientific community. There were concerns,

[29] *Single-pose* (SP) system refers to an AIT system that can screen a person without him/her having to turn to scan both sides. In this report any reference to the Rapiscan Secure 1000 relates to the SP system unless otherwise stated.

[30] Here, bystanders that are waiting in line can include passengers, operators, and airline personnel. These bystanders can be men, women, pregnant women, and children.

[31] According to NCRP, the level of average annual excess risk of fatal health effects attributable to radiation exposure below this level is so low that effort to further reduce the exposure to an individual is not warranted. See NCRP, *Limitation of Exposure to Ionizing Radiation*, Report No. 116, Bethesda, Md., 1993.

TABLE 1.1 Summary Findings from Selected X-ray Backscatter Investigations of the Rapiscan Secure 1000

Study	Number of Units Tested	Reference Effective Dose to Standard Man Being Screened (nSv)	Effective Dose to Sensitive Populations Considered	Absorbed Dose to Skin or Eye Lens	Air Kerma in Region Surrounding Inspection area per screening	Dose rate to bystanders from stray radiation[a]
JHU/APL	1	4.6	No	No	8.4 nGy	Up to 1285 nSv/hour
NIST	1 at NIST facility	18.5	Newborn infant: 29.8 nSv 5 year-old: 21.9 nSv	111 nGy to skin and eye[b]	<0.1-1.8 nGy	Up to 276 nSv/hour[c]
AAPM	3 at Factory and 6 at one airport	11.1[d]	No	40.4 nGy to skin	Below detection limit	Below detectable level
FDA	Multiple	29	N/A	N/A	1.9-2.6 nGy	N/A

[a] This value is based on 180 screenings per hour.

[b] Value based on dose calculated for the position of maximum exposure, which was at a height of 185 cm.

[c] This value would apply to an operator who spends 2,000 hours per year at the edge of the inspection zone, which cannot occur in light of current work practices.

[d] Calculated by the committee from kerma and half-value layer (HVL) reported by AAPM.

NOTE: The four studies presented here were selected because they are the most comprehensive studies to be performed on the Rapiscan Secure 1000 system.

The ANSI/HPS N43.17 standard limits the dose per screening for a general-use X-ray backscatter system to a reference dose of 250 nSv.

SOURCE: American Association of Physicists in Medicine, *Radiation Dose from Airport Scanners: Report from Task Group 217*, College Park, Md., 2013.

primarily by faculty members of the University of California, San Francisco,[32,33] that data supporting this conclusion came from studies[34] that were not *independent,*[35] and that the studies did not carefully examine the dose to the skin, which they

[32] J.W. Sedat, Ph.D., Marc Shuman, M.D., David Agard, Ph.D., and Robert Stroud, Ph.D., Letter to Dr. John P. Holdren, Assistant to the President for Science and Technology, April 6, 2010, available at http://www.whitehouse.gov/sites/default/files/microsites/ostp/ucsf-jph-letter.pdf.

[33] P. Mehta and R. Smith-Bindman, 2011, Airport full-body screening: What is the risk?, *Archives of Internal Medicine* 171(12):1112-1115.

[34] See, for example, Cerra, *Assessment of the Rapiscan Secure 1000 Body Scanner for Conformance with Radiological Safety Standards*, 2006; JHU/APL, *Radiation Safety Engineering Assessment Report for the Rapiscan Secure 1000 in Single Pose Configuration*, 2009.

[35] The authors do not define *independence*.

believe could be high even though the effective dose is low.[36] Another concern was that the studies did not address issues regarding AIT system malfunctions that could potentially cause a high radiation dose to be concentrated on a single spot.[37] Such studies were described as "difficult-to-impossible" to conduct using publicly available information.[38]

To ensure that malfunctions would not lead to overexposure[39] to radiation, manufacturers of the AIT systems include safety interlocks that, for example, prevent the AIT system from emitting X rays if the X-ray beam is not moving across the passenger being screened. These interlocks can be implemented in hardware and/or software. Hardware interlocks for AITs include switches that prevent X-ray generation if the X-ray electronics cabinet doors are open or if a number of other safety-related conditions are not met. With regard to software interlocks, at the highest level, the software provides password protection against changing AIT system settings that would increase the radiation dose. Within the AIT system, software interlocks monitor critical voltages and currents and prevent the generation of X rays if the operating conditions vary from nominal conditions. For AIT system maintenance and repair, the X-ray tube must sometimes be turned on with the cabinet doors open or in other non-standard AIT system configurations. For these cases, each AIT software design includes a "maintenance mode" or "engineering mode" that is restricted to trained and certified maintenance personnel.

THE STUDY REQUEST

Congress introduced legislation calling for an independent investigation of the safety of the X-ray backscatter AIT systems.[40] In response to this call, in November 2011, TSA made a commitment at the Senate Homeland Security and Governmental Affairs Committee hearing that it would conduct an independent

[36] In their April 6, 2010, letter, Sedat et al. express a number of concerns about the safety of backscatter X-ray inspection. Some of the points raised relate to the physics of energy deposition by ionizing radiation and the quantities used to quantify radiation exposure. However, some of the issues raised are based on mischaracterization of radiation concepts. For the committee's discussion of the letter and clarification of some of these misconceptions, see Chapter 6.

[37] D.J. Brenner, Are X-ray backscatter scanners safe for airport passenger screening? For most individuals, probably yes, but a billion scans per year raises long-term public health concerns, *Radiology* 259(1):6-10. 2011.

[38] J.E. Moulder, Risks of exposure to ionizing and millimeter-wave radiation from airport whole-body scanners, *Radiation Research* 177(6):723-726, 2012.

[39] For the purpose of this report, overexposure is defined as exposure to radiation above the dose limit set by the ANSI, 2009, ANSI/HPS N43.17-2002, Radiation Safety for Personnel Security Screening Systems Using X-Ray or Gamma Radiation standard.

[40] U.S. House of Representatives, 112th Congress, H.R. 4068, introduced February 16, 2012, https://www.congress.gov/bill/112th-congress/house-bill/4068/text.

study on the effects of X-ray backscatter AIT.[41] Around May 2012, DHS engaged the NRC to review current processes used by TSA and equipment manufacturers to estimate radiation exposures resulting from X-ray backscatter AIT use in screening air travelers and announced its intention to award a contract to the NRC in December 2012.[42] As specified in the statement of task (Appendix A) the request was to consider only the use of X-ray backscatter AIT technology and to address only the radiation issues related to standards and malfunction. Specifically, it was not to address the following:

1. The issue of *justification* of the use of X-ray backscatter AIT systems when an alternative technology that does not use ionizing radiation exists, or
2. Whether the standard this technology needs to comply with is appropriate and/or adequate to protect human health.

The NRC study started in May 2013. However, during that month, TSA completed the removal of the Rapiscan X-ray backscatter AIT systems from airports because of Rapiscan's inability to develop the ATR privacy software by the deadline directed by Congress. Despite removal of the X-ray backscatter AIT systems from all airports, DHS, the study sponsor, expressed their continuing interest for the NRC to perform an independent examination of the Rapiscan Secure 1000 previously deployed in U.S. airports. Given TSA's intention to potentially procure the second-generation X-ray backscatter AITs manufactured by AS&E, which are now in testing, DHS also expressed an interest in an independent examination of these second-generation AIT systems.[43]

STRATEGY TO ADDRESS THE STUDY CHARGE

This study was carried out by a committee of experts appointed by the NRC. The committee consisted of 14 members with expertise that spans the disciplines relevant to the study task: radiation physics and dosimetry, radiation biology, diagnostic and therapeutic radiology, materials science, systems and electrical engineering, manufacturing testing and evaluation, aviation safety, software safety, and statistics. In selecting the membership of the committee, the NRC sought to

[41] TSA, "TSA to Conduct an Independent Study with National Academy of Sciences on Backscatter X-ray Advanced Imaging Technology," press release, December 18, 2012, http://www.tsa.gov/es/node/1671.

[42] Federal Business Opportunities (FedBizOps.gov), "Airport Passenger Screening: Backscatter X-Ray Machines," Solicitation Number RSEN-13-00004, posted December 13, https://www.fbo.gov/?s=opportunity&mode=list&tab=list&tabmode=list2012.

[43] Oral communication with TSA representatives from the Office of Security Capabilities on February 3, 2014.

balance members who have direct experience with the design and operation of the X-ray backscatter AIT and members who have relevant disciplinary expertise but no direct experience. Biographical sketches of the committee members are provided in Appendix E.

As part of the NRC independent evaluation, DHS requested that the NRC subcontract with an appropriate testing organization or qualified consultants to conduct field studies to measure the radiation emitted by the AIT systems as they are used. According to the DHS-NRC agreement, the work of the subcontractors would be overseen by the NRC.

To identify appropriate subcontractors to conduct field studies to measure the radiation emitted by the AIT systems as they are used and to estimate doses received by the populations of interest, NRC staff solicited nominations for candidates by drawing upon a vast network of contacts and resources and invited the candidates to respond to two separate requests for proposals (RFPs) issued by the NRC on February 21, 2014. In both RFPs (field measurements and dose estimations), the technical requirements and specifications, statement of work, and deliverables were defined by the NRC in consultation with the study committee. Decision on the awards was made by NRC staff in consultation with a subgroup of committee members who declared no conflict of interest related to the individuals or companies that responded to the RFPs. When making a decision on the subcontractors, the following criteria were considered: expertise and knowledge on radiation physics and dosimetry; adequacy of response to the technical aspects of the RFP; availability of personnel and timely ability to respond to the task; absence of conflict of interest; and cost of services. Subcontracts were awarded in April 2014 to David Hintenland and Wesley Bolch, both in the Advanced Laboratory for Radiation Dosimetry Studies, J. Crayton Pruitt Family Department of Biomedical Engineering, University of Florida, to perform the field measurements and dose estimations, respectively. Brief biographical information for the subcontractors is presented in Appendix E.

Results of the subcontractors' work was used by the committee to draw its findings and recommendations for the first part of the statement of task related to whether exposures from the AIT systems comply with the applicable health and safety standard, ANSI/HPS N43.17-2009. The committee identified three possible approaches to respond to the second part of the statement of task related to whether system design, operating procedures, and maintenance procedures are appropriate to prevent overexposures:

1. Carry out a system design reliability analysis by reviewing the mechanical and electrical diagrams and other documentation of how critical AIT safety systems work.
2. Inspect and test AIT safety systems.

3. Identify a worst-case scenario for the AIT that could lead to exposure higher than intended and determine whether this scenario could lead to overexposure of the person being screened.

The committee did not have access to the needed material for the first approach (i.e., to carry out an AIT system design reliability analysis) because this material is proprietary information and is protected from public release. However, the committee was able to inspect and test some AIT safety systems and performed a detailed analysis of the dose received by the person being screened in a situation where safety interlocks fail and overexposure may be possible. The committee's findings and recommendations are described in Chapter 7.

At the time this study was conducted, all X-ray backscatter AIT systems manufactured by Rapiscan had been removed from airports. Also, the second-generation AS&E AIT systems were undergoing initial evaluations at TSA's Transportation Systems Integration Facility (TSIF), and none were deployed at airports. Therefore, the committee and its subcontractors were unable to test the AIT systems at airports. Instead, they had access to two AIT systems:

1. A Rapiscan Secure 1000 unit located at NIST, Gaithersburg, Maryland, that was previously deployed at LaGuardia Airport. This AIT system, now the property of NIST, was set up by Rapiscan to operate as previously used at airport checkpoints. Measurements on this unit took place July 14-16, 2014.
2. A second-generation AS&E SmartCheck AIT system located at the TSIF testing laboratory, Arlington, Virginia, that was undergoing product certification/qualification procedures for checking that the system meets TSA's requirements and specifications. The committee is not aware how this unit undergoing certification/qualification differs from the units possibly deployed to airports in the future. Measurements on this unit took place May 20-22, 2014.

The manufacturers of the units (Rapiscan and AS&E), TSA personnel, and NIST personnel had no oversight during the measurements process. The subcontractors who performed the measurements, with committee oversight, and dose estimations provided their expert opinions to the committee about the interpretation of the measurements and calculations of doses but did not have input on how the results were used in this report.

When analyzing the results from the measurements, the committee requested that the subcontractor conduct a sensitivity analysis determining how the dosage received by a person being screened with the X-ray backscatter AIT would be affected by differences in design and radiation emission from various possible AIT

systems. This analysis makes the results from the NRC study more broadly applicable than for only the two AIT systems studied.

INFORMATION GATHERING AND CHALLENGES

The committee held six meetings, three of which were information gathering, to receive briefings and documentation from TSA and DHS and subject-matter experts. The committee also visited NIST and TSIF to inspect the X-ray backscatter AIT systems and learn about their design and operation by engaging in discussions with experts and operators.

In addition, the committee requested and received written information from DHS, NCRP, JHU/APL, NIST, and AAPM. Requests for information were also sent to Rapiscan and AS&E, the manufacturers of the units examined. However, even though there was some dialog, the companies were unable to meet all of the requests from the committee for information.[44]

REPORT ORGANIZATION

Chapter 1 (this chapter) provides an introduction to the study. Chapters 2 through 7 address the statement of task (Appendix A) in its entirety.

- Chapter 2 describes the radiation physics behind the X-ray backscatter AIT.
- Chapter 3 describes the different backscatter AIT implementations.
- Chapter 4 describes dosimetric considerations for measurements of ionizing radiation emitted by the X-ray backscatter AITs.
- Chapter 5 provides an overview of the pertinent radiation standards.
- Chapter 6 provides a review of previous studies on the radiation emitted from X-ray backscatter AIT systems and an investigation of interlocks put in place.
- Chapter 7 describes the committee's measurements of radiation emitted and calculation of dose as well as the committee's observations of the fail-safe mechanisms.

Appendixes A-E provide detailed information about organ dose calculations and statistical considerations from previous studies as well as abbreviations, the statement of task, and committee biographical information.

[44] For example, the committee requested the mechanical and electrical diagrams of the AIT systems and information about safety interlocks. The companies could not respond to all of the committee's requests for a variety of reasons (national security, proprietary information, trade secrets, etc.).

There are two chapters in this report that lead to key findings and recommendations: Chapters 6 and 7. Chapter 6 contains the review of previous studies, while Chapter 7 contains the measurements and computations the committee and the subcontractors undertook during the course of the study. For the analysis of the previous studies in Chapter 6, the committee focused on the methodologies used to measure radiation emitted by the AIT systems as well as on the results reported. For the reports or papers in which assessments of the effective dose are based on estimates of AIT system characteristics rather than measurements, the committee provides a summary at the end of Chapter 6. Chapter 7 describes the committee's measurement procedures, provides the measurements for the Rapiscan Secure 1000 and the second-generation AS&E AIT systems, and discusses the dose computations used. Descriptions of possible failures related to interlocks, subcomponents, and other issues that are fundamental to a functional AIT system are assembled in Tables 6.5, 6.6, 7.5, and 7.11.

2

Radiation Physics Relevant to Advanced Imaging Technology

X-ray backscatter advanced imaging technology (AIT) exploits the physical properties of X rays to create images using photons backscattered from a scanned passenger. This chapter summarizes the physics principles and the associated transfer of energy to the passenger that enable image formation. Additional information, including details of these processes, can be found in radiological physics and health physics texts.[1]

THE PHYSICS OF X-RAY ABSORPTION

X-ray backscatter AIT uses a narrow beam of X-ray photons with energies, *hv*, less than 100 keV.[2] There are five basic interactions that can occur as X rays penetrate material. These are the photoelectric effect,[3,4] Compton scattering, Thompson scattering, Rayleigh scattering, and pair production. Figure 2.1 shows the rela-

[1] See for example, H.E. Johns and J.R. Cunningham, *Physics of Radiology*, Fourth Edition, Charles C Thomas Publisher, Springfield, Ill., 1983.

[2] An X-ray tube operating at 100 kV has a peak at a lower energy than 100 keV; for example, for 50 kV, the peak is at ~30 keV, as seen in Figure 2.2.

[3] When a photoelectric interaction occurs, the energy of a photon is completely transferred to an atomic electron. The electron may thus gain sufficient kinetic energy to be ejected from the electron shell. The energy of the incoming photon must, however, be higher than the binding energy for the electron.

[4] *Photoionization* is the physical process in which an ion is formed from the interaction of a photon with an atom or a molecule.

tive interaction cross sections (i.e., attenuation coefficients) for photoelectric, Compton, and Rayleigh scattering in soft tissue as a function of photon energy. Pair production requires a minimum photon energy of 1.022 MeV and is not of concern here.

The photoelectric effect is the dominant interaction for X rays with energies below 30 keV. This reaction results in the disappearance of the photon. The result is the ejection of a bound electron, usually from an inner shell, with a kinetic energy of $h\nu - E_B$, where E_B is the original binding energy of the electron. The ejected electron loses its kinetic energy by exciting additional atoms. In some cases, it transfers sufficient energy to liberate an additional electron capable of creating additional ionization. This initiates a cascade process that ends only when all excitations have been thermalized and the system returns to a ground state, which may include chemical changes. Each ionized atom returns to its ground state by emitting one or more secondary photons and/or electrons, which add their contributions to the process. The result is a rapid dissipation of the energy of the incident X ray, diffused through a volume extending some 10 to 30 micrometers (μm) from the site of the initial absorption.

Because no scattered photon is generated, the photoelectric effect does not contribute photons to a backscatter image, but its contribution to energy absorbed in the material is significant. Furthermore, because the probability of a photoelectric interaction increases rapidly with the atomic number, Z, of the target atom, photons are more likely to be absorbed than scattered by high Z materials such as metals. This provides contrast in the backscatter image, with metallic objects appearing dark (indicating a lack of backscattered photons).

Compton scattering is the main interaction for energies above 30 keV. As seen in Figure 2.1, it is the dominant energy-loss mechanism in tissue for X rays of energy greater than about 30 keV. Here, the incident photon scatters off an electron in the material, transferring a fraction of its energy to the electron, thereby reducing its energy and changing direction. Energy conservation requires

$$h\nu = h\nu' + E_e$$

where $h\nu$ is the energy of the incident photon, $h\nu'$ is the energy of the photon after scattering, and E_e is the energy of the scattered electron.

By considering momentum conservation, it is possible to determine the properties of the scattered particles as a function of the scattering angle. If the photon scatters at an angle θ from its trajectory prior to the interaction, the energy of the scattered photon is given by:

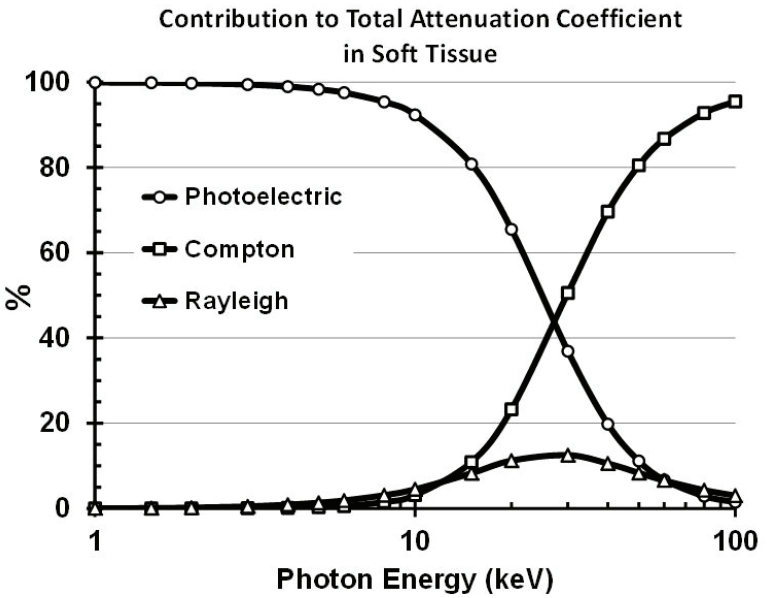

FIGURE 2.1 The relative interaction cross sections (i.e., attenuation coefficients) for photoelectric, Compton, and Rayleigh scattering in soft tissue as a function of photon energy. The cross section for Thompson scattering is too small to influence this figure. SOURCE: Courtesy of Tom Borak.

$$h\upsilon' = \frac{h\upsilon}{1+\frac{h\upsilon}{m_e c^2}(1-\cos\theta)}$$

where $m_e c^2$ is the rest mass energy of an electron. For example, a 50 keV photon scattered at $\theta = 180°$ emerges with an energy $h\nu' = 42$ keV. The energy transferred to the electron is $E_e = 8$ keV.

The energy of the electron is dissipated in the material, whereas the scattered photon either escapes or interacts in the material. While it is unlikely that an incident photon will backscatter at exactly 180°, several Compton scattering events can occur, resulting in the photon emerging in a backward direction or terminating in a photoelectric event. Detector systems with large geometrical acceptance angles have a good probability of registering these scattered photons. An image is formed by associating all of the photons detected in a time interval with the location of the incident beam on the subject at that time. In effect, the output of the detectors is stored in a memory location synchronized with the position of the beam.

The third interaction, Thompson scattering, is the emission of radiation generated by the acceleration of point charges (electrons) by the electric field of the incident X ray. Because accelerated charges radiate, there is a finite probability that an X ray of the incident beam will be backscattered with no change in energy. This backscattered intensity can be calculated. It is independent of incident energy and equal to the intensity of the incident beam times the square of the ratio of the nuclear diameter ($\sim 2 \times 10^{-15}$ m) to the distance between the scattering electron and the detector (~1 m). The resulting attenuation factor, $\sim 10^{-30}$, effectively prevents Thompson-scattered electrons from contributing to the image, even when generous estimates of collection solid angles and the number of electrons in a material up to the X-ray absorption depth are assumed.

The final interaction, Rayleigh scattering, also involves acceleration of charges but differs from Thompson scattering in that the atoms are treated as objects with a nucleus and surrounding electrons and therefore have a finite size. This introduces a length scale and, as a result, a wavelength dependence, $\sim \lambda^{-4}$, for the scattering probability. This dependence strongly favors short wavelengths. Applied to visible light, it accounts for the blue color of the sky. The contribution of Rayleigh scattering of X rays is that of Thompson scattering multiplied by a resonance factor. The resulting cross sections are not negligible, but they are still small compared to the photoelectric and Compton cross sections, as seen in Figure 2.1. Hence, neither Thompson nor Rayleigh scattering make important contributions either to backscatter image formation or to the deposition of energy in the scanned object.

BEAM ATTENUATION AND DEPOSITED ENERGY

If it were possible to use monochromatic 50 keV photons for backscatter screening, it would be relatively easy to estimate the intensity of backscattered radiation reaching the detector and the energy deposited in the scanned person. The incident X-ray beam would attenuate exponentially in the person's body, with an average penetration depth[5] of the order of 1 cm, generating scattered photons and secondary electrons by processes described above. The resulting electrons would travel distances on the order of tens of micrometers, resulting in the energy being deposited relatively near the locations of the energy transfer events.

Practical X-ray sources do not produce monoenergetic beams. X-ray tubes use electrons produced at the negative terminal, the cathode, of a vacuum diode. These electrons are accelerated for AIT systems, usually to an energy of about 50 keV, then strike the positive terminal, the anode, which is typically made of a heavy, electron-

[5] Penetration depth is a measure of how deep light or any electromagnetic radiation can penetrate into a material. It is defined as the depth at which the intensity of the radiation inside the material falls to $1/e$ (about 37%) of its original value.

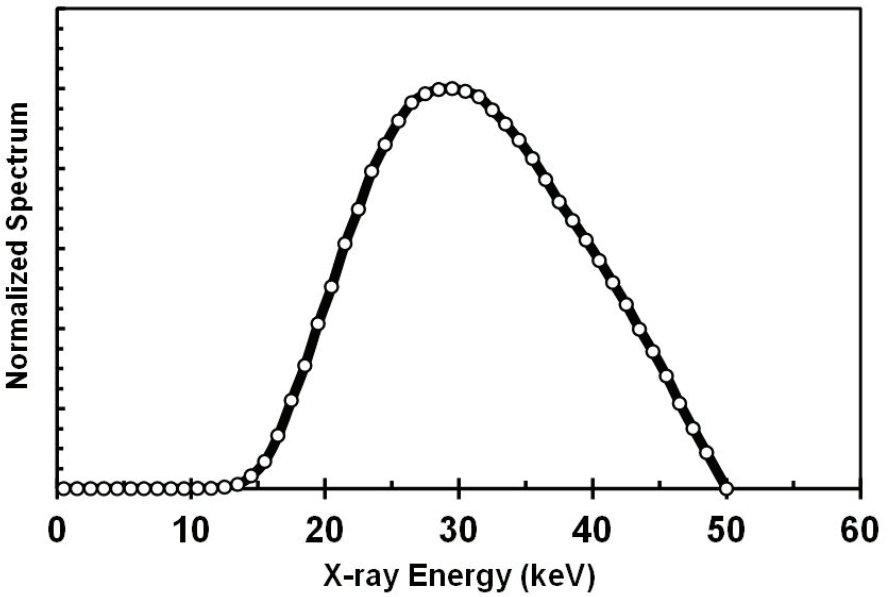

FIGURE 2.2 Typical energy spectrum of photons produced in an X-ray tube operating at 50 kV. SOURCE: Courtesy of Tom Borak.

dense metal such as tungsten. They lose energy either by interacting with the heavy nuclei to produce bremsstrahlung X rays or by interacting with the electrons of the anode to produce heat and characteristic X rays. The bremsstrahlung process produces a distribution of photon energies from zero to the electron energy itself. Because many electrons have slowed down before producing bremsstrahlung radiation, this results in a large number of photons at very low energies. The photons at very low energies are preferentially removed by absorption either in the tungsten anode or in the glass or metal body of the tube and any purposely inserted external filtration. The typical output spectrum peaks at around 30 keV, as shown in Figure 2.2.[6] However, the details of the spectrum depend on the atomic number of the anode material, the amount of anode material that the photons must traverse before exiting the tube (e.g., as a function of the exit angle), the atomic composition and thickness of the exit window, and other material (filters) in the beam path.

The average penetration depth of photons in a material such as the body of the person being scanned is the result of random absorption and scattering interactions. The number of unscattered photons per unit area typically decreases

[6] Note that any characteristic radiation from the tungsten anode is only produced when the voltage is higher than 69.5 kV.

exponentially with depth. The rate of decrease depends on the probability of the various interactions. Compton scattering depends on the number density of electrons in the material, and the probability of Compton scattering is therefore a function of the average atomic number of the elements in the material. However, the photoelectric cross section also depends on the binding of the electrons and increases rapidly with increasing atomic number. Soft tissue (such as muscle and skin) consists mainly of hydrogen, oxygen, carbon, and nitrogen with a trace amount of phosphorus. The atomic numbers of these elements are all relatively low, so photon attenuation is easily evaluated. Photons with energies below about 10 keV that are incident on muscle are absorbed almost entirely in 1 cm. At 20 keV, about 30 percent of the incident photons penetrate 1 cm. At 50 keV, the fraction that penetrates 1 cm rises to 80 percent. Thus, the backscatter images represent the outer 1 cm or so of material. Bone contains calcium and has a significantly higher rate of photon attenuation but is often behind more than 1 cm of soft tissue, so it is not considered further.

To determine the amount and location of energy deposited in biological material—the likely initiator of biological effects of irradiation—one must take into account the scattered X rays and energetic electrons generated by Compton scattering as well as the electrons energized by the photoelectric process. At any location within the material, this depends on the branching ratio between (relative importance of) Compton scattering and the photoelectric effect. The scattered photons add to the photons that have not been scattered, and the excited electrons carry energy away from their point of creation. But electron ranges are typically a small fraction of the mean penetration depths of photons, so the location where the incoming energy is deposited is determined by the photons. For example, the mean free path of a 30 keV photon in water is 2.7 cm, three orders of magnitude larger than the 18 μm range of a 30 keV electron in the same material. However, electron transport may be significant near boundaries between materials—for example, tissue adjacent to bone. This will be discussed in more detail in Chapter 4.

The quantitative analysis of backscatter image formation and patterns of energy deposition in the person being scanned requires sophisticated computational techniques. This will be discussed in detail in Chapter 7.

3

X-Ray Backscatter Advanced Imaging Technology

The X-ray backscatter advanced imaging technology (AIT) system is based on the backscatter imaging device described by Steven W. Smith in 1991.[1] In summary, a well-collimated pencil-beam of X rays is raster scanned across an area in which a person is positioned, and the X rays backscattered from a person toward the source are collected by large area detectors adjacent to and on the side of the X-ray source. The spatial resolution of the X-ray backscattered image is defined by the source collimator aperture and distance from the person to the source; the resolution is not defined by the detector.

Since the technology was first developed, X-ray backscatter AIT systems have evolved, and several models with distinct characteristics are available today. For example, there are at least three X-ray backscatter manufacturers: Rapiscan Systems, American Science and Engineering, Inc. (AS&E), and Tek84 Engineering Group, LLC. Each of these manufacturers produces a "general use" X-ray security screening AIT system.[2] The manufacturers use similar physics and differ only in their implementation of the physics and other aspects, as described in the sections below.

[1] Steven W. Smith, X-ray Backscatter Detection System, U.S. Patent 5181234, filed May 22, 1991, and issued January 19, 1993.

[2] The term *general use systems* was introduced by the National Council on Radiation Protection and Measurements (NCRP, 2003, "Screening of Humans for Security Purposes Using Ionizing Radiation Scanning Systems," Commentary No. 16, Bethesda, Md.) to describe X-ray security screening machines that expose the individuals being screened to a very low dose of radiation and, therefore, there is overall no need to limit the number of individuals screened or the number of screenings an individual can have in a year. This is in contrast to the second category of X-ray security screening

RAPISCAN SECURE 1000

There are two different Rapiscan Secure 1000 configurations: the first configuration uses a single X-ray source and a large area detector in a single housing and acquires data from a single side of a person, either anterior or posterior. Obtaining both anterior and posterior views requires the individual to pose twice, once facing the AIT system and once facing away, leading to what is called a dual-pose AIT system. The second configuration consists of two units facing each other, often referred to as "anterior" and "posterior" units. The two (front and back) sides of the person are scanned in succession. This equipment is referred to as a single-pose AIT system because the person does not have to turn to be scanned both front and back. Screening starts when an operator presses a start button on the anterior unit; the anterior unit scans the anterior of the person being screened, and after the anterior unit is done, the posterior unit scans the posterior of the person being screened.

The anterior and posterior units of the single-pose system take approximately 3 seconds each, and because scanning is performed sequentially, one screening (consisting of two scans) takes a total of about 6 seconds to complete. The dual-pose AIT system requires time for the person being screened to turn around for the second scan and thus takes longer than a single-pose AIT system does. The person being screened using a dual-pose AIT system is not subjected to twice the X-ray dose compared to the single-pose AIT system; they are receiving approximately half the X-ray dose for each of the poses for a total dose equivalent to that from the single-pose AIT system. The actual anterior and posterior doses are given in Chapter 7. The single-pose AIT system (Rapiscan Secure 1000 single pose) was predominantly deployed by TSA until it was removed in May 2013.

Each Rapiscan 1000 unit contains a tungsten anode X-ray tube that operates at a voltage of 50 kV and 5 mA. In the Secure 1000, the X-ray cone-beam emitted by the source is initially collimated by a slit (see Figure 3.1).

Downstream from the slit is a rotating chopper wheel with four equally spaced radial slits that go from near the center to the periphery of the wheel (see Figure 3.1); this is called a rotating geometry. The overlap of a stationary radial slit wheel aperture and the slit aperture results in a pencil beam at the center of the Secure 1000

systems defined by NCRP Commentary No. 16, named *limited use*. Limited use systems such as transmission X-ray systems expose individuals being screened to higher doses of radiation that penetrate the body in order to detect objects that have been swallowed or are hidden in cavities. NCRP recommends that these systems be used with consideration of the number of individuals screened and the number of screens per individual in a year. The basic criterion for distinguishing between the two categories is an effective dose of 250 nSv (or less) per screening. Both general use and limited use systems should meet the recommended administrative control for a member of the public of 250,000 nSv (or less) effective dose per year for a single source or set of sources under the control of one entity (committee communication with David Schauer, NCRP, January 15, 2014).

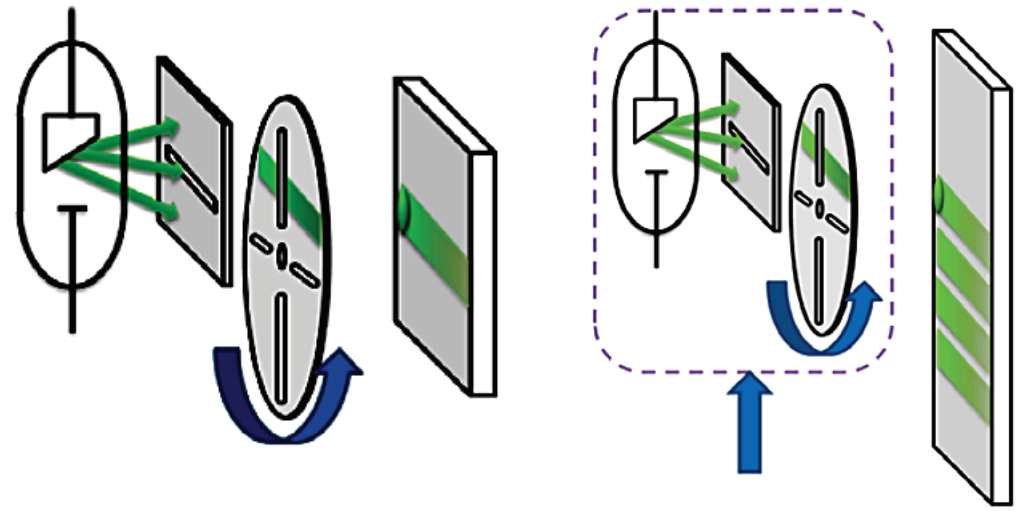

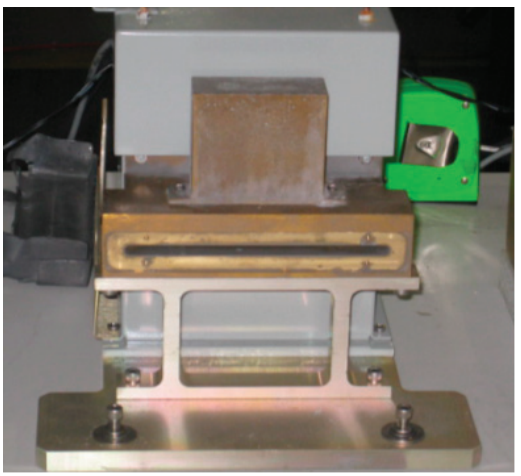

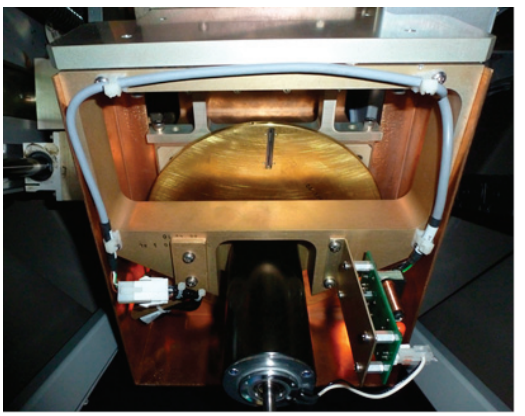

FIGURE 3.1 Drawings of the internal operation of the Rapiscan 1000 single-pose and dual-pose configurations showing the slit and chopper wheel radial apertures generation of a raster scanning pencil beam of X rays (*top left*). Vertical motion of this whole configuration (*top right*) allows the pencil beam to cover a large area and thus generate a two-dimensional X-ray backscattered image. The slit aperture (*bottom left*) and chopper wheel with radial apertures (*bottom right*) are shown. SOURCE: Courtesy of Erik Svedberg (*top*) and Mauro Sardela (*bottom*).

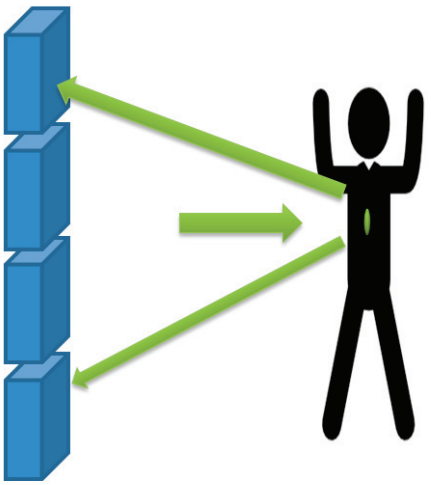

FIGURE 3.2 A backscatter AIT system in use. A small pencil beam illuminates a spot on some part of the scan area (i.e., the body) at any given time, and the large detector rows pick up the backscattered X rays continuously as the spot sweeps. SOURCE: Courtesy of Erik Svedberg.

AIT system. When the wheel rotates, the radial slits traverse across the length of the fan-beam and results in the pencil beam that scans in the horizontal direction; this combination of the horizontal slit and the rotating aperture produces what is commonly referred to as a raster scan. The large area detectors located beside the source integrate the X rays that are backscattered from the person. The resulting signal strength is recorded as a function of the position of the pencil beam. This results in a single horizontal line image of the X rays backscattered from the person.[3] The entire housing of the X-ray source, fan-beam collimator, and chopper wheel assembly is vertically translated during the scan so that successive horizontal image lines are displaced to form a two-dimensional image. Because the total vertical travel of the X-ray head is less than the desired scan height, the tube and collimator assembly also rotate about the horizontal axis. As the X-ray assembly approaches the lower limit of travel, it tilts down in order to image the feet of the subject, and as it reaches the top of its travel, it tilts up to cover the tallest individual. The AIT system can scan in both the upward and the downward direction. The result is a two-dimensional X-ray backscattered image of the person being screened. The large area detector consists of two vertical arrays of fluorescent screens that are viewed by large photomultiplier tubes (see Figure 3.2; only one vertical array is shown). An image is generated based on the intensity of backscattered X rays as a function

[3] For an additional description of the rastered spot used, see L.T. Hudson, J.L. Glover, and R. Minniti, The metrology of a rastered spot of X rays used in security screening, *Journal of Research of the National Institute of Standards and Technology* 119:540-553, 2014, http://dx.doi.org/10.6028/jres.119.021.

of the position of the pencil beam on the subject. Contrast in detected backscatter radiation provides depictive representations of the subject's body and exposes any concealed objects (e.g., a wallet or an explosive), generating an X-ray backscatter image for each AIT system unit.

AS&E SMARTCHECK

AS&E manufactures two X-ray backscatter AIT systems: SmartCheck and SmartCheck-HT. The SmartCheck is a dual-pose AIT system, while the SmartCheck-HT is a single-pose AIT system, where HT stands for high throughput. As stated earlier, the X-ray backscatter manufacturers use the same physics and differ mainly in their implementation.

The fundamental X-ray generation for SmartCheck is similar to the Rapiscan design in that AS&E's new AIT system employs a tungsten anode X-ray tube that operates at a voltage of 50 kV. They differ in that the AS&E's X-ray tube current is 12 mA, while Rapiscan's is 5 mA, and AS&E's AIT system generates its raster-scanning pencil beam of X-rays by collimating the X-ray cone-beam emitted by the source using a vertical hollow cylinder surrounding the X-ray tube and rotating about its central axis. Several round apertures or holes (see Figure 3.3) emit the desired X-ray beam.

The large area detector on the source side integrates the X rays that are backscattered from the person, and the signal is coordinated with the beam location.

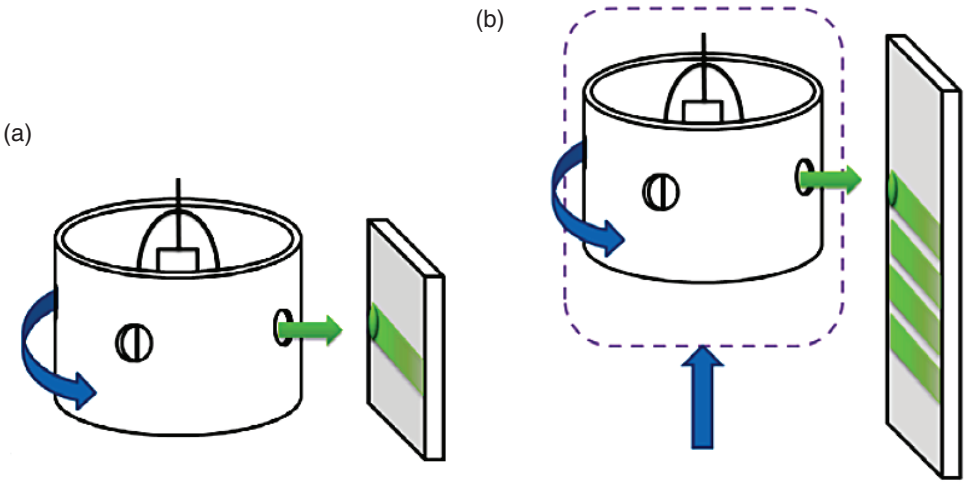

FIGURE 3.3 Apertures or holes in a rotating cylinder emit the sweeping X-ray beam in the AS&E SmartCheck AIT. As each hole traverses the cone-beam of X-rays from the source inside the cylinder, a scanning beam of X rays is generated. In diagram (a), only a line is swept out; in diagram (b), the unit is raised so that an area is swept out. SOURCE: Courtesy of Erik Svedberg.

This generates a single horizontal line (one-dimensional) image of the X rays that are backscattered from the person located in the scanning environment. Differences in backscatter intensity provide contrast in the line image. The entire housing of the X-ray source, fan-beam collimator, and canister assembly is vertically translated during the scan to move the horizontally raster-scanned pencil beam of X rays along the vertical direction. This results in a two-dimensional X-ray backscattered image of the person being screened. A second detector array, on the opposite side of the subject, produces an outline image of the subject. The AIT system can scan in both the upward and the downward direction.

Each scan takes about 3 seconds, or about 6 seconds for both anterior and posterior X-ray backscattered images. A dual-pose model requires time for the person being screened to turn for the second scan. As with the Rapiscan, persons being screened using a dual-pose AIT system are not being subjected to twice the X-ray dose compared to the single-pose AIT system; they are receiving approximately half the X-ray dose for each of the single poses for a total dose equivalent to that from the single-pose AIT system. The actual anterior and posterior doses are given in Chapter 7.

TEK84 AIT84

The design of Tek84's Ait84 is closely related to the Rapiscan Secure 1000; thus, Figure 3.1 best describes how the AIT system works. It is a single-pose AIT system and generates the raster-scanned X-ray spot using a similar horizontal collimating slit with rotating chopper wheel and vertical translation of the housing containing the X-ray tube, collimating slit, and rotating chopper wheel. Similar to the Secure 1000 single-pose AIT system, it completes the series of two scans in 6 seconds. The distinguishing feature of the Ait84 is that during each anterior or posterior X-ray scan, the Ait84 collects the X-ray intensity data from both the fluorescent screens on the active X-ray source side and the fluorescent screen opposite the X-ray source, generating two images, simultaneously X-ray backscattered and X-ray transmission, respectively.[4]

The fundamental X-ray generation for the Tek84 Ait84 is similar to the Rapiscan Secure 1000 and AS&E's SmartCheck design (see Figure 3.4). The Ait84 employs a tungsten anode 50 kV and 5 mA X-ray tube voltage and current, respectively. The Ait84 generates an X-ray beam ~6 mm × 6 mm at 75 cm. This AIT system is not equipped with automatic target recognition and, therefore, is not a candidate for deployment at U.S. airports. However, it is used for screening at airports outside the United States, such as airports in Israel.

[4] Presentation by Steven Smith, owner of Tek84, to the committee on April 29, 2014.

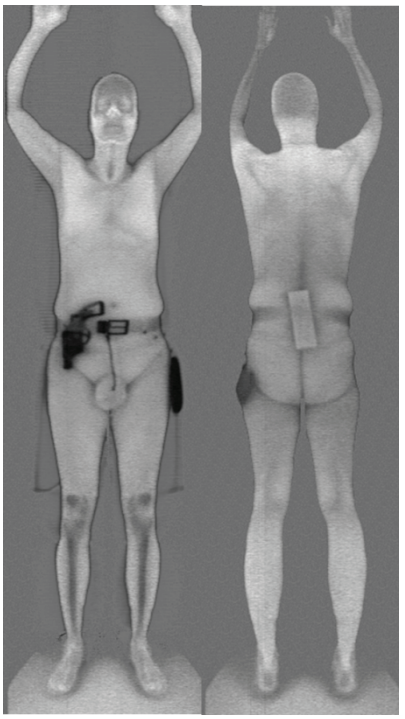

FIGURE 3.4 Composite images, including both transmission and backscatter image data are shown. SOURCE: Scanned images from the AIT84 security scanner, provided by Tek84 Engineering Group, LLC.

4

Dosimetry for X-Ray Backscatter Advanced Imaging Technology

In order to evaluate radiation exposures such as those produced by advanced imaging technology (AIT) systems, and to make it possible to estimate health effects that might result from those exposures, it is necessary to have a way to measure radiation exposure and to account for the different biological effectiveness of different types of ionizing radiation. Quantification of radiation exposure is complicated because a wide range of ionizing radiation is found in nature, and the interactions that those radiation types have with matter are complex. The International Commission on Radiation Units and Measurements (ICRU) has developed a self-consistent set of radiation quantities and units to resolve this problem (ICRU Report 85a, 2011). Because the AIT systems under consideration here use only photons with relatively low energy (less than 120 keV), this chapter will summarize only the quantities and units that are relevant to the determination and reporting of exposures to low-energy X-rays. The quantities that are needed for the work in Chapters 6 and 7 include the following:

- A measure of the energy spectrum of the photons,
- The amount of energy lost in a material by photons,
- The amount of energy deposited in tissue, and
- A quantity suitable for comparison with radiation protection limits when the type of radiation is different or when only a portion of the body is exposed to radiation.

X-RAY SPECTRA

The energy spectrum of photons incident on an exposed individual is related to the probability of each type of photon interaction and therefore affects the overall attenuation of the photon beam with depth. Consequently, it is essential to characterize the photon spectrum in order to determine the energy deposited in different parts of the body. The X-ray emission from conventional X-ray tubes is of much lower brightness than many other sources such as synchrotrons. Although it is possible to determine the spectra produced by X-ray tubes using semiconductor or other energy-sensitive detectors, when methods for characterization of X-ray beams were first developed, techniques for measuring X-ray intensity were used to characterize the photon spectrum, not spectroscopic principles.

In practice, determination of the intensity of photons emitted by an X-ray tube is generally accomplished by determining the accumulation of electrical charge collected in ionization chambers placed in the beam. This is possible because the photon energy required to produce an ion is nearly independent of the photon energy. Measurements of beam attenuation are used to confirm assumptions about the photon energy spectrum. In medical practice, knowledge of the tube's high voltage, anode material, the angle of the beam relative to the anode surface, and the amount of inherent and external filtration are sufficient to characterize a spectrum for most imaging applications.

The term generally used to characterize the spectrum of photons emitted by an X-ray tube is beam quality. It refers to the penetration capability of an X-ray beam emerging from a source. In clinical-diagnostic practice, beam quality is expressed as the first and second half-value layer (HVL) thicknesses, HVL_1 and HVL_2, respectively. The first half-value layer reduces the intensity of the incident beam by 50 percent, and adding the second half-value layer reduces the incident beam by another factor of two for a combined attenuation of 75 percent. If HVL_1 and HVL_2 are known, together with tube voltage, it is possible to estimate the energy spectrum of the emerging beam using established spectral models.

KERMA

In order to quantify X-ray beam intensity, a precise measure of the intensity is needed. The standard measure of energy transferred to matter by indirectly ionizing radiation (X rays and neutrons) is air kerma.[1] In the case of X rays, kerma is the kinetic energy transferred from photons to charged particles in a volume of

[1] When a quantity to characterize energy lost by radiation, as opposed to energy deposited in matter, was first introduced, it was identified by the acronym KERMA, kinetic energy released in matter. More recently, kerma has been adopted as the name of the quantity.

material, divided by the mass of material in that volume. It is typically expressed in gray (Gy) where 1 Gy = 1 J/kg.

Although other types of detectors can be used, gas-filled ion chambers are generally preferred for measuring kerma in the range of beam intensities produced by X-ray tubes. The radiation traversing the chamber produces positive and negative ions and free electrons, which are collected at two electrodes (typically concentric cylinders or parallel plates) by applying a potential difference between them. Ideally, all ions and electrons are collected. However, this is usually not achieved, and some corrections are generally necessary. Even the best chambers have small regions where the electric-field strength is reduced. This results in a local increase in recombination of electrons and ions in the gas and reduces the collected charge. Recombination can be reduced by reducing the density of the gas, but this negatively impacts sensitivity. Recombination can also be reduced by increasing the voltage difference between the plates. If the collected charge is found to be essentially independent of applied voltage for a range of voltages, it is a good indication that all of the charge that can be collected has been collected.

Ion-chamber design is also relevant. Most ion chambers necessarily have solid walls to define the gas volume where ionization is measured. The walls also provide secondary electrons that ionize the gas. In addition, a solid wall will preferentially attenuate low-energy photons. As a result, measurement of kerma is strongly dependent on the photon spectrum, and ion chambers must be calibrated in a radiation field that has the same quality as the radiation fields they will be used to measure. Size also matters, because sufficient charge must be produced to be measurable by the associated electronics. For example, a 1 cm^3 chamber exposed to 1 nGy would produce approximately 200 ion pairs, or 3.2×10^{-17} coulombs. This is much less than can be accurately measured even by high-quality electrometers. However, an 1,800 cm^3 ion chamber exposed to 1 nGy would produce 5.7×10^{-14} coulombs, which can be measured.

To minimize measurement uncertainty and provide a traceable standard, the National Institute of Standards and Technology (NIST) maintains precision free-air ion chambers to calibrate ion chambers in terms of air kerma for a variety of X-ray spectra.[2] The free-air ion chamber is a specialized instrument with no walls defining the sensitive volume of air. It measures the electric charge produced in a volume of air defined by two electrodes and a carefully collimated beam of photons. Because the radiation must be limited to a precisely defined beam, the free-air ion chamber cannot be used to measure kerma in a typical radiation environment. However, it can be used to cross-calibrate other ion chambers in well-defined beams. By sequentially placing the free-air reference chamber and the test cham-

[2] NIST website, Dosimetry Group, http://www.nist.gov/pml/div682/grp02/, accessed February 4, 2014.

bers in the same beam, NIST can determine the calibration factor for a given test chamber. Because each chamber has its own energy dependence, the calibration factor is specific to the spectrum used for the calibration. However, NIST provides a wide range of different spectra for calibration, as determined by the operating conditions of the X-ray tube and additional filtration.

ABSORBED DOSE

To predict the biological consequences of irradiation, kerma is not enough. The actual amount of energy deposited in tissue is more relevant because it is assumed that this energy initiates the biochemical processes that lead to the observable effects of irradiation. Because some of the electrons liberated by photon irradiation have ranges that are larger than the dimensions of cells in tissues, the energy deposited in tissue may not exactly equal the energy lost by photons. As a result, the *absorbed dose, D*, is defined as $d\varepsilon/dm$, where $d\varepsilon$ is the element of energy absorbed from ionizing radiation by an element of mass dm.[3] D and kerma have the same units but differ in that kerma describes the kinetic energy transferred to electrons without regard to their final destination, and D describes energy deposited without regard to origin. Thus, D does not include the energy escaping the volume but does include energy depositions within the volume from electrons initiated outside of the volume. Kerma and absorbed dose are numerically equivalent under the conditions of charged particle equilibrium (CPE). While proportional to the intensity of the incident X-ray beam, neither gives the intensity of the beam directly.

EFFECTIVE DOSE

For purposes of radiation protection, exposure to different types of radiation must be described in a way that can be compared to a single exposure limit, independent of the type of radiation or its spatial distribution in the body of the exposed individual. The quantity "effective dose," E, has been established by the ICRP for this purpose. E is the sum of doses to specific tissues or organs multiplied by the dimensionless weighting factors W_R (the radiation weighting factor) and W_T (the tissue weighting factor), which describe the different sensitivities of the different organs to different types of radiation (see Box 4.1). As with kerma and absorbed dose, the units of effective dose are J/kg, but because E is not a measurable physical quantity, its unit is given the special name sievert (Sv) instead of using the physical measurable quantity gray (Gy).

Several approaches can be used to determine the effective dose. Because expo-

[3] International Commission on Radiation Units and Measurements, ICRU Report 46: Photon, Electron, Proton and Neutron Interaction Data for Body Tissues, *Journal of the ICRU*, 1992.

BOX 4.1
Dosimetry Quantities and Units

The International Commission on Radiation Units and Measurements (ICRU) has developed a radiation measurement system using both stochastic and non-stochastic quantities.[1] The non-stochastic quantities are defined as expectation values at a point in space, that is, in the differential form. Since the non-stochastic quantities are used for radiation protection their definitions are given here.

Kerma, K, is defined as[1]:

$$K = \frac{dE_{tr}}{dm}$$

where dE_{tr} is the sum of initial kinetic energies of all charged ionizing particles liberated by uncharged ionizing particles in a volume of material having a mass dm.[1] Kerma has dimensions of energy divided by mass. It is described by the quantity gray (Gy) where

$$1\ \text{Gy} = 1\frac{\text{J}}{\text{kg}}$$

Absorbed dose, D, is defined as[1]

$$D = \frac{d\bar{\varepsilon}}{dm}$$

where $d\bar{\varepsilon}$ is the mean energy imparted by ionizing radiation in a volume of material of mass dm.[1] Absorbed dose has dimensions of energy divided by mass. It is also described by the quantity Gy. Absorbed dose and kerma differ in the sense that kerma represents the kinetic energy transferred to electrons, whereas absorbed dose represents the energy absorbed. One distinction is that kerma is based on the kinetic energy of electrons originating in a volume without regard to the final destination. Absorbed dose is based on energy deposition in a volume without restrictions on the origins or final destinations of the electrons. Kerma and absorbed dose are numerically equivalent under the conditions of charged particle equilibrium.

Effective dose,[2] *E,* is the tissue weighted sum of equivalent doses in specific tissues and organs of the body, and is given by the expression

sure to different organs depends on the attenuation of the beam at their locations, the most direct approach is to use a material phantom. This simulates a person of the desired height and weight and contains a large number of small dosimeters at appropriate locations. The dosimeters are used to evaluate the average absorbed dose to each of the organs. For X rays, the radiation weighting factor (W_R) is 1.0, so the effective dose is obtained by applying the appropriate tissue weighting factors

$$E = \sum_T w_T \sum_R H_{T,R} = \sum_T w_T \sum_R w_R D_{T,R}$$

where $D_{T,R}$ is the absorbed dose from radiation of type R averaged over a tissue or organ T, and w_R is a weighting factor for radiation of type R. For photons of all energies, $w_R = 1$.

The tissue weighting factor, w_T, is the factor by which the absorbed dose in a tissue or organ T is modified to represent the relative contribution of that tissue or organ to the total health detriment from a uniform irradiation of the whole body. It is normalized to

$$\sum_T w_T = 1$$

Tissue weighting factors are based on epidemiological studies of cancer induction, genetic alterations following exposure to radiation, and judgment. Furthermore, they represent mean values for humans averaged over both sexes and a span of ages. Effective dose is intended for use as a protection quantity derived from reference values and therefore is not recommended for epidemiological evaluations, nor should it be used for detailed assessment of exposure and risk to specific individuals.

Reference effective dose,[3] E_{REF}, is determined for full-body AIT systems from measurements of the half-value layer (HVL) and air kerma (Gy) as outlined below. It is given specifically by

$$E_{REF} = K_a \times C$$

where E_{REF} is the reference effective dose in sieverts (Sv), K_a is the measured air kerma per screen in grays (Gy), and C (in Sv/Gy) is given by C = 0.125 × HVL in millimeters of aluminum or 1.14, whichever is smaller.

---

[1] International Commission on Radiation Units and Measurements, ICRU Report 85a: Fundamental Quantities and Units for Ionizing Radiation, *Journal of the ICRU* 11(1), 2011.

[2] International Commission on Radiological Protection, ICRP Publication 103: The 2007 Recommendations of the International Commission on Radiological Protection, *Annals of the ICRP* 37(2-4), 2007.

[3] The American National Standards Institute/Health Physics Society standard ANSI/HPS N43.17-2009, "Radiation Safety for Personnel Security Screening Systems Using X-Ray or Gamma Radiation," is available at the Health Physics Society website at http://hps.org/hpssc/index.html.

to these data and adding the results. The process is difficult and time-consuming, with accuracy limited by the accuracy of the individual dosimeters and the number of dosimeters used to determine the average dose in specific tissues.

The alternative to direct measurement is computation. Here, radiation-transport calculations determine the absorbed dose at specified locations in a computational phantom. The computational phantoms originally used for this

purpose were collections of geometric shapes (cylinders, spheres, and intersecting planes) arranged to simulate a human body. Recently, phantoms of considerably improved detail and accuracy have been developed using computed-tomography images of individuals.

REFERENCE EFFECTIVE DOSE

The American National Standards Institute (ANSI) has adopted the concept of a reference effective dose, E_{REF}, for specifying exposures produced by X-ray AIT systems (see Box 4.1). E_{REF} is equal to the product of the air kerma of the beam and a function of its HVL. The justification for E_{REF} is based on the observation that "the effective dose for monoenergetic photons and for all the spectra having at least 1 mm of aluminum total filtration follows a relatively close-grouped pattern as a function of HVL."[4] The ANSI/Health Physics Society (ANSI/HPS) standard N43.17-2009 specifies that the reference effective dose from general-use AIT systems (such as AIT equipment) "shall not exceed 250 nSv (25,000 nrem) per screening" where a screening consists of an anterior and a posterior scan.[5] This recommendation is generic and does not specifically focus on specific at-risk populations.

RELATIONSHIP BETWEEN KERMA AND ABSORBED DOSE

To compare E produced by X-ray backscatter AIT systems to the maximum effective dose specified by National Council on Radiation Protection and Measurements (NCRP) and the ANSI/HPS N43.17-2009 standard, it is necessary to determine the average absorbed dose in each of the organs for which a weighting factor has been defined. To do this, it is necessary to consider the diffusion of electrons and the effect of boundaries. Diffusion is the process by which higher concentrations of electrons expand across a boundary into regions of lower concentrations. If the system is in local CPE, meaning that the local rates of in- and out-diffusion of energy are equal, then D is equal to the kerma, and its evaluation is straightforward. However, CPE does not occur near boundaries between materials of different atomic compositions. Of particular concern is the dose to the skin, because in most cases it is adjacent to air or in contact with another material and hence falls into this category.

For a beam of a given intensity, the concentration of secondary electrons cre-

[4] The ANSI/HPS N43.17-2009 standard, "Radiation Safety for Personnel Security Screening Systems Using X-Ray or Gamma Radiation," is available at the Health Physics Society website at http://hps.org/hpssc/index.html.

[5] ANSI/HPS N43.17-2009, p. 6.

ated in any material is proportional to the kerma in that material. Therefore, at a boundary between dissimilar materials, the concentration of secondary electrons is higher on one side than the other. As a result, electrons in the material with the higher kerma will diffuse across the boundary to the material with the lower kerma. Therefore, near the boundary, *D* will exceed the value calculated from kerma alone in the material with the lower kerma, and vice versa. This difference will die out on either side over distances of the order of the characteristic diffusion lengths for secondary electrons in the materials. The scale of these distances can be approximated as the range of the most energetic secondary electrons in the material, which for a 50 keV electron in tissue is 44 μm. Because most secondary electrons have much lower energies and therefore much shorter ranges, equilibrium between *D* and kerma is typically established well within 50 μm of the surface. Because the beam intensity decreases approximately exponentially with depth, diffusion causes *D* to be slightly different than the kerma, but this is usually a minor effect and can be ignored. Because nearly all radiation-sensitive cells are deeper than 50 μm in the body, *D* is essentially equal to the kerma for all radiation-sensitive cells.

If a material with a high energy transfer coefficient (μ_{tr}/ρ,) is in contact with the skin, *D* at the surface of the tissue can be much higher than is the kerma. For example, at 30 keV, the coefficient μ_{tr}/ρ of aluminum is 5.6 times that of muscle. The ratio for silicon is 7.4, and for calcium 23.4. If the skin is covered by a thin layer of one of these materials, energy transfer across the skin–material boundary needs to be taken into account.

Photon scattering also influences the kerma near boundaries between materials of different atomic compositions. Backscattered photons increase the kerma relative to that produced by the incident photons alone. The magnitude of this photon buildup depends on the geometry of the radiation field and of the object irradiated but is generally not large. It is included in the results of the Monte Carlo codes[6] used to calculate effective dose in a phantom.

[6] Monte Carlo codes are a type of computational algorithms that rely on repeated random sampling to obtain numerical results; typically, one runs simulations many times over in order to obtain the distribution of an unknown probabilistic entity.

5

Radiation Protection Standards

DOSE

The Transportation Security Administration (TSA) has required that the X-ray backscatter advanced imaging technology (AIT) systems approved for deployment conform to the American National Standards Institute/Health Physics Society (ANSI/HPS) Accredited Standards Committee N43 (Equipment for Non-Medical Radiation Applications) standard N43.17.[1,2,3] The ANSI/HPS N43.17 standard is a consensus standard that provides guidelines for both manufacturers and users of the systems and covers dose to subject, interlocks, operational procedures, and information to be provided to the travelers by the operators. Prior to this standard, there was little guidance for this type of intentional, nonmedical radiation

[1] Department of Homeland Security, Office of Health Affairs, "Fact Sheet: Advanced Imaging Technology (AIT) Health & Safety," http://www.tsa.gov/assets/pdf/ait_fact_sheet.pdf.

[2] The American National Standards Institute/Health Physics Society (ANSI/HPS) standard N43.17 is available at http://hps.org/hpssc/index.html, accessed March 2, 2014.

[3] There is a comparable international standard, International Electrotechnical Commission (IEC) 62463-2010, "Radiation Protection Instrumentation-X-Ray Systems for the Screening of Persons for Security and Carrying of Illicit Items," Geneva, Switzerland.

exposure. The current standard, ANSI/HPS N43.17-2009,[4] is a revision of ANSI/HPS N43.17-2002[5] in response to new system designs and new use requirements.

Manufacturers of electronic products that emit radiation also need to comply with the Federal Food, Drug and Cosmetic Act, Chapter V, Subchapter C; and manufacturers of personnel security screening X-ray AIT systems must comply with applicable requirements of Title 21 of the Code of Federal Regulations 1000-1005.[6] In addition, system operators need to comply with Occupational Safety and Health Administration ionizing radiation safety limits as promulgated in Title 29 of the Code of Federal Regulations, Part 1910.1096.[7] This regulation specifies radiation dose limits for the whole body, lens of the eye (same as whole body), and skin for occupationally exposed individuals.

The ANSI/HPS N43.17-2009 standard refers to the airport X-ray backscatter AIT systems as "general use" X-ray security screening systems and limits the dose per screening to 250 nSv, referred to as the *reference effective dose*. This description for dose is a simplified version of effective dose and is easier to calculate but still considered sufficiently accurate to ensure radiation safety (see Chapter 4 for a comprehensive discussion of reference effective dose.) Together with establishing a per-screening dose limit for the person being screened, the standard also recommends annual radiation dose limits of 250,000 nSv over a 12-month period (1,000 screens per year).

The annual dose limit of the ANSI/HPS N43.17-2009 standard is based on dose limit recommendations for the general public published in National Council on Radiation Protection and Measurements (NCRP) Report No. 116,[8] *Limitations of Exposure to Ionizing Radiation*, and endorsed in a later NCRP commentary,[9] "Screening of Humans for Security Purposes Using Ionizing Radiation Scanning Systems," prepared at the request of the Food and Drug Administration. NCRP[10] recommends limiting the annual effective dose from all sources (excluding back-

[4] The ANSI/HPS N43.17-2009 standard, "Radiation Safety for Personnel Security Screening Systems Using X-Ray or Gamma Radiation," is available at the Health Physics Society website at http://hps.org/hpssc/index.html.

[5] The ANSI/HPS N43.17-2002 standard, "Radiation Safety for Personnel Security Screening Systems Using X-rays," is available at http://hps.org/hpssc/index.html.

[6] Food and Drug Administration, "CFR—Code of Federal Regulations Title 21," last updated September 1, 2014, http://www.accessdata.fda.gov/scripts/cdrh/cfdocs/cfcfr/CFRSearch.cfm?CFRPart=1000.

[7] Department of Labor, Occupational Safety and Health Administration, Standard 1910.1096, "Ionizing Radiation," https://www.osha.gov/pls/oshaweb/owadisp.show_document?p_table=STANDARDS&p_id=10098.

[8] National Council on Radiation Protection and Measurements (NCRP), *Report No. 116, Limitation of Exposure to Ionizing Radiation,* Bethesda, Md., 1993.

[9] NCRP, "Screening of Humans for Security Purposes Using Ionizing Radiation Scanning Systems," Commentary No. 16, Bethesda, Md., 2003.

[10] NCRP, *Report No. 116*, 1993.

ground and medical)[11] for members of the public to 1,000,000 nSv. If a detailed assessment of all sources is not conducted, NCRP recommends that no single source or set of sources "under one control" should result in an individual being exposed to more than 250,000 nSv annually. For backscatter systems, "under one control" refers to the use of ionizing radiation AITs at one or more security checkpoints at a given venue (e.g., multiple checkpoints at a given airport).[12] In other words, NCRP recommends that a passenger not receive a dose of more than 250,000 nSv in 1 year from being scanned in a single airport. However, if this same passenger received a dose of more than 250,000 nSv in 1 year from being scanned in airports in different cities, NCRP's recommended administrative control is still met. Administrative controls are essential for keeping radiation exposure levels in compliance with the radiation safety principle of as low as (is) reasonably achievable (ALARA).[13]

The ANSI/HPS N43.17-2009 standard also addresses the issue of various subgroups (for example, pregnant women and children) of the general population being more susceptible to the radiation-induced health effects compared to others. Again, the standard refers to NCRP Report No. 116,[14] which recommends limiting the annual effective dose from all sources (excluding background and medical) for members of the public to 1,000,000 nSv. It does not issue different limits for these subgroups of the general population, implying that the 1,000,000 nSv dose limit offers sufficient protection to them also. However, NCRP issues a different limit for the embryo or fetus of an occupationally exposed woman and recommends a maximum occupational dose[15] of 500,000 nSv per month. For comparison, the occupational dose limit is 50,000,000 nSv per year.

ANSI/HPS N43.17-2009 provides detailed guidance not only for acceptable radiation dose levels for individuals and radiation workers but also for radiation-producing systems, manufacturing, installation, safety performance, and regular maintenance. Radiation-producing instruments are required to include fail-safe mechanisms that would halt the operation in case of major failures in mechanical

[11] These sources include activities such as nuclear power generation, decommissioning of radioactive waste, industrial and research activities, and security inspection systems.

[12] D.A. Schauer, Does security screening with backscatter x-rays do more good than harm?, *Radiology* 259:12-16, 2011.

[13] *As low as (is) reasonably achievable* is defined in Title 10, Part 20.1003 of the Code of Federal Regulations (CFR) to mean "making every reasonable effort to maintain exposures to radiation as far below the dose limits in this part as is practical consistent with the purpose for which the licensed activity is undertaken, taking into account the state of technology, the economics of improvements in relation to state of technology, the economics of improvements in relation to benefits to the public health and safety, and other societal and socioeconomic considerations, and in relation to utilization of nuclear energy and licensed materials in the public interest."

[14] NCRP, *Report No. 116*, 1993.

[15] *Occupational dose* refers to dose of ionizing radiation received by workers (often referred to as *radiation workers*) in the course of employment. See OSHA 29 CFR 1910.1096.

or electronic components. Periodic maintenance and inspection of such instruments must include testing of those fail-safe mechanisms.[16]

RADIATION HEALTH EFFECTS AND RISKS AT LOW DOSES[17]

Some background on the potential health effects and associated risks of the use of X-ray backscatter AIT systems may help to put dosimetric concerns in context. Current understanding of the potential health risks at very low doses of ionizing radiation is far from complete. Some things, however, are clear. First, the doses that an X-ray backscatter AIT system is capable of producing are far below the levels required to produce symptoms of acute radiation syndrome,[18] even in unusually sensitive individuals. Similarly, the doses are well below the threshold required for the production of late effects, such as cardiovascular or neurological damage, which only appear to occur at higher doses (approximately 500,000,000 nSv),[19] so these are also not of concern for X-ray backscatter AIT system exposures. In contrast, carcinogenesis is thought to be a stochastic event, meaning that exposure to a low level of a carcinogen could slightly increase the chance of cancer occurrence. Therefore, radiation protection limits for X-ray backscatter AITs have been designed with a focus on protecting against increased cancer risks to the exposed public.

Projections of cancer risks from exposure to radiation are based largely on epidemiological studies, with much of the information coming from studies of the atomic bomb survivors in Hiroshima and Nagasaki, Japan. More than 27,000 atomic bomb survivors had exposures in the 5,000,000 to 100,000,000 nSv range, and statistically significant excess cancer incidence has been detected.[20] In the Oxford Survey of Childhood Cancers, a study of 15,000 case control pairs, an increase in childhood cancer was found after in utero X-ray exposure to a mean dose of about 6,000,000 nSv.[21] Very large studies such as these are needed to detect effects

[16] ANSI/HPS N43.17-2009, Section 8.1.6.

[17] *Low dose* in this report refers to a dose lower than that used in radiation therapy. The amount of radiation used in photon radiation therapy is usually measured in gray (Gy) and varies depending on the type and stage of cancer being treated. For curative cases, the typical dose for a solid epithelial tumor ranges from 60 to 80 Gy. In this report, low is in the range nanogray (nGy), a billion times lower.

[18] For acute syndrome to manifest, doses need to be high, possibly higher than 0.7 Gy. See Centers for Disease Control and Prevention, "Acute Radiation Syndrome: A Fact Sheet for Clinicians," http://www.bt.cdc.gov/radiation/arsphysicianfactsheet.asp, accessed March 3, 2014.

[19] International Commission on Radiological Protection (ICRP), ICRP statement on tissue reactions/Early and late effects of radiation in normal tissues and organs—Threshold doses for tissue reactions in a radiation protection context, Publication 118, *Annals of the ICRP* 41(1/2), 2012.

[20] D.L. Preston, E. Ron, S. Tokuoka, S. Funamoto, N. Nishi, M. Soda, K. Mabuchi, and K. Kodama, Solid cancer incidence in atomic bomb survivors: 1958-1998. *Radiation Research* 168: 1-64, 2007.

[21] R. Doll and R. Wakeford, Risk of childhood cancer from fetal irradiation, *British Journal of Radiology* 70: 130-139, 1997.

from low-dose exposures because of the high background incidence of cancer (around 40 percent in the United States) and the relatively small expected increase in cancer due to small radiation doses such as those from screening with an X-ray backscatter AIT. Linear extrapolation indicates that measurable increases in cancer incidence will not occur at the doses used in X-ray backscatter AITs.

Epidemiological studies are limited in detecting increases in cancer risks following small doses of radiation (less than 100,000,000 nSv). Therefore, alternative ways to characterize risks at low doses are used, such as projecting the risks of very small exposures by extrapolating from existing studies where doses are higher. However, characteristics of the exposure or the populations exposed in these existing studies may vary substantially from those of interest.[22] Risk estimates at low doses (often defined as less than 100,000,000 nSv)[23] may be greatly affected by the choice of the model used to extrapolate to low doses. Currently, the linear nonthreshold dose-response model for extrapolation to low and very low doses is used as the basis for U.S. radiation protection standards.[24] However, the possibility of other shapes for dose-response curves at low doses cannot be ruled out because there are insufficient low-dose data.

SYSTEM DESIGN, INTERLOCKS, AND OPERATING PROCEDURES

In addition to providing guidance on radiation dose limits as discussed earlier in this section, ANSI/HPS N43.17-2009 also provides guidance as to the acceptable protection systems (interlocks to protect against accidental excess radiation) and operational procedures. Below, the requirements for general use systems are outlined because the X-ray-emitting passenger screening AIT systems fall into that category.

Indicators and Safety Interlocks

Although the radiation levels emitted from general use systems are low, ANSI/HPS N43.17-2009 requires a certain level of protection against accidental excess radiation as well as suitable notifications that the X-ray-emitting AIT system is in operation (Box 5.1).

[22] For example, atomic bombing survivors received a dose acutely while other low-dose exposure may happen chronically; the exposed individuals were Japanese, who may vary in their genetic makeup and susceptibility to cancer from the U.S. populations.

[23] NRC (National Research Council), *Health Risks from Exposure to Low Levels, of Ionizing Radiation: BEIR VII—Phase 2*, The National Academies Press, Washington, D.C., 2005.

[24] NRC, *Health Risks from Exposure to Low Levels of Ionizing Radiation: BEIR VII—Phase 2*, 2006.

BOX 5.1
ANSI/HPS 43.17-2009, Sections 7.2.1 and 7.2.2

7.2.1 Requirements for All Systems: The requirements of this subsection apply to all the systems regardless of category or type of radiation source. In addition to these requirements systems must comply with the requirements of one of the sections 7.2.2 through 7.2.5 as appropriate.

a. There shall be at least one indicator, clearly visible from any location from which a scan can be initiated, that indicates when a scan is in progress.

b. There shall be at least one lighted indicator clearly visible from the inspection zone. For portal systems the indicator shall be visible from any approach to the inspection zone to indicate that a scan is in progress.

c. Power to the system shall be controlled by a key switch. The key shall be captured (unable to be removed) whenever it is in a position that allows exposures to be initiated. Turning on the key switch shall never result in the external emission of radiation.

d. Each system shall have a means for the operator to initiate the emission of radiation other than the function of an interlock or the main power control.

e. Each system shall have a means for the operator to terminate the emission of radiation other than the function of an interlock.

f. Means shall be provided to ensure that operators have a clear view of the scanning area. This can be a direct, mirror view, or real-time video of the scanning area. Engineering controls should be provided to ensure that individuals do not reenter the scanning area from the exit while x-rays are being produced (e.g., one way turnstile, see also specific requirements in Sections 7.2.2 through 7.2.5).

g. A ground fault shall not result in the generation of x-rays or activate a scan beam from a sealed radioactive source.

h. Failure of any single component of the system shall not cause failure of more than one safety interlock.

i. A tool or key shall be required to open or remove access panels. Access panels shall have at least one safety interlock.

j. For stationary-subject systems, the scanning motion of the x-ray beam relative to the subject shall be interlocked and the exposure shall terminate when the rate of motion of the beam in any direction falls below a preset minimum speed. The minimum speed shall be chosen so that the dose during the exposure period is within the applicable limit.

k. For portal systems, the minimum walking or driving velocity through the inspection zone shall be determined by the manufacturer. The minimum speed shall ensure that the dose during the exposure period is within the applicable limit.

l. Operational interlocks shall terminate the primary beam in the event of any system problem that could result in abnormal or unintended radiation emission. This shall include, but is not limited to, unintended stoppage of beam motion, abnormal or unintended x-ray source output, computer safety system malfunction, termination malfunction, and shutter or beam stop mechanism malfunction.

m. In the event of a malfunction, the system shall terminate radiation exposure rapidly enough so that no location on the subject's body shall receive an ambient dose equivalent (H*10) exceeding 250 μSv (25 mrem), regardless of the size of the exposed area.

continued

BOX 5.1 Continued

n. Following interruption of x-ray production or external gamma emission by the functioning of any safety interlock, resetting the interlock shall not result in the production of x-rays or emission of gamma radiation. Use of the normal control sequence shall be necessary for resumption of x-ray generation or gamma radiation emission.

7.2.2 Requirements for General-use Systems Using X-ray Sources: In addition to the requirements of Section 7.2.1, "Requirements for All Systems," the following requirements apply to general-use systems using x-ray sources:

a. For any x-ray system that normally keeps high voltage applied to the x-ray tube at times other than during a scan, there shall be at least one lighted "xray on" indicator at the control console where x rays are initiated indicating when x-rays are being produced.

b. Technique factors[1] for each mode of operation shall be preset by the manufacturer and shall not be alterable by the system operator. If there is more than one mode, prior to each scan, a mode indicator shall be clearly visible to the operator.

c. Each access panel to the x-ray source shall have at least one safety interlock to terminate the x-ray production when opened.

d. The following warning label shall be permanently affixed or inscribed on the x-ray system at the location of any controls used to initiate x-ray generation: "CAUTION: X-RAYS PRODUCED WHEN ENERGIZED."

e. X-ray emission shall automatically terminate after a preset time or exposure.

f. For portal systems, motion sensors shall monitor the speed of pedestrians or vehicles through the inspection zone (in the forward direction) and the radiation exposure shall terminate when the speed drops below the minimum (as determined according to Section 7.2.1k).

[1] Technique factors relate to the X-ray beam configuration and include accelerating potential, beam current, beam filtration, and stand-off distance.

SOURCE: The ANSI/HPS N43.17-2009 standard, "Radiation Safety for Personnel Security Screening Systems Using X-Ray or Gamma Radiation," is available at the Health Physics Society website at http://hps.org/hpssc/index.html.

Operational Procedures

In addition to the technical requirements related to radiation levels and the engineering of an airport screening AIT system, ANSI/HPS N43.17-2009 lays out the following requirements on the operation of the AIT system as well as the operators using the AIT system:

- The compliance with required operational procedures must be ensured by a designated responsible individual. The operational procedures for the particular installation must be documented and be provided to the

operators of the AIT system. ANSI/HPS N43.17-2009 outlines the minimal amount of information that must be included in this operational procedures document. In addition, all operators must receive appropriate training, including information about the types of radiation present, comparison to other radiation sources, units of measurement, hazards with the system, and security procedures.

- The manufacturer must provide adequate installation procedures so that the installed AIT system complies with its operational specification. This includes a qualified individual to perform a radiation survey to verify that the dose to the scanned passenger, to the operators, as well as to the bystanders[25] is within acceptable guidelines. Such radiation surveys must also be performed at least once every 12 months to ensure that the AIT system stays within its operation parameters. Finally, radiation surveys shall also be performed after maintenance and after any incident that might damage the system to prevent unintended radiation emission.
- The facility operating the system must provide the person to be screened with information that the system emits radiation, basic information about the dose expected in the screening, and information so that the dose can be compared to other radiation sources (for example, background radiation or a chest X ray).
- Finally, the institution operating the AIT system must maintain records for at least 5 years, documenting operator training, maintenance and upgrade, radiation surveys, and the number of scans performed. Current information on the responsible individual designated for the site as well as a complete set of operating procedures must be readily available.

[25] In general, this report differentiates only between the *scanned passenger* and *anyone else* using the term *bystander*. An *operator* can be seen as a *bystander* that spends more time and in closer proximity to the equipment than *anyone else*.

6

Review of X-Ray Backscatter Advanced Imaging Technology Studies

The committee performed a comprehensive analysis of previous studies of X-ray backscatter advanced imaging technology (AIT) systems. This chapter focuses on the following reports:

- Johns Hopkins University/Applied Physics (JHU/APL), *Radiation Safety Engineering Assessment Report for the Rapiscan Secure 1000 in Single Pose Configuration* (2010);[1]
- National Institute of Standards and Technology (NIST), *Assessment of the Rapiscan Secure 1000 Single Pose (ATR version) for Conformance with National Radiological Safety Standards* (2012);[2]
- American Association of Physicists in Medicine (AAPM), *Radiation Dose from Airport Scanners: Report of AAPM Task Group 217* (2013);[3]

[1] JHU/APL, *Radiation Safety Engineering Assessment Report for the Rapiscan Secure 1000 in Single Pose Configuration*, NSTD-09-1085,Version 2, Laurel, Md., August 2010.

[2] J.L. Glover, R. Minniti, L.T. Hudson, and N. Paulter, *Assessment of the Rapiscan Secure 1000 Single Pose (ATR version) for Conformance with National Radiological Safety Standards*, NIST report for the TSA, interagency agreement HSHQDC-11-X-00585, April 19, 2012; latest version available is J.L. Glover, R. Minniti, L.T. Hudson, and N. Paulter, *Assessment of the Rapiscan Secure 1000 Single Pose (ATR version) for Conformance with National Radiological Safety Standards*, NIST report for the TSA, interagency agreement HSHQDC-11-X-00585, September 28, 2012.

[3] AAPM, *Radiation Dose from Airport Scanners: Report of AAPM Task Group 217*, College Park, Md., 2013.

- U.S. Army Public Health Command (USAPHC), *Radiation Protection Consultation No. 26-MF-0E7K-11*, Rapiscan Secure 1000 Single Pose Dosimetry Study (2012);[4] and
- Food and Drug Administration (FDA), *Assessment of the Rapiscan Secure 1000 Body Scanner for Conformance with Radiological Safety Standards* (2006).[5]

The committee briefly describes how it considered radiation measurements from these previous reports, followed by an analysis of each report, including subsections on measurements, calculations, procedures. and interlocks. The chapter also includes a summary of measurements and interlock information from the reviewed studies and a discussion of other studies and their considerations—studies that usually lacked the level of measurements and calculations that the first set of studies had. The chapter concludes with findings and recommendations on exposure and dose.

COMPARING RADIATION MEASUREMENTS

In its analysis of previous reports, the committee focused on the methodologies used to measure radiation emitted by the AIT systems as well as the results. It also looked at AIT system design, such as interlocks. In interpreting and comparing the results from these reports, the committee identified two issues that may result in variations in effective dose to scanned individuals:

1. The model of the AIT system evaluated, and
2. The techniques used to measure kerma and half-value layer (HVL).

With respect to the model of the AIT systems, all systems evaluated in the reviewed reports were produced by the same manufacturer, Rapiscan Systems, and represent different stages in the evolution of the instruments installed in airports. As the instrument was refined, it is not unlikely that small changes were made in the physical components, operating parameters, and procedures. However, there is no evidence that major changes that would affect the radiation emitted were made during the interval covered by the reports reviewed.

Four physical quantities are characteristic of the AIT system and are the primary determinants of the effective dose to a standard subject when scanned. These

[4] USAPHC, *Radiation Protection Consultation No. 26-MF-0E7K-11*, Rapiscan Secure 1000 Single Pose Dosimetry Study, Aberdeen Proving Ground, Md., 2012.

[5] F. Cerra, *Assessment of the Rapiscan Secure 1000 Body Scanner for Conformance with Radiological Safety Standards*, Food and Drug Administration, Arlington, Va., July 21, 2006.

are the photon spectrum, fluence rate, scan duration, and the location of the subject in the AIT system. Additional physical quantities that describe the subject being scanned determine the effective dose for the individual, including weight, height, and shape.

The photon spectrum and fluence rate produced by a specific AIT system are controlled by the X-ray tube used, the anode voltage applied, the anode current, and the X-ray filtration inherent in the AIT system. It appears that the same tube type was used in all of the AIT systems described in the reviewed reports. Within a given tube type, the variations in output at a fixed anode voltage and current are very limited. The most significant source of variation in output is the thickness of the photon exit window of the tube. This window is a component of the photon filtration for the AIT system and thus can influence the photon spectrum. The X-ray tube used in these AIT systems has a glass window 1.5 mm thick. From 10 keV to 30 keV, the mass attenuation coefficient of borosilicate glass is 65 to 70 percent of that of aluminum; thus, this glass window contributes approximately 1 mm aluminum equivalent beam filtration. As a tube is used, a small amount of the anode material, tungsten, evaporates and deposits as a thin metallic film on the inside of the tube, including the window. Thus, the effective filtration may increase slightly with tube use.

The photon spectrum is essentially independent of the anode current, but at a fixed anode voltage, the fluence rate is directly proportional to the anode current. The standard practice for X-ray backscatter AIT systems is to control the anode current by adjusting the cathode temperature, achieved by adjusting the filament current. The filament current is provided by a regulated power supply using a sample of the anode current compared to a reference current. The anode current specified for late-model AIT systems is 3 mA, but the maximum-rated anode current for the tube is 5 mA, and the tube can probably survive a slightly higher current for short times. Consequently, it may be possible to adjust the anode current to produce a photon fluence rate and effective dose rate as much as a factor of two higher than would be obtained using the 3 mA currently specified.

The photon spectrum and the fluence rate both change with a change in anode voltage. For a tungsten target at 50 kV, a 10 percent increase in anode voltage produces approximately a 10 percent increase in the photon yield. For example, an increase in anode voltage from 50 to 55 keV results in approximately a 20 percent increase in the energy emitted as photons, the result of a 10 percent increase in the power to the anode and a 10 percent increase in the radiation yield as well as a 10 percent increase in the maximum photon energy.[6] Differences of this magnitude (or larger) might exist between early prototype AIT systems and production models

[6] F.H. Attix, *Introduction to Radiological Physics and Radiation Dosimetry*, Wiley, New York, N.Y., 1986.

but are extremely unlikely during the operation of a production unit because the regulation of high-voltage power supplies is typically better than 0.05 percent for line voltage variations from 102 to 132 VAC.[7]

The HVL of the photon spectrum is also influenced by any additional material in the photon path to the scanned object. It appears that the only material in addition to the glass tube window is the case of the AIT system, approximately 3 mm of plastic. Although the type and thickness of plastic may have been different on early prototype units, it is unlikely that they would differ significantly from one production AIT system to another.

When other parameters are constant, the effective dose varies directly with the scan duration. Although the scan rate, and therefore the duration, are under software control and can be adjusted by someone with the appropriate software access, it is unlikely in the usual course of operation that scan duration could be modified by more than 30 percent (i.e., increased from 3 seconds to 4 seconds) without being noticed by the operator. The fourth parameter, the location of the subject, is controlled by "footprints" painted on the floor indicating the proper pose.

With respect to the techniques used to measure kerma and HVL, one major difference in the various studies was the modification of the scanning process to increase the photon fluence available for measurement by repeating the scan at a single vertical location. The X-ray beam includes a penumbra of photons scattered by the collimator, and the contribution of these lower-energy photons to the ion chamber current may differ if the whole detector, or one line across it, is irradiated. This could lead to a small difference in the HVL, depending on the measurement conditions. This difference is expected to be very small because the collimator components appear to be made of high Z materials, and the photoelectric effect will dominate the interactions in the collimator.

Additional differences in measured HVL and kerma may result from differences in the instrumentation or techniques used for the measurements. The measurement of kerma was generally done with an ion chamber calibrated for a specific photon spectrum. If the photon spectrum produced by the AIT system does not exactly match the spectrum used for the calibration, small errors in the measurement of kerma may occur. The measurement of HVL is simpler in one way: only relative measurements are needed, but it is technically more challenging because the structure of the measuring device may be modifying the measurement. Ideally, HVL measurements would be made using a wall-less detector thin enough such that there is no variation in photon spectrum through the detector. For gas-filled detectors, the second half of this requirement is easily met, but the presence of an ion chamber wall is the equivalent of adding material to the filtering inherent

[7] Glassman High Voltage, Inc., http://www.glassmanhv.com/, accessed September, 5, 2014.

in the AIT system.[8] Thus, if the ion chamber used to measure HVL has a 5-mm-thick plastic wall, it will determine the HVL present at a depth of 5 mm of plastic. Differences in the structure of the ion chambers used to measure HVL may be responsible for significant differences in the measured result.

The JHU/APL Report

The purpose of the JHU/APL study[9] was to conduct a radiation safety engineering assessment of the Rapiscan Secure 1000 in single-pose configuration.[10] Measurements were made at the Rapiscan factory using two dual-pose engineering units (dated 2005 and 2007) and other components from inventory. The resulting AIT system was configured to be equivalent to a unit then being evaluated by the Transportation Security Laboratory.

Measurements

- *Person being scanned*
  — *Air kerma measurements* were made using a 10X5-1800 ionization chamber manufactured by Radcal Corporation.[11] This chamber was constructed with a polycarbonate wall (i.e., Lexan^{TM}) with a conductive graphite coating. The wall thickness was 3.175 mm (0.125 in.) corresponding to an areal density of 0.38 g/cm^2. This corresponds to the aluminum equivalent thickness of 1.4 mm. The active volume was 1,800 cm^3. The central collector was a cylinder centrally located in the sensitive volume of the detector with a length of 7.8 cm (3.0 in.) and diameter of 3.6 cm (1.4 in.) and 0.07 cm (0.028 in.) wall thickness.

    Measurements were made using the full vertical and horizontal raster-scanning conditions at a standard location, representative of the exposure received by the individual being scanned. The detector was centered midway between the entry and exit portals and 30 cm from the surface of the wall where the beam exits. The ion chamber was orientated so that the incident beam was parallel to the long axis of the cylindrical detector. To shield the ion chamber from extraneous radiation, a piece of lead was placed on top

[8] Calibration to a specified photon spectrum corrects the measured kerma for attenuation in the detector wall, but that attenuation continues to be included in a depth per dose or HVL measurement.

[9] JHU/APL, *Radiation Safety Engineering Assessment Report for the Rapiscan Secure 1000 in Single Pose Configuration*, 2010.

[10] Single-pose configuration means that the subject is scanned only a single time by two AIT systems, one for the front and one for the back.

[11] Radcal Corporation, "10X5-1800," https://www.radcal.com/10x5-1800, accessed September 5, 2014.

(a)

(b)

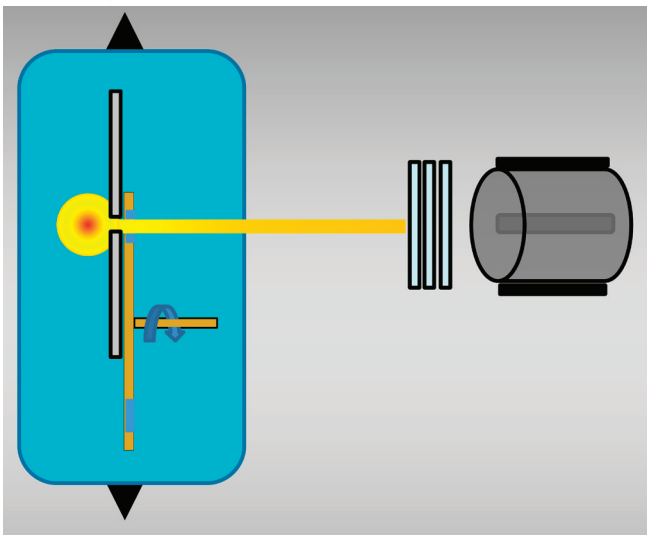

FIGURE 6.1 (a) The location of the 1800 cc ion chamber with lead shield for the JHU/APL kerma measurements. (b) Schematic of the configuration used by JHU/APL to determine half-value layer. SOURCE: (a) Department of Homeland Security, *Radiation Safety Engineering Assessment Report for the Rapiscan Secure 1000 in Single Pose Configuration*, August 2010, http://www.dhs.gov/advanced-imaging-technology-documents; (b) Courtesy of Tom Borak.

of the chamber and wrapped around the sides (Figure 6.1a). The date of calibration was indicated, but details of calibration vendor and beam quality were not indicated. The report indicated that "as a conservative measure, the dose conversion coefficients were selected based on an operating potential of 50 kV." The average air kerma was found to be 41 nGy per scan (82 nGy per screening).

— *HVL measurements* were made using the 1800 cc ionization chamber with the long axis oriented parallel to the beam. The Rapiscan was operated in the full scanning mode with vertical translation of the X-ray assembly, horizontal collimator, and rotating chopper wheel. Lead shielding was wrapped around the ionization chamber to shield from ambient radiation and inscatter, but the beam was not collimated before the attenuation foils (Figure 6.1b). The first HVL for the anterior unit was found to be 1.18 mm of aluminum, but the first HVL of the posterior unit was 1.63 mm of aluminum. No explanation was given for this unusually large difference in HVL for nominally identical sources.

- *Bystander.* Geiger-Mueller and scintillator probes were used to survey the radiation outside the inspection volume. In order to simulate radiation scattered by a person being scanned, a phantom consisting of four 5-gallon containers of water supported by stacked bins was placed at the position of the person being scanned. Locations of maximum count rate were recorded and measurements were made at those locations with the 1800 cc ion chamber and with the AIT system in normal full-scanning operation. Background measurements for the same total time were made and subtracted from the readings of dose during scanning. A maximum of 10 nGy per screening was observed in locations above the inspection volume. The maximum in a location that could be occupied by the equipment operator was 8.4 nGy per screening.

Calculations

- *Person being scanned.* Applying the ANSI/HPS N43.17-2009 method,[12] a reference effective dose of 14.6 nSv per screening was calculated.
- *Bystander.* Dose rate to bystanders was calculated to range from up to 1,285 nSv per hour, assuming 180 screenings per hour.

[12] The ANSI/HPS N43.17-2009 standard, "Radiation Safety for Personnel Security Screening Systems Using X-Ray or Gamma Radiation," is available at the Health Physics Society website at http://hps.org/hpssc/index.html.

Procedures and Interlocks

JHU/APL considered several potential failure mechanisms that could result in X-ray overexposure to the person being screened or the bystanders and screeners. On the engineering AIT system used for exposure dose measurements, investigators verified through measurements that the X-ray source is activated only by the "scan" button and that the X-ray source will not power on if any of the panel doors are not completely closed. They also measured the X-ray fluence as zero at the end of the scan, which indicates that the X-ray beam is off. They verified that the key used to turn the AIT system on cannot be removed unless it is in the "off" position, indicating that there can be no power to the X-ray source unless the key is present and in the "on" position. Additionally, JHU/APL reviewed the AIT system documentation and determined that the AIT system design operates the X-ray tube at its maximum voltage. Thus, it cannot produce X-rays of a higher energy or a higher fluence than the design settings, and the AIT system interlocks limit the "beam on" time to 3 seconds; there is no risk of increased exposure time.

The NIST Report

The NIST report[13] describes radiation-exposure testing of the Rapiscan Secure 1000 Single Pose ATR (automatic target recognition) version (serial number 1041001, manufactured October 2010) in the laboratories of the Dosimetry Group at NIST.

Measurements

- *Person being scanned*
  — *Air kerma measurements* were made using a 10X5-1800 ionization chamber manufactured by Radcal Corporation.[14] This chamber was constructed with a polycarbonate wall (i.e., Lexan^{TM}) with a conductive graphite coating. The wall thickness was 3.175 mm (0.125 in.) corresponding to an areal density of 0.38 g/cm^2. This corresponds to an aluminum equivalent thickness of 1.4 mm. The active volume was 1,800 cm^3. The central collector was a cylinder centrally located in the sensitive volume of the detector with a length of 7.8 cm (3.0 in.) and diameter of 3.6 cm (1.4 in.) and 0.07 cm (0.028 in.) wall thickness.

    Measurements were made using the full vertical and horizontal raster

[13] Glover et al., *Assessment of the Rapiscan Secure 1000 Single Pose (ATR version) for Conformance with National Radiological Safety Standards*, 2012.

[14] Radcal Corporation, "10X5-1800," https://www.radcal.com/10x5-1800, accessed September 5, 2014.

scanning conditions. Measurements were made at a standard location representative of the exposure received by an individual, 100 cm above the floor midway between the entry and exit portals and 30 cm from the surface of the wall where the beam exits to the center of the ion chamber (Figure 6.2a). The ion chamber was orientated so that the incident beam was perpendicular to the long axis of the cylindrical detector. Measurements of air kerma were also taken at the ANSI-specified Reference Location representing the point of maximum exposure, but no closer than 30 cm to the surface where the beam exits, at a height of 185 cm above the floor, midway between the entry and exit portals and 30 cm from where the beam exits the front panel. The ionization chamber was calibrated using the M50 beam quality at the NIST X-ray calibration facility. This beam had a HVL of 1.04 mm of aluminum. The measured air kerma at the standard location was 47 nGy while at the maximum location 185 cm above the floor; it was 92 nGy when averaged over the area of the ion chamber.

— *HVL measurements* were made using the 1800 cc ionization chamber with the long axis oriented vertically and perpendicular to the beam. The Rapiscan was operated in an engineering mode with vertical translation of the X-ray assembly disengaged. The X-ray source remained at a fixed height. The horizontal collimator and rotating chopper were in place and operated normally such that the flying spot made a repeating horizontal trace. A collimator was placed outside of the X-ray assembly upstream of the aluminum absorbers. This restricted the horizontal dimensions of the raster scanned beam incident upon the aluminum absorber. Another circular collimator was placed between the aluminum absorbers and ionization chamber to intercept scattered radiation from the aluminum and to create conditions for narrow beam geometry (Figure 6.2b-c). No significant difference was found between the first HVL for the anterior and posterior units. The HVL was found to be 1.09 mm of aluminum.

- *Bystander.* Air kerma was measured at representative locations outside the inspection area with a RANDO phantom being scanned. Measurements were made using the 1800 cc ion chamber by averaging the charge collected over 20 scans occurring in a 5-minute interval. At many locations, the kerma was found to be less than 0.1 nGy per scan, the minimum detectable. At locations expected to have the highest kerma, based on results of a dose rate survey using a Technical Associates Neon-P8 probe, the kerma was found to range from 0.5 to 0.9 nGy per scan.

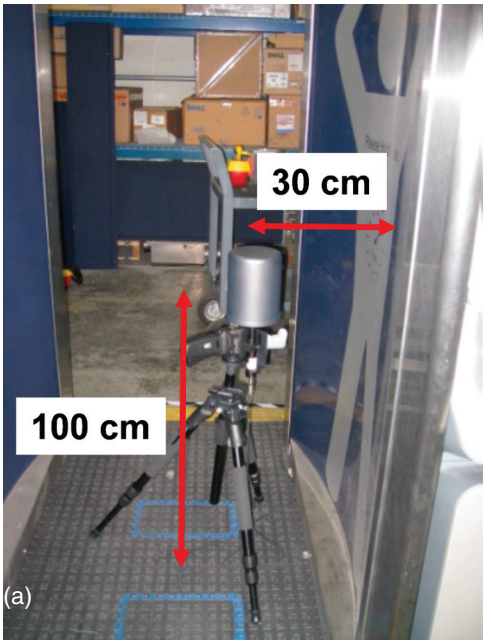

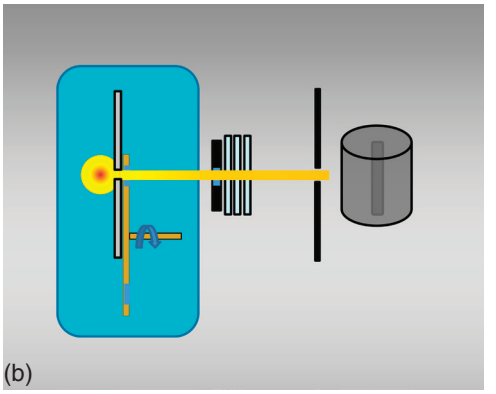

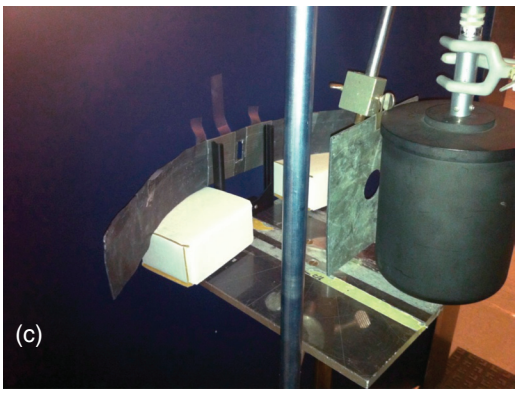

FIGURE 6.2 (a) Configuration of the 1800 cc ion chamber used by NIST to evaluate kerma. (b) Schematic and (c) photograph of the detector arrangement used by NIST to measure half-value layer. SOURCE: (a) American Association of Physicists in Medicine Task Group 217; (b) Tom Borak; (c) NIST.

Calculations

- *Person being scanned*
  — *Reference effective dose* was calculated using the ANSI N43.17 relationship. The result was 12.6 ± 0.8 nSv per screening at the position that resulted in the maximum kerma, near the top of the scan range. A more realistic reference effective dose, typical of potentially occupied spaces, was 9.23 nSv per scan (18.5 nSv per screen).

— *Effective dose* was calculated using the PCXMC Monte Carlo code that uses age dependent Cristy-Eckerman (geometric shape based) computational phantoms. This code uses the X-ray tube characteristics plus the "aluminum-equivalent filtration" to calculate the photon spectrum used to evaluate organ doses. The aluminum-equivalent filtration of 1.21 mm was obtained from the spectrum generator program in order to match the measured 1.085 mm of aluminum first HVL. The calculated effective dose for a properly positioned adult was 14.7 nSv. The effective dose for an adult ranged from 11.9 to 22.4 nSv, depending on positioning in the inspection area (10 cm from front panel of anterior unit to 10 cm from front panel of posterior unit). The effective dose to a standard 5-year-old child (19 kg, 109.1 cm tall, trunk thickness 15 cm) was 21 nSv when properly positioned in the scanning area.

- *Bystander.* Ambient dose equivalent to bystanders was calculated using conversion factor 0.85 Sv/Gy derived from ANSI N43.17, Figure C1, assuming an HVL of 1.1 mm of aluminum. Using the maximum kerma measured and assuming a workload of 180 scans per hour, the maximum ambient dose equivalent rate for bystanders was 276 nSv/hour.

Procedures and Interlocks

The NIST report did not indicate that potential failure mechanisms or verified safety interlocks were considered during the AIT system evaluation.

The AAPM Report

The aim of the AAPM report[15] was to utilize the expertise of the medical physics community to make independent, detailed measurements of the Rapiscan Secure 1000 single-pose system output. The goal was to make measurements on multiple commercial AIT systems, both at the factory and in the field (i.e., in AIT systems in actual use in an airport setting).

Measurements

- *Person being scanned*
  — *Air kerma* measurements were made using a 10X5-1800 ionization cham-

[15] AAPM, *Radiation Dose from Airport Scanners: Report of AAPM Task Group 217*, College Park, Md., 2013.

ber manufactured by Radcal Corporation.[16] This chamber was constructed with a polycarbonate wall (i.e., Lexan™) with a conductive graphite coating. The wall thickness was 3.175 mm (0.125 in.), corresponding to an areal density of 0.38 g/cm^2. This corresponds to an aluminum equivalent thickness of 1.4 mm. The active volume was 1,800 cm^3. The central collector was a cylinder centrally located in the sensitive volume of the detector with a length of 7.8 cm (3.0 in.) and diameter of 3.6 cm (1.4 in.) and 0.07 cm (0.028 in.) wall thickness.

Measurements were made on three AIT systems (1.5 SP systems) at the Rapiscan factory and three AIT systems at Los Angeles International Airport. Measurements were made at a standard location representative of the exposure received by the individual being screened. This was similar to the NIST study reviewed above, but the height is 91 cm above the floor, midway between the entry and exit portals, and 30 cm from the surface of the wall where the beam exits. The ion chamber was orientated so that the incident beam was perpendicular to the long axis of the cylindrical detector. The ionization chamber was calibrated using the M50 beam,[17] which has a HVL of 1.04 mm of aluminum. The average air kerma at the reference point for nine AIT systems was 46 nGy with a standard deviation of 3 nGy and a range of 40 to 52 Gy.

— *HVL measurements* were made both at the factory and at the airport. Measurements at the factory were made with a 6 cc thimble ion chamber suitable for mammography beams with the scanning mechanisms completely disassembled. This created a stationary beam defined only by the horizontal slit attached to the X-ray tube housing. Measurements were made with beam collimation before and after the aluminum absorber (Figure 6.3). Measurements at the airport were made with the 1800 cc ion chamber described above. For the factory bench top configuration, which did not include the AIT system faceplate, the HVL was 0.81 mm of aluminum. For the measurements at the airport, the HVL was 0.93 mm of aluminum.

- *Bystander.* An attempt was made to determine the dose to bystanders using both the 1800 cc chamber and a Fluke 451P survey meter. Measurements were made at the airport, with an anthropomorphic torso phantom in the AIT system. Locations expected to have maximum scattered radiation were measured by integrating the reading for 10 screenings, but no exposure above background was detected.

[16] Radcal Corporation, "10X5-1800," https://www.radcal.com/10x5-1800, accessed September 5, 2014.

[17] For a definition of M50 beam, see Table 3 in NIST Handbook 150-2D, *Calibration Laboratories: Technical Guide for Ionizing Radiation Measurements*, 2004.

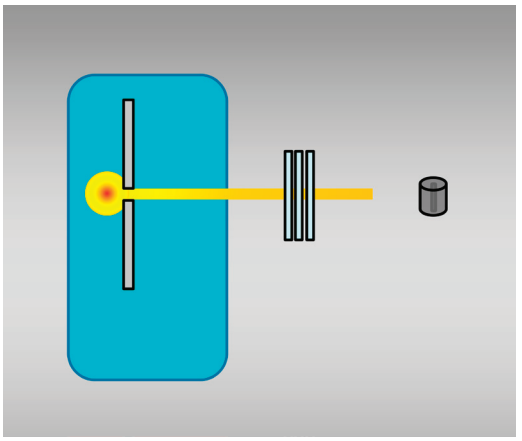

(a)

(b)

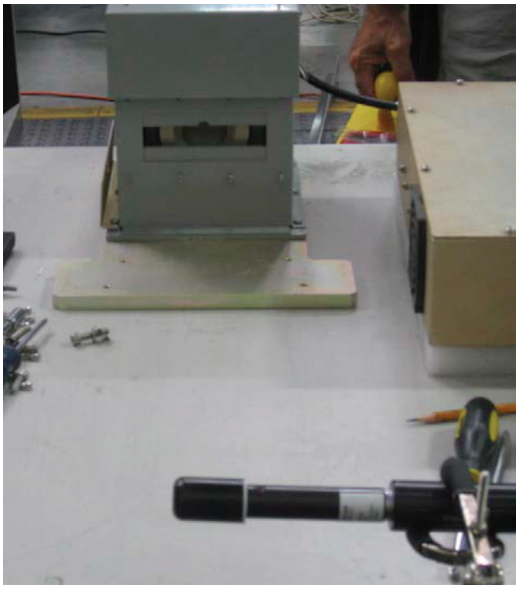

FIGURE 6.3 (a) Schematic and (b) photograph of the system used by AAPM to measure half-value layer. SOURCE: (a) Tom Borak; (b) American Association of Physicists in Medicine Task Group 217.

Calculations

- *Person being scanned*
  — *Reference effective dose* was calculated using the ANSI N43.17 formula. The result was 11 nSv per screening.
  — *Effective dose* and average absorbed dose for three organs were calculated for the standard man, a 10-year-old child (height 1.398 m, mass 32.4 kg), a Centers for Disease Control and Prevention (CDC) average U.S. adult, and a CDC 90th percentile adult using the PCXMC Monte Carlo code. The input data for beam quality was 50 kV, 20 degree anode angle, and 1 mm of aluminum total filtration to give the measured 0.93 mm of aluminum HVL. The results are summarized in Table 6.1.

- *Bystander.* No calculations were made for the bystander.

Procedures and Interlocks

The AAPM report includes potential failure mechanisms that could result in overexposure to the person being screened or the bystanders or screeners, including

TABLE 6.1 Effective Dose and Three Organ Doses Calculated Using PCXMC and Measured Kerma

Phantom	Effective Dose (nSv)	Skin Dose (nGy)	Breast Dose (nGy)	Thyroid Dose (nGy)
Standard man	11.1	40.4	20.0	21.0
10–year-old child	14.8	42.4	32.8	22.4
CDC average adult	10.4	41.0	19.2	20.0
CDC 90th percentile	9.4	40.9	18.7	18.2

NOTE: CDC, Centers for Disease Control and Prevention.

overvoltage of the X-ray tube and the vertical scan stopping during the screening and increasing the exposure dose to one area of the passenger. They did not verify design or interlocks that would prevent these scenarios but indicated that the power supply to the X-ray tube is already operating at its maximum voltage and that the image would be affected in a noticeable manner if the vertical or horizontal beam motion stopped.

The USAPHC Report

The primary focus of the USAPHC report was to estimate the effective dose per screening to individuals being scanned and to operators and others in the area of the AIT system using passive dosimeters. Dosimeters have response characteristics that are essentially independent of dose rate. The use of these passive dosimeters avoids the possible complications of high dose rate in the beam, which has been mentioned as a concern when the effective dose, *E,* is determined based on measurements of kerma, *K,* using a large ion chamber. The most sensitive passive dosimeters available for this type of measurement are aluminum oxide crystals, with the absorbed dose determined by optically stimulated luminescence (OSL).

A commercial dosimetry service was used for these measurements. The minimum dose reported by the vendor for OSL dosimeters used in this experiment was 10,000 nSv, and the resolution for higher doses was also 10,000 nSv. In order to produce data with nanosievert-per-screening resolution, the dosimeters were subjected to 93,105 screenings in a Rapiscan Secure 1000 single-pose system before being returned to the dosimetry service for reading. For each dosimeter, utilizing a system of physical filters over the OSL chip, the dosimetry service provided estimates of the deep dose equivalent (DDE), lens dose equivalent, and shallow dose equivalent. They also interpreted the readings behind the separate filters slightly differently, assuming that the ambient radiation field is a mixture of photon and

electron radiation, unless they were informed that it was a pure photon field. In this report, it was assumed that the true dose at each depth is between the values obtained assuming a pure photon field and a mixture of photons and electrons.

Measurements

- *Person being scanned.* In order to evaluate the radiation exposure produced by the Rapiscan Secure 1000 single-pose system, a physical phantom consisting of plastic containers of water was assembled on a wooden framework in the inspection area. OSL dosimeters were placed on the surface of the plastic containers facing the anterior AIT system unit at nine different locations representing specific locations on the body. These dosimeters do not provide a value for air kerma. In addition, measurements of HVL and kerma were made using a Radcal Model 10X5-1800 ion chamber. The results were as follows: a HVL of 1.646 (anterior unit) and 1.281 (posterior unit); kerma of 63 (anterior) and 55 (posterior) nGy.
- *Bystander.* Dosimeters were also placed at the outer edges of the shielding wings of the AIT systems and on a plastic framework just outside the inspection area in order to determine the dose to AIT system operators.

Calculations

- *Person being scanned.* The use of dosimeters on only the surface of the phantom did not provide the data needed to evaluate the average dose to each organ, as is required for evaluation of effective dose. Instead, it was assumed that the DDE, which estimates the dose at 1 cm depth, would overestimate E because most of the organs used to evaluate E are deeper than 1 cm and therefore receive less dose when exposed to the soft X rays used for scanning. Thus, the DDE was assumed to be an acceptable estimate of E.

  The average DDE to the nine locations on the water phantom was 49 nSv per screening using the photon-only algorithm to evaluate the OSL reading and 38 nSv per screening using the mixed-radiation algorithm. These values are somewhat higher than the values of E obtained in other studies, as expected, but confirm that the effective dose is substantially less than the 250 nSv limit. These results also indicate that measurements of kerma made with a large-volume ion chamber do not have serious errors due to the dose rate in the beam and possible recombination issues.

  The reference effective dose was calculated using the ANSI N43.17 formula and ion chamber data, resulting in E_{REF} equal to 33 nSv.

- *Bystander.* DDE measured outside the inspection area ranged from below the detection limit to 140,000 nSv with an average (counting below limit readings as 10,000 nSv) of 11,300 nSv for the 93,105 screenings. Per screening, this is a maximum of 1.5 nSv and an average of 0.12 nSv.

Procedures and Interlocks

The USAPHC report includes potential failure mechanisms that could result in overexposure to the person being screened or the bystanders or screeners, including overvoltage of the X-ray tube and the vertical scan stopping during the screening and increasing the exposure dose to one area of the passenger. They did not verify design or interlocks that would prevent these scenarios but indicate that the operator cannot adjust the power to the X-ray tube or the scan speed, so these failure modes cannot be caused by operators.

The FDA Report

In 2006 a Rapiscan Secure 1000 dual-pose AIT system (serial number S701201213, dated May 2001) was evaluated at the FDA's Center of Devices and Radiological Health.[18] The AIT system was evaluated against ANSI N43.17-2002, which was the current standard at the time. Tests confirmed that the tube anode potential was 50 kV, the same as the units later installed at airports.

Measurements

- *Person being scanned*
  — *Exposure (proportional to kerma)* was mapped using the solid-state detector and measured using a 10X5-1800 ion chamber manufactured by Radcal Corporation[19] mounted with its axis vertical and 30 cm from the face of the AIT system. Ion collection efficiency at the operating voltage of 300 V was evaluated by decreasing it to 270 V. This decrease resulted in only a 2.3 percent decrease in charge per scan, indicating that very little recombination was occurring at 300 V. The measured exposure per scan was 9,600 nrem, equivalent to kerma of 84 nGy at 30 cm from the face of the AIT system and 100 cm above the floor (the height of maximum kerma in the range of 0 to 180 cm). The kerma decreased to approximately 60 percent of this value at

[18] Cerra, *Assessment of the Rapiscan Secure 1000 Body Scanner for Conformance with Radiological Safety Standards*, 2006.

[19] Radcal Corporation, "10X5-1800," https://www.radcal.com/10x5-1800, accessed September 5, 2014.

heights of 0 cm and 180 cm, but a peak value of 2.5 times the value at 100 cm was found at 197 cm for alternate scans.
— *HVL* was determined using a R100B solid-state detector placed at 50 cm from the AIT system face and 90 cm above the floor. HVL was measured during normal scan operation. To ensure good (narrow beam) geometry, a 6.25 mm thick lead shield with a 25 mm diameter aperture was placed 35 cm from the face of the AIT system, in line between the X-ray tube and the detector. High-purity aluminum absorbers were placed on the detector side of the shield. The first HVL was found to be 1.1 mm of aluminum, but a second HVL was not determined.

- *Bystander.* The AIT system was monitored for leakage radiation using an array of eight Geiger-Muller detectors 5 cm in diameter. No detectable leakage was found over the majority of the AIT system surface, but leakage was found along a line up both sides and across the top of the unit, approximately 29 cm from the front edge of the unit. Using the 1800 cc ion chamber, the maximum leakage rate was found to be 75 nR (0.65 nGy) per scan. Radiation scattered from a phantom was measured with the 1800 cc ion chamber (calibrated for the M50 spectrum) at two locations, on the mid-plane of the phantom and on the plane of the AIT system back plate (100 cm above the floor and 30 cm outside the plane of the AIT system side surface in both cases). The scattered radiation was found to be 200 nR (1.8 nGy) per scan and 110 nR (0.96 nGy) per scan, respectively.

Calculations

- *Person being scanned*
  — Based on fitting the kerma as a function of distance (r) from the AIT system face to a $1/r^2$ relationship, it was concluded that the effective position of the X-ray source was 91 cm behind the face of the AIT system.
  — The first HVL was compared with data for HVL as a function of total filtration for a 50 kV spectrum, and it was determined that the effective filtration was 1.4 mm of aluminum, which was supplied to the PCXMC program for determining an effective dose of 23.6 nSv per frontal scan.
- *Bystander.* No results were provided.

Procedures and Interlocks

Not applicable.

SUMMARY OF MEASUREMENTS FROM REVIEWED STUDIES

The characteristics of the detectors used and the AIT system operation mode utilized to make the measurements reported in the reports reviewed in the previous sections are summarized in Table 6.2. The results are summarized in Tables 6.3 and 6.4.

The studies described above do not define how they reached margins of error for their estimates of average exposure. At a minimum, all of the studies deviate from standard statistical methods for describing the uncertainty in key parameters. A more detailed discussion on the statistics for some of the available studies is available in Appendix D.

TABLE 6.2 Characteristics of the Rapiscan Secure 1000 Measurements in the Reviewed Reports

Report	AIT System Type (Pose)	Kerma Detector	Kerma Scan	Kerma Calibration Spectrum	HVL Detector	HVL Scan	Leakage Detector
USAPHC	Single	1800 cc	Full	Unknown	1800 cc	Full	OSL
FDA	Dual	1800 cc	Full		Solid state	Full	1800 cc GM survey
JHU/APL	Single	1800 cc	Full	Unknown	1800 cc	Full	1800 cc GM survey
AAPM	Single	1800 cc	Full	M50	6 cc thimble 1800 cc	None full	1800 cc
NIST	Single	1800 cc	Full	M50	1800 cc	Line	1800 cc GM survey

NOTE: GM, Geiger-Muller tube; HVL, half-value layer; N/A, not applicable; OSL, optically stimulated luminescence.

TABLE 6.3 Summary of Rapiscan Secure 1000 Measurement Results in the Reviewed Reports

	K_{Std} (nGy) per Scan	K_{max} (nGy) per Scan	HVL_1 (mm of aluminum)
USAPHC	63	N/A	1.646 (anterior) 1.281 (posterior)
FDA	84	212	1.1
JHU/APL	41 ±1	N/A	1.18 (anterior) 1.63 (posterior)
AAPM	46 ±3	N/A	0.93
NIST	68 ±1	95 ±6	1.09

NOTE: HVL, half-value layer; N/A, not applicable.

TABLE 6.4 Effective Dose per Rapiscan Secure 1000 Screening Results in the Reviewed Reports

	Person Screened	
	E_{REF} (nSv)	E (nSv)
USAPHC	38-49[a]	NA
FDA	29	23.6[b]
JHU/APL	14.7	NA
AAPM	10.7	11.1
NIST	18.5	14.7

[a] Deep dose equivalent.
[b] Per anterior scan.

SUMMARY OF THE INTERLOCK TOPIC FROM REVIEWED STUDIES

Three of the reviewed studies considered the potential for accidental or deliberate malfunction of the Rapiscan Secure 1000 that could result in X-ray overexposure to the person being scanned, bystanders, or the operators. The USAPHC, JHU/APL, and AAPM reports indicate that increasing the voltage or current to the X-ray tube could result in increasing maximum X-ray energy or increasing the X-ray photon flux, either of which would result in an increased X-ray dose to the person being screened. All three studies concluded that the X-ray tube is operated at its maximum voltage and that the operator does not have access to increase the voltage or current to the X-ray tube. In addition, the JHU/APL report refers to an interlock documented in the AIT system manual that includes a photodiode measurement that reflects the X-ray photon flux and is interlocked to turn off the voltage to the X-ray tube if the flux increases from nominal by more than 17 percent or is more than 23 percent below nominal.

The USAPHC, JHU/APL, and AAPM reports also consider a malfunction where the vertical scan slows or stops, resulting in increased X-ray exposure to the person being scanned. Both the USAPHC and AAPM reports note that the operator cannot adjust scan speed and that if the beam stops, the image would be affected and noticed by the screener reviewing the images. The JHU/APL report review of the AIT system manual also notes that an interlock prevents the "beam on" time from exceeding 3 seconds, which would not result in overexposure to the person being screened. The JHU/APL report also notes that the Secure 1000 meets the ANSI N43.17-2002 standard requirement 6.2.2, "Subject exposure during a malfunction."

The JHU/APL group verified several other interlocks against potential malfunctions on a Secure 1000 engineering AIT system built for their measurements at the Rapiscan factory. They verified that the X-ray beam cannot be activated

without the power key present and in the "on" position, and the X-ray source does not remain on after the scan is complete. Additionally, the panel doors are interlocked, and the group verified that the X-ray source cannot be activated if the panel doors have been removed.

It is worth mentioning that Mowery et al.[20] investigated potential cyber physical threats and discusses software and hardware issues that could compromise the safety of the device. The paper (reviewed in the section below) makes the following observations: the PC controlling the AIT system could potentially be infected with malware; there is a bypass signal that disables the hardware interlocks; all safety interlocks can be bypassed by the software; and corrupt firmware could potentially deliver the whole radiation dose from a scan to a single random point on the body. The authors tried to cause the code on the PC to malfunction but failed.

In summary, none of the reports identified a potential AIT system malfunction that would result in overexposure to the person being screened or to the operator. For an overview of all the information this far, see Tables 6.5 and 6.6.

OTHER STUDIES AND CONSIDERATIONS

There have been additional studies and reports that examined the dose received during X-ray backscatter AIT screening. Three are described here in some detail. These studies are based on previous measurements and estimates of AIT system parameters.

The Dose from Compton Backscatter Screening

Retz et al.[21] report an effort to determine the effective dose per screening by estimating the number of scattered photons per pixel that must be detected to produce a usable image. They then estimate the number of photons that must be incident on the surface of the scanned individual in order to produce the needed number of scattered photons. Finally, they estimate the effective dose from the number of incident photons per pixel. In order to make these calculations, a great deal of information is required about the scanning AIT system, including the beam spot size, the photon spectrum, the beam scanning rate, the location and efficiency of the scattered photon detectors, and much more. However, most of this information was not available to the authors because it was considered proprietary by the

[20] K. Mowery, E. Wustrow, T. Wypych, C. Singleton, C. Comfort, E. Rescorla, S. Checkoway, J.A. Halderman, and H. Shacham, Security analysis of a full-body scanner, *Proceedings of the 23rd USENIX Security Symposium*, 2014, https://www.usenix.org/conference/usenixsecurity14/technical-sessions/presentation/mowery.

[21] P. Retz, R.L. Metzger, and K.L. Mossman, The dose from Compton backscatter screening, *Radiation Protection Dosimetry* 145:75-81, 2010.

TABLE 6.5 Summary of Rapiscan Secure 1000 Malfunction Investigations from the Reviewed Reports

Report	Potential Malfunction	Page	Conclusion	How Verified
JHU/APL	X-ray source activated by "on" switch without pressing "scan" button	36	X-ray source activated only by "scan" button	Verified by measurement on engineering AIT system
	X-ray source can be activated with power key removed	36	Key can be removed with power switch only in "off" position	Verified on engineering AIT system
	X-ray source can be activated for a scan with panel doors removed	37	Panel doors are interlocked, and AIT system will not scan if interlock is tripped	Verified on engineering AIT system
	X-ray beam fails to turn off at the end of a scan	41	No X-rays are emitted after a scan is complete	Verified by measurement on engineering AIT system
	X-ray tube can be operated with higher voltage resulting in higher X-ray photon flux and higher X-ray photon energies	38	X-ray tube is operated at the maximum voltage. Photodiode measures X-ray photon intensity and is interlocked if the flux varies from nominal by <–23% or +17%	Confirmed in AIT system documentation
	Vertical scan stops and X-ray exposure is focused on one area of the body for enough time to overexpose the passenger	40	AIT system interlock limits "beam-on" time to 3 seconds, which would not result in overexposure. Meets ANSI requirement N43.17.2002 6.2.2 "Subject exposure during a malfunction"	Confirmed in AIT system documentation
AAPM	X-ray tube can be operated with higher voltage resulting in higher X-ray photon flux and higher X-ray photon energies	13	Power supply cannot provide voltage higher than tube specification	No evaluation
	Vertical scan stops and X-ray exposure is focused on one area of the body for enough time to overexpose the passenger	13	If beam stops, the image would be affected and the operator would notice "immediately"	No evaluation

TABLE 6.5 Continued

Report	Potential Malfunction	Page	Conclusion	How Verified
USAPHC	X-ray tube can be operated with higher voltage or current resulting in higher X-ray photon flux or higher X-ray photon energies	2	Operator cannot adjust X-ray tube voltage or current	No evaluation
	Vertical scan speed is lower than set value and increases X-ray exposure, resulting in overexposure to the passenger	2	Operator cannot adjust scan speed	No evaluation

TABLE 6.6 Summary of Rapiscan Secure 1000 Malfunction Investigations from the Committee's Investigation of the Unit at NIST

Report	Potential Malfunction	Conclusion	How Verified
Committee	X-ray source stays on after emergency-off (EMO) button is pressed	X-ray source turns off when EMO button is pushed; vertical scan bar completes full travel to top or bottom	Verified by EMO activation on engineering AIT system
	X-ray source activated by "on" switch without pressing "scan" button	X-ray source only activated by "scan" button	Verified by measurement on engineering AIT system
	X-ray source can be activated with power key removed	Key can be removed only with power switch in "off" position	Verified on engineering AIT system
	X-ray source can be activated for a scan with panel doors removed	Panel doors are interlocked, and AIT system will not scan if interlock is tripped	Verified on engineering AIT system
	X-ray beam fails to turn off at the end of a scan	No X-rays are emitted after a scan is complete	Verified by measurement on engineering AIT system
	Vertical scan can be locked into a single position	Cannot initiate scan if vertical scan motor is turned off; can activate X-ray source with vertical scan locked only in engineering mode, which requires a separate password	Verified on engineering AIT system

AIT system manufacturers. In order to proceed with the calculations, the authors made estimates of the needed information based on a simple analysis of published images made by commercial scanning equipment (for pixel size and gray scale resolution) and on scanning AIT system size and shape (for detector size and location).

Assuming a 50 kV X-ray source, 2 mm square pixel size, a scan duration of 8 seconds, and a maximum of 3,200 photons detected per pixel, they estimated the effective dose of 0.880 nSv per screening, on the order of 20 times the value reported for measurements.[22] The authors point out that if the number of scattered photons per pixel is held constant, the effective dose is proportional to 1/(pixel area); similarly, if the pixel area is constant, the effective dose is proportional to 1/(scattered photon number per pixel). Thus, if they had assumed a pixel size of 4 mm square and a maximum of 640 photons, they would have predicted an effective dose of 44 nSv. Although they express the opinion that the difference between their calculation and measured results is likely due to recombination in the ion chambers used to measure air kerma, considering the tenuous nature of their estimates of pixel size and number of scattered photons it is perhaps more likely that the difference is due to differences between their estimated input values and those actually used in AIT systems. The authors also assert that if there is a failure of the scanning AIT system, the beam would have to be turned off within ~15 milliseconds to avoid exceeding an effective dose of 250,000 nSv. This conclusion is apparently based on a misinterpretation of effective dose. Effective dose is the sum of the average dose to each organ times that tissue's weighting factor. The average dose to an organ (e.g., the skin) is the same if 1,000 pixels receive a dose of 100 nGy or if 1 pixel in a population of 1,000 receives a dose of 100,000 nGy. Thus, the effective dose is relatively insensitive to scanning failures if the total beam time is unchanged.[23]

Letter to the Presidential Science and Technology Advisor

Four professors at the University of California, San Francisco, questioned the safety of the X-ray backscatter AITs in a letter to the presidential science and tech-

[22] They also estimate that an X-ray tube operating at 125 kV would require an anode current of 3.5 mA. An anode current of over 17 mA would be required to produce the same photon energy fluence for a tube operating at 50 kV. This is at least three times the anode current actually used, indicating that they have also overestimated the number of photons required.

[23] The effective dose will depend on which organs and tissues are in the beam when scanning fails. This is because different tissues have different weighting factors and occur at different depths in the body. However, the absorbed dose to the skin is much higher than that to deeper organs and, therefore, dominates the effective dose. Although other organs may or may not be in the beam if scanning fails, the skin will be, and thus the effective dose will be relatively insensitive to the beam location.

nology advisor.[24] Many of the concerns expressed in the letter deal with specific aspects of radiation biology or segments of the population with unusual sensitivity to radiation and are outside the scope of this report. However, some of the points raised relate to the physics of energy deposition by ionizing radiation and the definitions of quantities used to describe radiation exposure. These concerns bear, indirectly, on the accuracy and relevancy of measurements of exposure from AIT systems that have been reported previously and would also apply to the measurements made specifically for this report.

The letter asserts that because backscatter screening utilizes a small beam of relatively low-energy photons, it produces unique forms of damage. While it is true that these photons scatter from electrons involved in maintaining molecular structures, and thus break molecular bonds, the vast majority of the bonds broken by any dose of ionizing radiation are broken by the secondary electrons liberated by Compton scattering, or the photoelectric effect. A 28 keV photon will typically interact twice: once by Compton scattering transferring some of its energy to an electron, and then by photoelectric effect, transferring the rest of its energy to an electron and disappearing in the process. These two electrons produce on the order of 1,000 ionizations and many more excitations in the molecules they interact with. Similar ionizations and excitations are produced by the secondary electrons released by photons of any energy above a few hundred electronvolts. Although differences in the energy spectra of electrons produced by photons of different energy produce differences in the average distance between ionizations along the path of an electron, and this may produce small differences in the biological effectiveness of the radiation,[25] the interactions produced by the X rays used for backscatter screening are essentially the same as those produced by X rays used in many medical procedures.

The letter also asserts that because the energy delivered by an AIT system is mostly absorbed in the skin, it may produce an excessive risk of skin cancer. Most radiation exposures, including those delivered by inspection systems, do not deliver the same energy per mass to all parts of the body. However, the exposures received by the survivors of the nuclear bombs used in Japan, the source of most of the data used to set radiation protection limits, were nearly uniform. Radiation protection standards in the United States and internationally are based on maintaining the risk of lethal effects at an acceptable level based on an assumption of linear, no threshold, response. Assuming the linear response, the risk of a lethal effect in

[24] J.W. Sedat, Ph.D., Marc Shuman, M.D., David Agard, Ph.D., and Robert Stroud, Ph.D., Letter to Dr. John P. Holdren, Assistant to the President for Science and Technology, April 6, 2010, available at http://www.whitehouse.gov/sites/default/files/microsites/ostp/ucsf-jph-letter.pdf, accessed February 2014.

[25] A committee of the National Council on Radiation Protection and Measurements is currently attempting to determine the magnitude of such differences.

a nonuniformly irradiated individual can be evaluated by summing the risks of lethal events in each of the tissues of the body. The bomb survivor data provide the radiation sensitivity information needed to relate the average dose in an organ to the risk in that organ. Following this logic, the International Commission on Radiation Protection developed the quantity "effective dose," which is the sum of the average dose to each organ times the weighting factor for that organ, a version of the radiation sensitivity as described above. For example, the weighting factor for the skin is 0.01 and the sum of the weighting factors for all other organs is 0.99. It is thus possible to state:

> *An absorbed dose of 1,000 nGy to the skin only, or 10 nGy to each of the organs of the body (including the skin), results in the same effective dose, 10 nSv.*

In addition, a dose of 1,000 nGy to the skin only, or 10 nGy to each of the organs of the body, is expected to result in the same risk of a lethal event. If the irradiation is uniform, that lethal event could occur in any organ, but if the dose is limited to the skin, the lethal event has to occur in the skin. Thus, if the dose is limited to the skin, the risk of skin cancer is no more than the total risk of all cancers that would have occurred if the same effective dose was distributed uniformly.

Furthermore, the letter asserts that the correct quantity for measuring the exposure from an AIT system would be the photon flux. For some types of irradiation, there are significant advantages to the use of charged particle flux—or the equivalent, fluence rate—to characterize the exposure.[26] However, for photons over a wide range of energies, there is a simple relationship between fluence and kerma. If the photon spectrum and atomic composition of the target are known, the fluence can be calculated from the kerma, and the kerma can be calculated from the fluence. In the case of the X-ray backscatter AIT systems currently under consideration, the fluence is relatively low because it is limited by the X-ray tube voltage, the anode current, and anode composition, all of which are comparable to that used for a conventional dental X ray. However, the fluence (photons per area) is lower than in a dental X ray because an area is exposed to the beam for only a few thousandths of a second. One way to put the fluence or kerma into prospective is to estimate the number of radiation events in a cell of the skin. If one assumes that the photon spectrum produces an average linear energy of 5 keV/μm and that cells are 10-μm diameter spheres, the average dose to a cell hit by the radiation is 0.01 Gy, and at a kerma of 100 nGy, more than the kerma per screening produced by most AIT systems, the chance of a cell being hit is 10^{-5}—that is, about 1 in 100,000 of the cells in the skin are hit.

[26] International Commission on Radiation Units and Measurements, Report 85: Fundamental Quantities and Units for Ionizing Radiation, *Journal of the ICRU* 11(1):1-31, 2011.

Estimation of Organ and Effective Dose Due to Compton Backscatter Security Scans

Hoppe and Schmidt[27] calculated the organ and effective doses for four voxelized phantoms using published data for incident kerma and X-ray filtration. They did the calculations for a 34-year-old male, a 26-year-old female, an 11-year-old female, and a 6-year-old male, all using 2 mm cubic voxels. They used the air kerma values provided by the JHU/APL report cited above, 41 nGy, to determine the photon fluence. They estimated the photon spectrum using the SPEC78 software assuming the X-ray anode voltage of 50 kV, tube description, and filtration of 1.0 mm of aluminum, the minimum consistent with the ANSI/HPS N43.17-2009 reference effective dose method. They used the estimated photon spectrum to calculate energy deposited in the 1800 cc ion chamber used by JHU/APL in order to determine the kerma to fluence conversion, but they did not do additional calculations to test the accuracy of the photon spectrum. This process has been contested because the ion chamber was simulated as a water cylinder instead of air, which results in an overestimate by a factor of about 3 in the source fluence.[28] They found the effective dose for a person at 30 cm from the beam exit surface to range from 50 nSv for an adult male to 70 nSv for the 6-year-old male child. The other two phantoms, female adult and child, both showed 60 nSv per screening. They found the highest organ doses in the adipose tissue, ranging from 37.3 nGy in the adult male to 63.3 nGy in the female child, per scan. They present numbers for the skin, but the 2 mm pixel size averages the skin dose with that of adjacent tissue and introduces significant errors due to partial pixels in the field, so these numbers are not reliable.

Security Analysis of a Full-Body Scanner

Mowery et al. [29] performed a radiation dose assessment of the Rapiscan Secure 1000 by measuring the dose from a total of 4,033 scans totaling 6 hours and

[27] M.E. Hoppe and T.G. Schmidt, Estimation of organ and effective dose due to Compton backscatter security scans, *Medical Physics* 39:3396-3403, 2012.

[28] A revised estimate of effective dose to passengers was published in *Medical Physics*, based on comments from NIST (see J.L. Glover and L.T. Hudson, Comment on "Estimation of organ and effective dose due to Compton backscatter security scans" [Med. Phys. 39, 3396 (2012)], *Medical Physics* 39(9):5782-5787). However, the committee did not have access to the revised material while working on the report and have, therefore, not been able to comment on it.

[29] Mowery et al., Security analysis of a full-body scanner, 2014.

23 minutes using 21 InLight[30] dosimeters placed on a RANDO[31] chest phantom (neck-to-floor distance of 144 cm and source-to-detector distance of 66 cm). As the authors point out, the detectors are sensitive to the angular placement in the radiation field as well as the time from exposure to signal readout (fading). Following the manufacturer's suggested calibration procedures and using the dose equation algorithm,[32] the authors deduce an average DDE per scan to be 73.8 nSv, the average shallow dose equivalent (SDE) to be 70.6 nSv, and the eye lens dose to be 77.9 nSv with a DDE standard deviation of 7.5 and a coefficient of variation of 0.10. The authors do note the higher deep dose than shallow dose and suggest further investigations to account for this unexpected behavior. The authors conclude the paper by stating that the dose equivalent[33] measured is below the recommendation of 250 nSv per screening established by the applicable ANSI/HPS standard and that a person would have to undergo approximately 3,200 scans per year to exceed the standard's annual exposure limit of 250,000 nSv/year. It is also worth mentioning that DDE and SDE are operational quantities used in radiation protection for external radiation. DDE is defined as the dose equivalent at a tissue depth of 1 cm and is not an assessment of the dose equivalent to organs and tissues distributed throughout the entire body; therefore, it should not be used as a surrogate for effective dose received by airline passengers from bilateral scans during a backscatter screen.

FINDINGS AND RECOMMENDATIONS ON EXPOSURE AND DOSE

Individual Being Screened

Key Finding: Previous radiation dose studies employed different methodologies and instrumentation to estimate the dose delivered by Rapiscan Secure 1000 X-ray backscatter AIT systems. The reports reviewed by the committee generally agreed that the effective dose per screening to an average passenger

[30] See Landauer, Inc., "Dosimeters," http://www.landauer.com/Industry/Products/Dosimeters/Dosimeters.aspx, accessed October 9, 2014. These are aluminum oxide (Al2O3:C) crystals functioning through optically stimulated luminescence (OSL).

[31] The Phantom Laboratory, "RANDO® Phantoms," http://www.phantomlab.com/products/rando.php, accessed October 9, 2014.

[32] The shallow dose equivalent (SDE) and deep dose equivalent (DDE) are obtained from a proprietary algorithm using a combination of ratios of the OSL dosimeters behind each of the filters.

[33] The authors did not measure HVL in aluminum or air kerma and thus could not determine the ANSI reference effective dose for the scanning unit. The exact definition of DDE and the extent to which it represents effective dose to the passenger is not clear. Estimating DDE for soft X rays emitted from a tube operating at 50 kV may be problematic because the X rays are not mono-energetic, and most of the incident photons are less than 35 keV.

is about a factor of 10 below the limit of 250 nSV per screening, the dose set by ANSI/HPS N43.17-2009.

Kerma Measurements

Finding: In most cases, kerma was measured with a large cylindrical ion chamber with a relatively thick wall that was calibrated for the M50 NIST spectrum. This chamber averages the kerma over a relatively large area, and the distance between the face of the AIT system and the effective center of the ion chamber is not known exactly. This may have resulted in a small error relative to the kerma at a specified point, the quantity needed to calibrate effective dose calculations.

Recommendation: During kerma measurements, one should use a parallel-plate ion chamber with precisely known effective center and a relatively small diameter.

Half-Value Layer Measurements

Finding: In most cases, the HVL was measured using a large cylindrical ion chamber with relatively thick walls (3 mm air equivalent plastic) and varying degrees of control of scattered radiation. In other cases, detectors with unknown cover thicknesses were used. These measurements may misrepresent the first HVL because of attenuation of the lowest energy photons by the wall of the detector or detector cover. None of the measurements included the second HVL.

Recommendation: One should measure first and second half-value layers (HVLs) using a thin-window, parallel-plate ion chamber with effective shielding to ensure narrow beam geometry. The increments of aluminum thickness should be small compared to the HVL in order to maximize the information for comparison with Monte Carlo simulations of attenuation using different photon spectra.

Depth Dose Distribution Measurements

Finding: Depth dose distribution with a resolution of approximately 25 μm in tissue is needed to ensure that the dose to critical cells of the skin in scanned individuals is not being underreported and to provide a test of the photon spectrum used to calculate the effective dose. None of the reports provided the depth dose distribution in tissue in the broad beam geometry.

Recommendation: One should measure depth dose distributions in tissue using a thin-window, parallel-plate ion chamber. Embed the ion chamber in a tissue-equivalent phantom large enough to simulate broad beam geometry, and use tissue-equivalent absorbers with 25 μm depth increments.

Dose Outside Inspection Area Potentially Affecting Bystanders

Outside the inspection area, the dose rate and the photon energy are very low, so using the correct detector is important. Detectors are typically calibrated for a specific photon spectrum—for example, M50—which is expected to approximate the spectrum of the radiation source being measured. However, the average energy of the photon spectrum scattered from a person being scanned will be less than the average energy of the incident spectrum. As a result, an ion chamber calibrated to detect radiation from the incident spectrum may not accurately detect radiation scattered from a person being screened.

Key Finding: Measurements of radiation outside the inspection area have generally been made with detectors that are calibrated for X-ray energies higher than those scattered from a passenger being scanned by the Rapiscan Secure 1000 AIT system. As a result, the detectors may indicate a lower dose than is actually present. The detectors have sometimes failed to distinguish a signal from the background radiation.

Finding: Dose measurements outside the inspection area were often made with radiation survey instruments using pressurized ion chambers or other detectors with unknown, but likely very low, response for photons below 30 keV. Because most of the dose outside the inspection area is probably due to scattered photons, and because the peak of the scattered photon spectrum is well below 30 keV, such detectors may indicate a significantly lower dose than is present.

Recommendation: Dose per screening outside the inspection area should be measured with a thin-window ion chamber or other detector with relatively uniform response to photons down to approximately 10 keV.

Based on all the detailed recommendations from this chapter, it is possible to state a key recommendation.

Key Recommendation: To estimate X-ray radiation exposure outside the inspection area, measurements should be made with detectors calibrated for X-ray energies below the maximum for the advanced imaging technol-

ogy (AIT) system's X-ray tube and for the radiation levels expected. Use of detectors that are appropriate for other applications but not ideal for measuring dose in a X-ray backscatter AIT system may result in inaccurate measurements.

As discussed in Chapter 7, for both AIT systems the committee studied, the radiation measured outside the inspection area by the National Research Council subcontractor was found to be so low as to be statistically indistinguishable from zero (7.3 ±8.0 nGy) when using appropriate detectors calibrated for the correct energies.

7

Measurements, Dose Calculations, and System Design for X-Ray Backscatter Advanced Imaging Technology Systems

This chapter contains the measurement procedures developed by the committee, including half-value layer (HVL) measurements, percent depth dose (PDD) measurements, air kerma measurements, and determination of the kerma per screening outside the inspection area. After the section describing the measurement procedures there follows the measurement results acquired by the National Research Council (NRC)[1] subcontractor for the Rapiscan Secure 1000 advanced imaging technology (AIT) system and the AS&E SmartCheck AIT system and the committee's review of each system's design. The next section makes use of the measured data for the dose computations. The dose computations include descriptions of the X-ray source term; features of the reference AIT system used; validation of Monte Carlo sampling procedures; description of the passenger irradiation geometry, including phantoms; and dosimetry results for standard screening conditions. Additional information extracted from the dose computations include variations in X-ray tube voltage, dose to radiosensitive cells in the skin, and failure mode analysis. The chapter concludes with findings and recommendations.

Evaluation of effective dose from an unknown X-ray source, such as an AIT scanner, can be accomplished by measuring HVL, depth dose, and air kerma and then using the HVL and depth dose data to calculate the photon spectrum. With the photon spectrum and a suitable mathematical model of the person being scanned,

[1] Effective July 1, 2015, the institution is called the National Academies of Sciences, Engineering, and Medicine. References in this report to the National Research Council are used in an historic context identifying programs prior to July 1.

Monte Carlo calculations can be used to determine the organ dose per incident photon, and the effective dose per photon can be calculated using organ weighting factors. Finally, the measured air kerma can be used to determine the number of incident photons and, therefore, the effective dose. The ANSI reference effective dose (E_{REF}) is determined through a simple mathematical relationship[2] based on measurements of the HVL and air kerma.

MEASUREMENT PROCEDURES

The National Research Council (NRC) subcontractor David Hintenland, Advanced Laboratory for Radiation Dosimetry Studies, J. Crayton Pruitt Family Department of Biomedical Engineering, University of Florida, performed field measurements of HVL, PDD, air kerma, and dose outside the scanning area for two AIT systems: (1) the AS&E SmartCheck-HT dual-pose system being evaluated at the Transportation Security Administration (TSA) Systems Integration Facility (TSIF) and (2) a Rapiscan Secure 1000 single-pose system located at the National Institute of Standards and Technology (NIST). Both systems operate with an applied voltage of 50 kV, although they use different X-ray tubes, anode currents, and scan mechanisms and scan rates.

Measuring Half-Value Layer

Background

The HVL in aluminum provides a common description for characterizing the spectrum of an X-ray beam. With the addition of aluminum, the lower-energy components of the X-ray spectrum are preferentially attenuated and create a difference between the first and second HVLs. Measured values of the first and second HVLs were utilized to characterize the energy spectrum of the AIT systems. The attenuation curve in aluminum was evaluated in increments as small as 0.05 mm of aluminum (mm Al) across the expected range. This not only permitted the first and second HVLs to be extracted from the data but also provided a continuous curve of the attenuation in aluminum against which the X-ray spectrum of the simulated X-ray source term could be precisely matched.

[2] Formulas for calculating E_{REF} are provided in Section 6.1.3 of American National Standards Institute/Health Physics Society (ANSI/HPS), "Radiation Safety for Personnel Security Screening Systems Using X-Ray or Gamma Radiation," ANSI/HPS N43.17-2009, 2009, http://hps.org/hpssc/index.html.

Experimental Approach

HVL measurements were made utilizing a Keithley model 96035b 15 cc parallel-plate ion chamber interfaced with a Univision electrometer from PTW.[3] The ion chamber has two windows. The thinner window, 32 mg/cm^2 or 320 μm tissue equivalent (mammography focus), was utilized for characterizing the HVLs of the expected, relatively soft X-ray spectrum generated by the AIT systems. The determination of HVL requires a series of measurements of beam intensity performed with increasing aluminum attenuator thicknesses relative to the unattenuated beam intensity. An absolute calibration of the chamber is not critical to the measurement results. The chamber was, however, calibrated to a molybdenum/molybdenum target/filter mammography X-ray standard at 28 kV.

To obtain improved signal-to-noise ratio for this set of measurements, both types of AIT systems were operated in a partially fixed scanning mode; in this mode, only one AIT system module (either the anterior or the posterior) is operating for a series of measurements. The mode is partially fixed, meaning that the vertical movement of the X-ray source is stopped but the horizontal is not; hence, only a line, and not an entire area, is scanned by the pencil beam. The service/engineering mode was utilized to perform measurements with the X-ray tube raised to a fixed vertical location while the beam continued to scan in the horizontal direction. Although the X-ray source and associated beam-forming equipment generates a pencil beam, the continual horizontal scanning at a fixed vertical location results in irradiating a vertical line or band across the face of the ion chamber. Although only a portion of the chamber is exposed, the same portion is exposed for each attenuator thickness, and all measurements are referenced to the same geometry exposure with no attenuator present. A series of at least three replicate measurements were made for each attenuator thickness under these conditions. Six replicate measurements were made for an aluminum attenuator thicknesses of less than 0.6 mm, where the relative change in exposure is expected to be the greatest due to the fact that the thin attenuators affect the low-energy portions of the X-ray spectrum.

The coordinate system for describing measurements on the AIT systems is set up along the central medial (longitudinal) axis of a subject undergoing the scanning process, which was defined as being collocated with the geometric central axis of the AIT system. This position is designated in the Cartesian coordinate system as x = 0 cm, y = 0 cm, where x is the dimension toward or away from the anterior X-ray source (−x is closer to the source), and y is left or right as the screening subject faces the anterior source (−y is to the left, +y is to the right) (Figure 7.1).

For the HVL measurements, the 15 cc parallel-plate ion chamber (approximately 4 cm in diameter) was centered in the AIT system halfway between the

[3] See the PTW Freiburg GmbH website at http://www.ptw.de, accessed January 13, 2015.

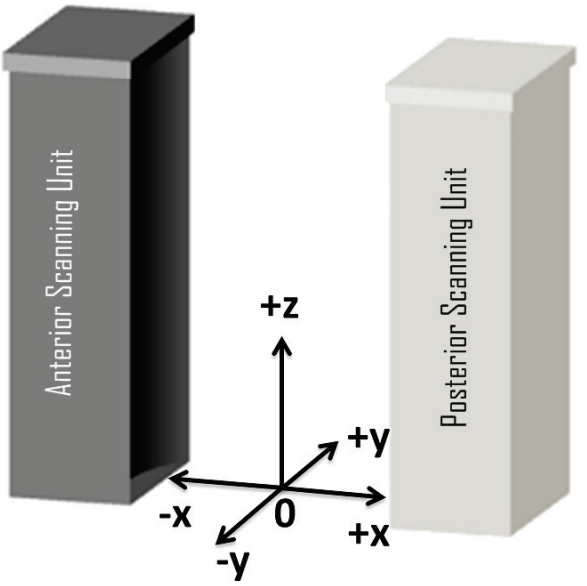

FIGURE 7.1 The coordinate system for describing measurements on the AIT systems. X is the dimension toward or away from the anterior (dark gray) X-ray source (–x is closer to the source), and y is left or right as the screening subject faces the anterior source (–y is to the left, +y is to the right), +z is pointing upward, with z = 0 at the base of the AIT system modules.

entrance and exit portals, at x = 0 cm, and centered between the anterior and posterior[4] (or transmission detector), at y = 0 cm. The vertical position of the chamber was adjusted by trial and error to correspond with the position of the X-ray beam and correspondingly provides the greatest signal response by having the maximum exposed chamber area. The beam was further collimated by utilizing a sheet of lead that was custom fitted to the chamber and located behind the aluminum attenuators to reduce scatter contributions from the aluminum attenuators and to provide narrow beam geometry.

[4] This is the case for the Rapiscan Secure 1000; for the AS&E AIT system, the manufacturer's suggested position (footprints) were used.

Measuring Percent Depth Dose

Background

Percent depth dose (PDD) profiles are a relative measurement of dose as a function of depth into tissue.[5] PDD is defined as a function of depth in tissue maintaining a constant source-skin distance (SSD), although it is more practical to directly measure the tissue-maximum ratio (TMR), where the reference depth remains constant, and subsequently transform the acquired data to the PDD. One objective for the PDD measurements is to elucidate the skin dose that may be delivered to radiobiologically sensitive layers of the skin such as the epithelial layer. Another is to provide relative PDD depth profiles that can be used to validate the computationally determined radiation doses to the radiobiologically sensitive regions of the skin. The shallow skin layers for which these measurements are desired present technical challenges due to the low energy of the X-ray sources of interest, requiring that thin layers of tissue-equivalent materials be produced and that measurements be made using an ion chamber with a very thin window in order to minimize secondary electron production prior to the X-ray beam's reaching the sensitive volume of the chamber. To minimize the effects of dose buildup at these relatively low energies, it is important to utilize an ion chamber that has a very thin (and therefore fragile) entrance window. Such chambers have small volumes (a few cubic centimeters), however, so that the entrance window does not break from the detector being moved and handled, with resulting low sensitivity. The NRC subcontractor selected a Capintec PS-033 parallel-plate ion chamber to perform these measurements. This chamber provides a thin mylar window (0.5 mg/cm^2 or 5 μm tissue-equivalent thickness) and a relatively large sensitive volume (4.9 cm^3) for a chamber of this type with a diameter of 2.5 cm and a total thickness of 1 cm. The PS-033 parallel-plate ion chamber was integrated with a PTW Unidose electrometer for this set of measurements. Because the PDD measurement is a relative measurement, the chamber was not calibrated ahead of time, although the response at 50 kV was well characterized by the NRC subcontractor and compared to other parallel-plate ion chambers used in this study.

To develop the PDD curves, it is necessary to have a tissue-equivalent material of appropriate thicknesses. For a 50 kV X-ray source with little filtration, quite thin layers of tissue-equivalent material are required. The NRC subcontractor, therefore, fabricated custom-made layers of tissue-equivalent materials and a tissue-equivalent phantom-block in which the thin-window ion chamber was embedded. The lateral extent of the phantom-block is 10 cm × 10 cm with an additional 5 cm of tissue-equivalent material behind the chamber in order

[5] The dose values are divided by the maximum dose.

to capture the scatter contributions to the PDD. The subcontractor fabricated a series of tissue-equivalent material thicknesses as thin as 25 μm and up to 10 mm thick.[6] The precise thickness of the tissue-equivalent slabs were individually determined by measurements performed with an analog dial indicator with 25 μm increments.[7] The tissue-equivalent materials were evaluated against several other commonly used phantom materials, including BR12 (a breast tissue-equivalent material having a lower density) and acrylic (a plastic having a higher density but lower attenuation coefficient), at 50 kV in the NRC subcontractor's laboratory. The materials produced performed as expected relative to these benchmarks and were determined to have a density of 1.04 g/cm^3, matching that of skin and soft tissue. These materials permitted the development of a PDD from 0 to over 60 mm with high spatial resolution.

Experimental Approach

The general procedure utilized for performing the PDD measurements closely followed the procedure used for performing the HVL measurements where the tissue-equivalent material was used in place of aluminum sheets and with no lead collimation for the ion chamber. In order to maximize the signal-to-noise ratio for this set of measurements, the AIT system was operated in a partially fixed scanning mode (described in detail under the section "Half-Value Layer Measurements"). This was particularly important for this set of measurements because of the small physical dimensions of the thin-window chamber. A series of at least three replicate measurements were made for each attenuator thickness under these conditions.

An additional set of PDD measurements was made using the Keithley model 96035b 15 cc parallel-plate ion chamber with the low-energy (32 mg/cm^2) window oriented toward the beam for comparison with the PS-033 chamber. While the 15 cc chamber has a relatively thin window at 32 mg/cm^2, it is significantly thicker than the 0.5 mg/cm^2 window of the PS-033 chamber.

The thin-window parallel-plate ion chamber (approximately 2.5 cm in inner diameter) was centered in a 10 cm × 10 cm block of phantom material with 5 cm of backscatter material behind it. The center of the chamber was positioned at x = 0 cm and y = 0 cm. The vertical position of the chamber was adjusted by trial and error to correspond with the position of the X-ray beam that correspondingly

[6] The committee is not familiar with any previous study that has successfully measured PDD curves at these low energies, in part because they call for very thin layers of tissue-equivalent materials to be fabricated.

[7] The University of Florida has extensive experience with the development and fabrication of tissue-equivalent materials and developed these materials specifically for this application and in order to provide empirical data that could be used for the verification of the parallel computational effort.

provided the greatest signal response by having the maximum exposed chamber area. This was determined to occur for the center of the chamber at z = 19.5 cm.

In order to measure the exposure as a function of tissue depth, the desired thickness of tissue was placed directly in front of the ion chamber. A 1 cm air gap was maintained between the tissue-equivalent materials and the chamber to prevent inadvertent contact and potential damage to the thin window of the ion chamber. Note that the geometry selected here differs from the usual approach to measure PDD because of experimental practicality. To assure accuracy, the detector block was not moved back with each additional layer of tissue but was kept at a fixed location. The data were then transformed to the PDD by the Mayneord factor,[8] which in this case simplifies to a correction using the inverse square law; because the beam is broad, distances are large compared to the tissue thicknesses, and the scatter phantom area is fixed.

Measuring Air Kerma

Background

Air kerma measurements provide an absolute measure of the air kerma (in Gy) at discrete locations in the AIT system X-ray field. These measurements provide an absolute reference against which any computational efforts can calibrate their calculations in order to predict dose to the scanned subject. In contrast to the measurements performed for HVL and PDD, the measurement of air kerma is performed with the AIT system operated in its normal scanning mode. In this mode of operation, the X-ray exposure is quite low, and it is most appropriate to use a large-volume parallel-plate ion chamber to obtain the best possible signal-to-noise ratio. Corrections for temperature and pressure, relative to the chamber calibration conditions, are applied to ensure the precision of these measurements.

Experimental Approach

Air kerma measurements were performed utilizing a Keithley model 96020C 150 cc parallel-plate ion chamber in conjunction with a PTW Unidose electrometer. The ion chamber was previously calibrated using an H60 spectrum.[9] Due to the time limitations of this study, it was not possible to perform a chamber calibration

[8] W.V. Mayneord and L.F. Lamerton, A survey of depth dose data, *British Journal of Radiology* 14:255, 1941.

[9] The H60 spectrum, formed at NIST by filtration using 4 mm Al and 0.61 mm of copper, was used for air kerma calibrations.

using an M50[10] spectrum until after all the measurements were done on both X-ray backscatter AIT systems. However, the post calibration allowed for a correction of all affected data so that no incorrect values were used or included in this report. The M50 is expected to be most representative of the beam for both the AS&E SmartCheck and the Rapiscan Secure 1000 AIT systems that were tested.

Measurements for the air kerma were performed with the electrometer operated in integrating mode over the course of a normal screening subject scan. The total charge (picocoulombs) was recorded for each case. The charge was subsequently converted to air kerma using the appropriate chamber calibration factor and making air temperature and pressure corrections relative to the chamber's calibration conditions.

For each of the air kerma measurements, the 150 cc parallel-plate ion chamber was centered at x = 0 cm, y = 0 cm, with the vertical dimension (z) referenced to z = 0 cm at floor level. Air kerma was measured at four vertical locations: z = 32 cm, z = 120 cm, z = 150 cm, and z = 202 cm. The measurement locations were designed to roughly evaluate any variations in beam intensity as the beam scans vertically. Because of the low intensity of the scanning beam, a series of 10 individual measurements were recorded at each vertical location.[11]

Determination of the Kerma per Screening Outside the Inspection Area

Background

In view of the unique conditions of low X-ray energy and exposure times on the order of a few seconds, typical low-dose-rate survey instruments are limited in their ability to accurately respond to these fields. In order to accurately determine the exposure outside of the inspection area, the NRC subcontractor utilized a large-area parallel-plate ion chamber (Keithley model 96020C, 150 cc) interfaced with the PTW Unidose electrometer.

In order to accurately account for the scatter contributions from the passenger being screened, a scatter medium that simulates the presence of the human as a scatter source must be included. A variety of scatter sources were considered. The University of Florida has previously constructed a series of anthropomorphic phantoms representing a variety of human anatomies. The full human-sized phantom is constructed of tissue-equivalent materials designed to mimic the response of

[10] The M50 spectrum, formed at NIST by filtration using 1.07 mm Al, was used for air kerma calibrations.

[11] Note that there is a platform that can be inserted into the screening system that screening subjects would normally stand on that is 14 cm tall at its midpoint. Thus, the bottom of subjects' feet would be at z = 14 cm when the platform is used. The platform was removed for the measurements performed in this study.

tissues in the low-energy X-ray range and includes a realistic internal anatomy. The phantom development and details are available in the published literature.[12] These phantoms have been utilized extensively for radiation dosimetry studies of clinical X-ray systems. They are fabricated as physical analogs to selected phantoms in the Computational Phantom Library, accurately reproducing the anatomy and incorporating appropriate tissue-equivalent materials.

Dose outside the screening area may arise from two sources: radiation scattered from scanned subjects to the area outside the scanning region and X-ray leakage from the X-ray tube housing area.

Experimental Approach

For each set of measurements, a large-area Keithley model 96020C 150 cc parallel-plate ion chamber interfaced with a PTW Unidose electrometer was used. The electrometer was utilized in integration mode[13] for each of these measurements. A Fluke 451B survey ion chamber was also positioned in close proximity to the parallel-plate ion chamber and was operated in integration mode utilizing the thin mylar window.

Measurements for the air kerma were performed with the electrometer operated in integrating mode over a repeated series of normal screening subject scans. Measurements were performed at several locations outside of the subject inspection area to individually quantify the contributions from each of these sources, as described below. The measurements integrated over at least 40 scans performed at each of the measurement positions. The total charge (picocoulombs) was recorded for each case and divided by 40; in this way, smaller charges could be measured. The charge was subsequently converted to air kerma using the appropriate chamber calibration factor and including air temperature and pressure corrections relative to the chamber's calibration conditions.

A measurement location on the backside of the scanning unit was selected to evaluate leakage radiation that may be exiting the unit in that direction. The 150 cc parallel-plate ion chamber was positioned against the rear exterior of the AIT system assembly at a height of z = 150 cm, centered on the path that the X-ray source travels while vertically scanning.

Again, a series of 40 normal subject-screening scans were performed while the detection systems continuously integrated. Here, an anthropomorphic phantom

[12] J.F. Winslow, D.E. Hyer, R.F. Fisher, C.J. Tien, and D.E. Hintenlang, Construction of anthropomorphic phantoms for use in dosimetry studies, *Journal of Applied Clinical Medical Physics* 10(3):195-204, 2009.

[13] Integration mode accumulates charge over a specified time and can be more sensitive, albeit slower, than the rate mode, which detects the current.

representative of an adult male was used for this purpose. The region from the bottom of the pelvis to the top of the head was used as the scatter source. The phantom was positioned on a stool such that the base of the pelvis was located at z = 74 cm and the top of the head was z = 170 cm. The phantom was positioned such that the center of the longitudinal axis of the phantom was centered in the AIT system at x = 0 cm, y = 0 cm.

The parallel-plate ion chamber was positioned at the two positions along the edge of the AIT system exit on the side toward the operator position. The detector was centered at a height z = 120 cm for each scatter measurement, essentially even with the midpoint of the vertical extent of the phantom. The lateral positions were characterized by x = 0 cm, y = −66 cm, and x = −27 cm, y = −66 cm.

AS&E SMARTCHECK SYSTEM MEASUREMENT RESULTS AND SYSTEM DESIGN

Under the direction of the committee, the NRC subcontractor made measurements on the AS&E SmartCheck (Serial No. 1004) AIT system using the same protocol used for the Rapiscan Secure 1000. The AS&E SmartCheck AIT system has not been approved by TSA for airport deployment yet; thus, the system inspected by the committee may not be the final version that may be deployed in airports in the future.

Half-Value Layer Results

Measurements of HVL were made at a fixed height using a SmartCheck software command that caused the tube head to come up to a fixed height and operate for the 3 seconds required for a normal scan. This mode of operation requires a password that would be available only to maintenance personnel. The vertical position of this beam was z = 19.5 cm (with x = 0 cm and y = 0 cm). HVL measurements provided highly reproducible data and high resolution of spectral hardening with increasing thicknesses of aluminum attenuators. The data permit not only the extraction of a first and second HVL but also a detailed attenuation curve as a function of aluminum filter thickness that can be used to refine estimates of the incident X-ray spectrum for computational dose determination. Aggregate measurements of the HVL and associated uncertainties are tabulated in Table 7.1 and

TABLE 7.1 Half-Value Layer Measurements for the AS&E SmartCheck

Aluminum Thickness (mm)	Exposure Measurement (pC)	Uncertainty (pC)
0.0	5.52	0.06
0.1	5.15	0.08
0.2	4.70	0.13
0.3	4.47	0.06
0.4	4.16	0.10
0.5	3.92	0.04
0.6	3.65	0.03
0.7	3.39	0.04
0.8	3.19	0.04
0.9	3.04	0.04
1.0	2.90	0.02
1.5	2.31	0.02
2.0	1.87	0.03
2.5	1.53	0.03
3.0	1.28	0.02
3.5	1.11	0.02
4.0	0.97	0.01
4.5	0.82	0.01
5.0	0.71	0.02

NOTE: Each measurement is the average of at least three measurement scans. The uncertainty represents the observed standard deviation in the replicate measurements for each aluminum thickness. pC, picocoulomb.

graphically illustrated in Figure 7.2. The specific values that are identified as the first and second HVLs are 1.1 and 1.7 mm Al, respectively.[14]

Percent Depth Dose Measurements

The PDD measurements are tabulated in Table 7.2 for the PS-033 thin-window (0.5 mg/cm^2) 4.9 cm^3 chamber and illustrated graphically in Figure 7.3.

Again, a second set of PDD data was collected using the larger 15 cc parallel-plate ion chamber with a 32 mg/cm^2 window thickness. A comparison of the response for the two chambers is illustrated in Figure 7.4.

For this AIT, standard deviations for each set of exposure measurements were

[14] The high spatial resolution of the HVL data for thin layers of aluminum will permit the low-energy components of the X-ray beam to be incorporated into any computational candidate spectrum. Thus, the complete aluminum attenuation curve can provide improved fitting of the X-ray spectrum compared to previous models that incorporated simply the first, and sometimes second, HVL. This process and the effects on the PDD simulation process are discussed in more detail in the "Measuring Percent Depth Dose" section.

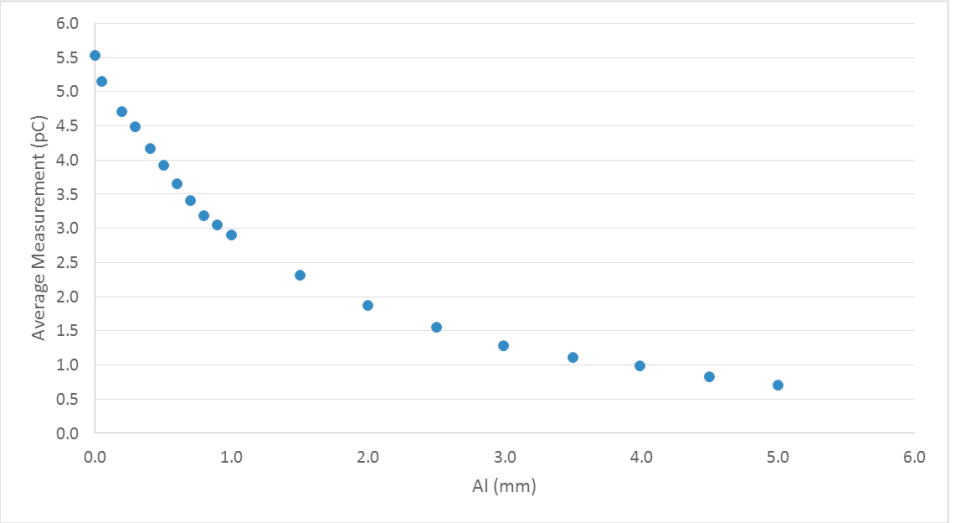

FIGURE 7.2 High-value layer measurements as a function of aluminum thickness for the AS&E SmartCheck. Error bars are not shown since they are approximately the size of or smaller than the symbols.

calculated based on the replicate data set and averaged less than 2 percent of the mean value, the largest being 4.2 percent for the thin-window (0.5 mg/cm^2) 4.9 cm^3 chamber. For the 15 cc chamber, the standard deviation for each set of exposure measurements averaged less than 1 percent of the mean value with the largest being 1.5 percent.[15]

It is important to point out here why extra efforts were taken to acquire extremely high-resolution PDD data. Because concerns have been expressed that the short range for dose buildup at low energies generated by an X ray tube, with a voltage of 50 kV applied, delivers a peak dose to radio-sensitive portions of the skin and that this may be great enough to produce significant risk of skin cancer. Accurate PDD data are needed in order to investigate this claim. While PDD profiles are commonly characterized for radiation therapy beams operated at much higher energies (in the ~ 10 MV energy range), they are not commonly characterized for energies at which AIT systems operate. This presents a unique challenge because any peak dose for 50 kV systems is expected to occur at very shallow tissue depths and requires a specialized ion chamber having a very thin entrance window, which

[15] Uncertainties in the tissue depth are substantially smaller than the size of the symbols in the accompanying figures. Hence, you might not see them even though they are there.

TABLE 7.2 Percent Depth Dose for the AS&E SmartCheck Using the PS-033 Thin-Window (0.5 mg/cm^2) 4.9 cm^3 Ion Chamber

Tissue Depth (mm)	PDD (%)	Standard Deviation (%)
0.0	92.2	3.6
0.0	91.7	1.6
0.2	93.5	1.6
0.3	89.8	3.2
0.3	92.6	1.6
0.5	99.0	1.6
0.7	100.0	1.6
1.0	92.4	4.2
2.0	92.2	4.2
3.1	88.3	1.6
4.2	79.9	1.6
5.9	77.7	3.2
8.0	67.4	1.6
9.6	56.4	1.6
15.6	44.1	1.6
20.4	35.8	1.6
26.2	28.3	1.6
31.0	20.4	1.6
40.7	14.9	1.6
51.4	8.90	1.6
62.2	7.88	1.6

minimizes production of secondary electrons as the beam enters the chamber, and specialized phantom materials to represent tissue attenuation and the thin thicknesses of interest.

Phantom materials were successfully produced in thin layers, as small as 25 μm. A series of thicknesses were fabricated in 10 cm × 10 cm cross sections so that these could be assembled in various combinations to develop the data for the PDD curves. The PDD data demonstrated a peak dose occurring at a depth around 0.5-0.7 mm. The peak, however, is not significantly greater than is the entrance skin dose—it exceeds the entrance skin dose by approximately 8 percent. Consequently, there should not be concern that the shallow dose is preferentially deposited to radio-sensitive layers of the skin.

The remainder of the PDD curve demonstrates the attenuation of the 50 kV X-ray beam for thicknesses up to 62 mm. A first HVL of 13 mm and a second HVL of 15 mm in tissue is observed for this beam. About 10 percent of the entrance dose is delivered at a depth of 62 mm.

A second set of PDD data was collected using the larger-volume (15 cc), thicker-window ion chamber. This data set provided enhanced measurement accuracy over all but the smallest range of tissue depths. When normalized to the

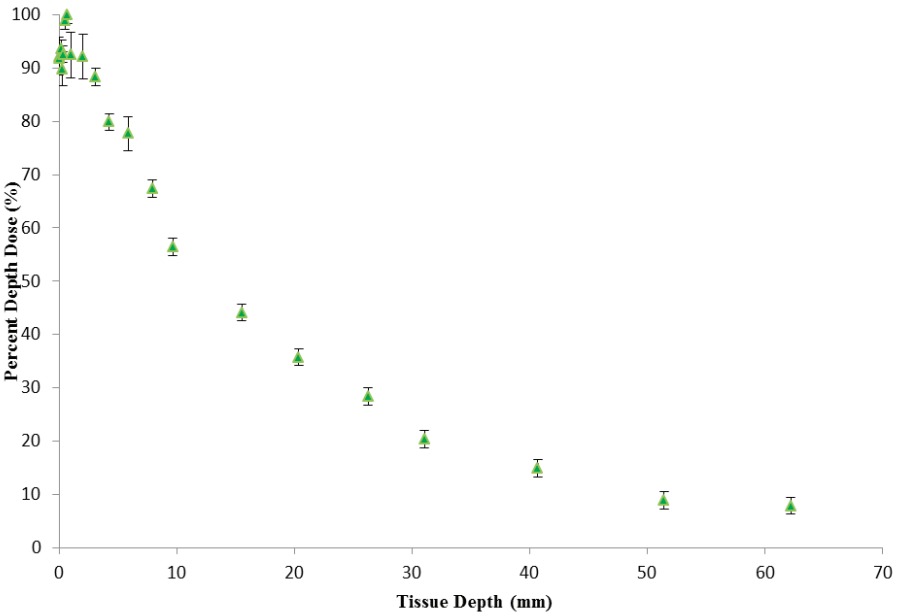

FIGURE 7.3 Percent depth dose collected for the AS&E SmartCheck using the PS-033 thin-window (0.5 mg/cm^2) 4.9 cm^3 ion chamber.

maximum, the PDD curves from the two ion chambers match within the measurement uncertainties for tissue depths greater than 1 mm. At depths less than 1 mm, the larger-volume chamber does not resolve the dose peak due to the thicker window that generates secondary electrons prior to the X-ray beam entering the sensitive volume of the ion chamber. While this effect must also occur to some degree in the thin-window PS-033 chamber, the curves demonstrate the need to utilize a thin-window ion chamber to more accurately resolve the details of the PDD curve at this low energy and this tissue depth.

The PDD data were also used as a validation tool for the computational simulations. Good agreement (see Figure 7.13) was obtained between the computational and empirical evaluations of the PDD curves.

The initial simulations were not particularly good matches to the empirical PDD curves. Through a series of discussions and a review of both the HVL and the PDD data, it was recognized that the candidate X-ray spectrum that was being utilized based on previously collected data was overly hard (i.e., excessively filtered, low-energy beam components). By developing a softer candidate spectrum (reducing the filtration to include more low-energy components), a good match was obtained for both HVL and PDD curves. This demonstrates the value of obtain-

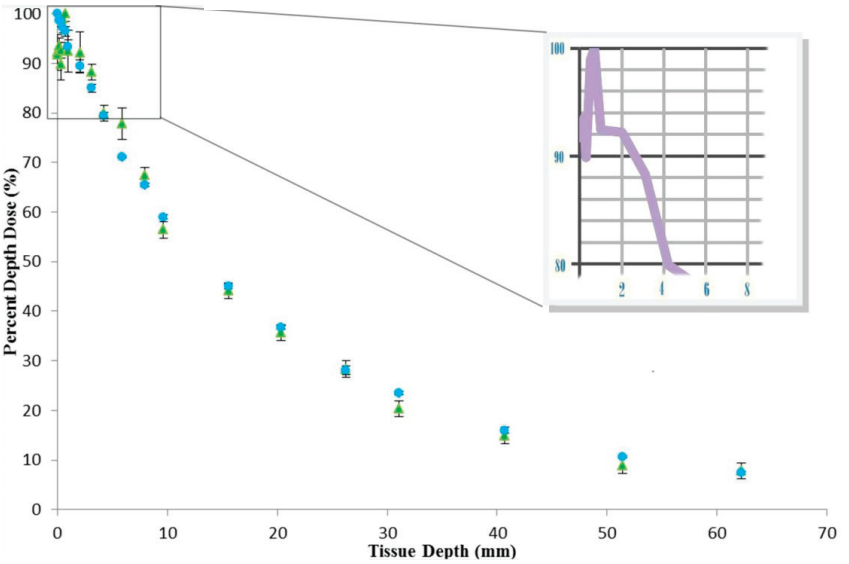

FIGURE 7.4 Comparison of percent depth dose data collected for the AS&E SmartCheck using the thin-window (0.5 mg/cm^2) 4.9 cm^3 chamber (green triangles) and the 32 mg/cm^2 window 15 cc chamber (blue circles). The inset shows the region from 0 to 8 mm enlarged, indicating a peak around 0.5 to 0.7 mm.

ing high-spatial-resolution measurements for HVL and PDD curves to accurately characterize the X-ray spectrum for AIT systems.

Air Kerma Results

Person Being Screened

A series of 10 individual air kerma measurements were made at each measurement position. Each measurement was made with the ion chamber positioned as previously described, and a normal subject scan was made along the central axis (x = 0 cm, y = 0 cm) at several vertical positions (z). The two z = 32 cm results represent two separate sets of 10 individual scans performed under the same conditions. The average and standard deviations for the air kerma at each vertical position are provided in Table 7.3.

The measurements of air kerma provided good reproducibility at each location. A slight variation of air kerma was observed as a function of z. The air kerma aver-

TABLE 7.3 Air Kerma Measured Along the Central Axis (x = 0 cm, y = 0 cm) for the AS&E SmartCheck at Transportation Security Administration's Systems Integration Facility

Vertical Position-z (cm)	Air Kerma per Scan (nGy)	Standard Deviation (nGy)
32	113	4
32	113	4
120	108	5
150	105	4
202	111	3

aged 110 nGy per scan and was observed to be a few percent higher at the upper and lower regions of the scan. Because the system utilizes a fixed, horizontally oriented tube geometry that is translated vertically (there is no tube angulation), it would be expected that the air kerma should be nearly constant along the vertical extent of the scan. The small variations of air kerma observed may result from the time required for tube acceleration and deceleration at the beginning and end of the scan, respectively. Uncertainty in the absolute value of the air kerma is also subject to uncertainty in the chamber calibration. Comparisons among various chamber calibrations performed on a 50 kV beam (2.08 mm HVL) performed at the University of Florida indicates that the uncertainty in the 150 cc chamber calibration performed for the L60 beam should be less than 4 percent different from the spectral response of this 50 kV beam.

Bystander (Outside the Screening Volume)

Leakage Radiation Geometry

The low levels of radiation encountered during the bystander set of measurements required continuous integration over a period of 4-5 minutes. The Fluke 451B was operated in integration mode and never recorded any values above 0 nGy. Results presented are based on the Keithley model 96020C 150 cc ion chamber with charge collected by the PTW Unidose electrometer. At low exposure levels, the background and electrometer/chamber leakage can produce a significant contribution to the measured result. In order to reduce this contribution, a baseline measure of background electrometer/chamber leakage rate was made. An estimate of this total contribution was made based on the resulting integration time and subtracted from the gross charge accumulated over the period. The net accumulated charge was subsequently converted to air kerma using the appropriate chamber calibration factor and making air temperature and pressure corrections relative to the chamber's calibration conditions. The integrated results were then divided

TABLE 7.4 Air Kerma per Scan Outside the Inspection Area for the AS&E SmartCheck

Position	Air Kerma per Scan (nGy)	Standard Deviation (nGy)
Leakage—Rear exterior x = –100 cm, y = 0 cm, z = 150 cm	0.23	0.83
Scatter—Center of exit x = 0 cm, y = –66 cm, z = 120 cm	1.7	0.45
Scatter—Operator side of exit x = –27 cm, y = –66 cm, z = 120 cm	2.8	0.25

by the number of scans included for each measurement position to provide the average air kerma per scan at each measurement position, illustrated in Table 7.4.

Standard deviation is relatively large at the very low exposure levels for each of these measurements. The standard deviation observed between multiple sets of measurements average around 0.5 nGy per scan. Consequently, the reported values of the leakage radiation are so low as to be statistically indistinguishable from the background radiation. This should not be surprising because the X rays produced by a 50 kV beam are readily attenuated by quite modest thicknesses of lead that may be expected to be incorporated into the scanning system.

Scatter Radiation Geometry

Measurement of the scatter radiation fields was performed at a very conservative position (the very edge of the AIT system) and produced small but measurable radiation exposures. The reported values suggest that there may be slightly more scatter intensity in the direction toward the X-ray source. This may be expected because a greater surface area of the phantom is available to scatter into this direction, and the generation of scatter within the phantom is expected to be mostly isotropic at these energies. Measurements were thus not made at the operator position, only at the edge of the AIT system. It should also be noted that the operator position can be altered from side-to-side (i.e., it can be located on either the entrance or the exit side) on this system, but it is confined to the side housing the anterior X-ray source. Radiation fields are expected to be symmetrical in the +/– y directions based on the system geometry and measurements performed on a previous generation AS&E AIT system by NIST.

Committee Review of the AS&E SmartCheck System Design

The committee did not have the same level of access to the AS&E system that it had to the Rapiscan Secure 1000 system at NIST. This difference in access is due to the AS&E system being subjected to TSA qualification tests that impose restrictions on how it can be handled, but an AS&E representative pointed out and described the various interlocks and safety features. From these descriptions, the committee developed a summary of the committee's findings, given in Table 7.5. As with the Rapiscan Secure 1000 installed at NIST, the committee was able to confirm that the AS&E AIT system installed at TSIF met the same 6 of 14 requirements for all radiation-emitting devices in ANSI/HPS N43.17 (Section 7.2.1) and the same 5 of the 6 requirements for general-use radiation-emitting devices (Section 7.2.2). An additional 3 requirements (Sections 7.2.1 j and l, and 7.2.2 e) could not be confirmed because the operational AIT system cannot be forced to perform the action. The interlocks, safety, and control requirements in ANSI/HPS N43.17-2009 that could be verified for the AIT system are listed in Box 7.1.

> **Key Finding:** Based on the committee's inspection of the AS&E SmartCheck system with the AS&E representative present, the committee was unable to identify any circumstances where an accidental failure or deliberate reconfiguration of the AIT system could result in either a person being screened or the operator receiving a larger X-ray dose than the normal screening dose.

Because there is no failure mechanism that would give more than a normal screening dose, as stated in the key finding, scanning time is the only factor left. The AIT system would have to operate for more than 16 hours to exceed the dose limit of 250,000 nSv, as stated in Table 7.5 (row 7.2.1 m); it is unreasonable to expect that a person being scanned would be exposed for that amount of time.

THE RAPISCAN SECURE 1000 SYSTEM MEASUREMENT RESULTS AND SYSTEM DESIGN

A Rapiscan Secure 1000 (serial number S51023005) became available for measurements in July 2014. This AIT system had been in service at LaGuardia Airport and was later transferred to NIST, where it was installed and calibrated by the manufacturer's technicians. This AIT system can thus provide information indicative of the performance of the AIT systems that were installed previously in airports. For the purposes of the measurements done by the NRC subcontractors, the software used by TSA and NIST were identical. During some measurements, the engineering mode was used to control scan motion.

TABLE 7.5 Summary of the Committee's Review of the AS&E SmartCheck Compared to the Requirements in Sections 7.2.1 and 7.2.2 of ANSI/HPS N43.17-2009

Text	Committee Comments
ANSI/HPS Section 7.2.1	
a. There shall be at least one indicator, clearly visible from any location from which a scan can be initiated, that indicates when a scan is in progress.	Confirmed on AS&E prototype AIT system at TSIF.
b. There shall be at least one lighted indicator clearly visible from the inspection zone. For portal systems the indicator shall be visible from any approach to the inspection zone to indicate that a scan is in progress.	Confirmed on AS&E prototype AIT system at TSIF.
c. Power to the system shall be controlled by a key switch. The key shall be captured (unable to be removed) whenever it is in a position that allows exposures to be initiated.	Confirmed on AS&E prototype AIT system at TSIF.
d. Each system shall have a means for the operator to initiate the emission of radiation other than the function of an interlock or the main power control.	Operator initiates scan from computer console. Observed on AS&E prototype.
e. Each system shall have a means for the operator to terminate the emission of radiation other than the function of an interlock.	"Stop scan" icon included on computer screen. Confirmed on AS&E prototype AIT system at TSIF.
f. Means shall be provided to ensure that operators have a clear view of the scanning area.	Operational requirement that is site specific. Not confirmed on AS&E prototype AIT system at TSIF.
g. A ground fault shall not result in the generation of X rays or activate a scan beam from a sealed radioactive source.	Committee unable to confirm impact of a ground fault.
h. Failure of any single component of the system shall not cause failure of more than one safety interlock.	Committee unable to determine the impact of component failure.
i. A tool or key shall be required to open or remove access panels. Access panels shall have at least one safety interlock.	Confirmed on AS&E prototype AIT system at TSIF.
j. For stationary-subject systems, the scanning motion of the X-ray beam relative to the subject shall be interlocked and the exposure shall terminate when the rate of motion of the beam in any direction falls below a preset minimum speed.	Not confirmed. Committee believes this verification is part of the qualification testing under way at TSIF.
k. For portal systems, the minimum walking or driving velocity through the inspection zone shall be determined by the manufacturer.	Not applicable to stationary subject AIT systems.
l. Operational interlocks shall terminate the primary beam in the event of any system problem that could result in abnormal or unintended radiation emission.	Not confirmed. Committee believes this verification is part of the qualification testing under way at TSIF.
m. In the event of a malfunction, the system shall terminate radiation exposure rapidly enough so that no location on the subject's body shall receive an ambient dose equivalent (H*10) exceeding 250 μSv (250,000 nSv), regardless of the size of the exposed area.	In this report it is shown that the computed effective doses for a normal scan are about an order of magnitude lower than the recommended ANSI standard of 250 nSv/screen. Comparing the 6 second scan and ~25 nSv/screen versus a 250,000 nSv limit, the exposure would have to last for more than 16 hours.

TABLE 7.5 Continued

Text	Committee Comments
n. Following interruption of X-ray production or external gamma emission by the functioning of any safety interlock, resetting the interlock shall not result in the production of X rays or emission of gamma radiation.	Confirmed on AS&E prototype AIT system at TSIF.
ANSI/HPS Section 7.2.2	
a. For any X-ray system that normally keeps high voltage applied to the X-ray tube at times other than during a scan, there shall be at least one lighted "X ray on" indicator at the control console where X rays are initiated indicating when X rays are being produced.	Confirmed on AS&E prototype AIT system at TSIF.
b. Technique factors for each mode of operation shall be preset by the manufacturer and shall not be alterable by the system operator.	Confirmed on AS&E prototype AIT system that technique factors cannot be changed when AIT system is in operator mode. Verified in discussion with TSA.
c. Each access panel to the X-ray source shall have at least one safety interlock to terminate the X-ray production when opened.	Confirmed on AS&E prototype AIT system at TSIF.
d. The following warning label shall be permanently affixed or inscribed on the X-ray system at the location of any controls used to initiate X-ray generation: "CAUTION: X-RAYS PRODUCED WHEN ENERGIZED."	Confirmed on AS&E prototype AIT system at TSIF.
e. X-ray emission shall automatically terminate after a preset time or exposure.	Not confirmed. Committee believes this verification is part of the qualification testing under way at TSIF.
f. For portal systems, motion sensors shall monitor the speed of pedestrians or vehicles through the inspection zone (in the forward direction) and the radiation exposure shall terminate when the speed drops below the minimum (as determined according to Section 7.2.1k).	Not applicable to stationary subject AIT systems.

Half-Value Layer Results

In order to stop the vertical scan motion, the power to the vertical positioning motor was turned off and the X-ray head was manually moved to the desired height and clamped in place. In this position, the top of the tube housing was horizontal, at approximately z = 85 cm. The engineering software was utilized to override interlocks and allow X-ray production in this configuration. One AIT system unit was turned off while measurements were made for the other one. The results for both the anterior and the posterior unit are shown in Table 7.6 and Figures 7.5, 7.6,

BOX 7.1
ANSI/HPS N43.17-2009 Requirements Verified for the AS&E SmartCheck

7.2 Indicators, Controls, and Safety Interlocks

7.2.1 Requirements for All Systems: The requirements of this subsection apply to all the systems regardless of category or type of radiation source. In addition to these requirements systems must comply with the requirements of one of the sections 7.2.2 through 7.2.5 as appropriate.

a. There shall be at least one indicator, clearly visible from any location from which a scan can be initiated, that indicates when a scan is in progress.

b. There shall be at least one lighted indicator clearly visible from the inspection zone. For portal systems the indicator shall be visible from any approach to the inspection zone to indicate that a scan is in progress.

c. Power to the system shall be controlled by a key switch. The key shall be captured (unable to be removed) whenever it is in a position that allows exposures to be initiated. Turning on the key switch shall never result in the external emission of radiation.

i. A tool or key shall be required to open or remove access panels. Access panels shall have at least one safety interlock.

j. For stationary-subject systems, the scanning motion of the X-ray beam relative to the subject shall be interlocked and the exposure shall terminate when the rate of motion of the beam in any direction falls below a preset minimum speed. The minimum speed shall be chosen so that the dose during the exposure period is within the applicable limit.

l. Operational interlocks shall terminate the primary beam in the event of any system problem that could result in abnormal or unintended radiation emission. This shall include, but is not limited to, unintended stoppage of beam motion, abnormal or unintended X-ray source output, computer safety system malfunction, termination malfunction, and shutter or beam stop mechanism malfunction.

m. In the event of a malfunction, the system shall terminate radiation exposure rapidly enough so that no location on the subject's body shall receive an ambient dose equivalent (H*10) exceeding 250,000 nSv (25 mrem), regardless of the size of the exposed area.

7.2.2 Requirements for General-use Systems Using X-ray Sources: In addition to the requirements of Section 7.2.1, "Requirements for All Systems," the following requirements apply to general-use systems using X-ray sources:

c. Each access panel to the X-ray source shall have at least one safety interlock to terminate the X-ray production when opened.

d. The following warning label shall be permanently affixed or inscribed on the X-ray system at the location of any controls used to initiate X-ray generation: "CAUTION: X-RAYS PRODUCED WHEN ENERGIZED."

e. X-ray emission shall automatically terminate after a preset time or exposure.

SOURCE: The ANSI/HPS N43.17-2009 standard, "Radiation Safety for Personnel Security Screening Systems Using X-Ray or Gamma Radiation," is available at the Health Physics Society website at http://hps.org/hpssc/index.html.

TABLE 7.6 Rapiscan Secure 1000 Half-Value Layer Measurement Results

Aluminum Thickness (mm)	Normalized Exposure Anterior Unit	Uncertainty Anterior Unit	Normalized Exposure Posterior Unit	Uncertainty Posterior Unit
0.0	1.00	0.005	1.00	0.007
0.05	0.95	0.008	0.94	0.003
0.1	0.90	0.005	0.89	0.004
0.15	0.86	0.018	0.84	0.004
0.2	0.83	0.003	0.81	0.003
0.25	0.79	0.012	0.77	0.004
0.3	0.76	0.005	0.75	0.000
0.35	0.73	0.009	0.71	0.005
0.4	0.71	0.002	0.68	0.008
0.45	0.68	0.004	0.65	0.002
0.5	0.65	0.006	0.63	0.003
0.55	0.63	0.003	0.60	0.003
0.6	0.61	0.007	0.58	0.002
0.65	0.59	0.003	0.56	0.003
0.7	0.58	0.004	0.56	0.005
0.8	0.55	0.010	0.52	0.002
0.9	0.51	0.004	0.48	0.003
1.0	0.48	0.007	0.46	0.005
1.1	0.45	0.000	0.43	0.002
1.2	0.44	0.003	0.42	0.000
1.3	0.41	0.002	0.39	0.000
1.4	0.40	0.002	0.37	0.004
1.5	0.37	0.007	0.35	0.002
2.0	0.30	0.003	0.28	0.000
2.5	0.24	0.002	0.22	0.004
3.0	0.20	0.003	0.19	0.005
3.5	0.17	0.000	0.16	0.003
4.0	0.15	0.004	0.13	0.002
4.5	0.13	0.006	0.12	0.002
5.0	0.11	0.003	0.10	0.003

NOTE: Each measurement result shown is the average of at least three measurement scans. The uncertainty represents the observed standard deviation in the replicate measurements for each aluminum thickness.

and 7.7. Each measurement is the average of at least three measurement scans, as measured in coulombs, and then normalized to the value at zero aluminum thickness. HVL_1 and HVL_2 were 0.92 and 1.47 mm Al for the anterior unit and 0.85 and 1.42 mm Al for the posterior unit, respectively.

Percent Depth Dose Results

Depth dose measurements were at the same height as the HVL measurements, z = 85 cm, with x = 0 cm and y = 0 cm. The results are tabulated in Table 7.7 and shown in Figures 7.6 and 7.7.

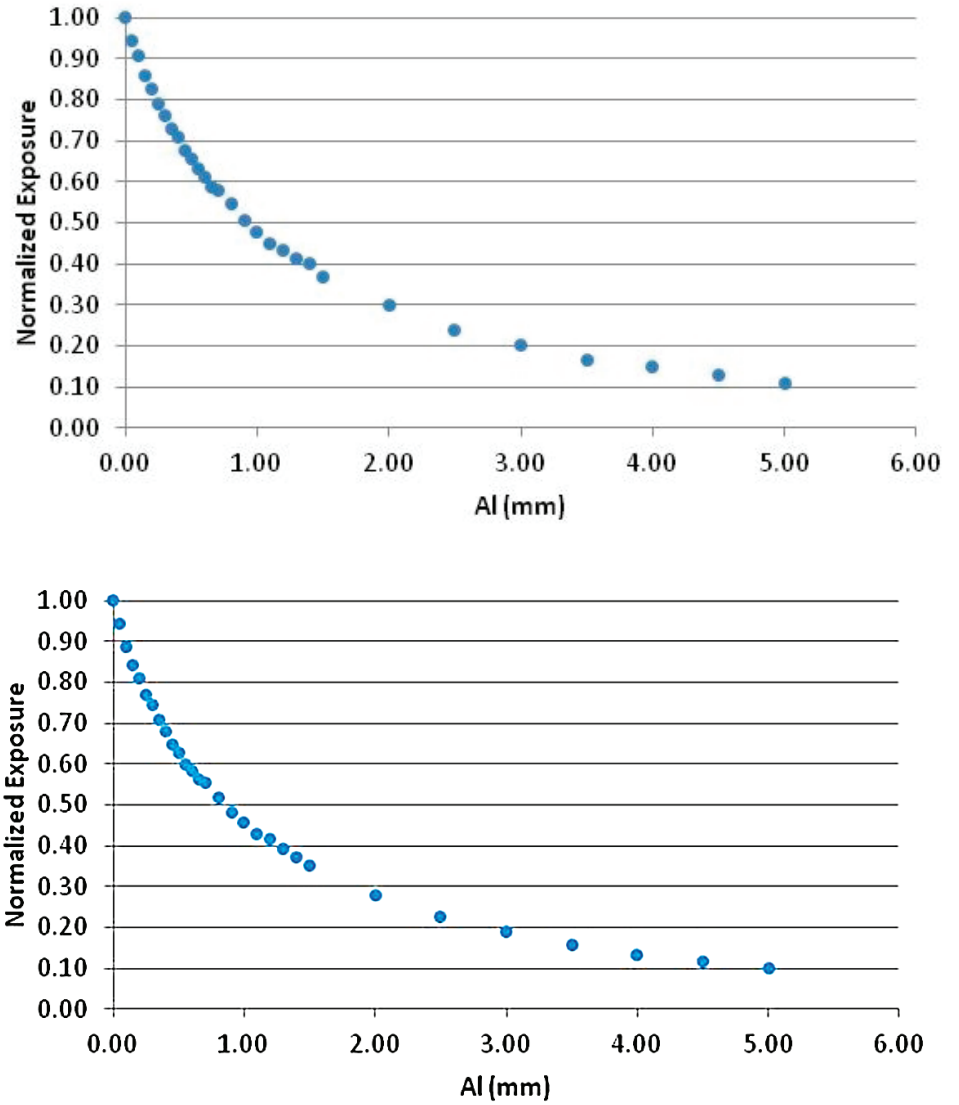

FIGURE 7.5 Normalized exposure as a function of aluminum thickness for the Rapiscan Secure 1000 for (a) the anterior unit and (b) the posterior unit. Error bars are not shown since they are approximately the size of or smaller than the symbols.

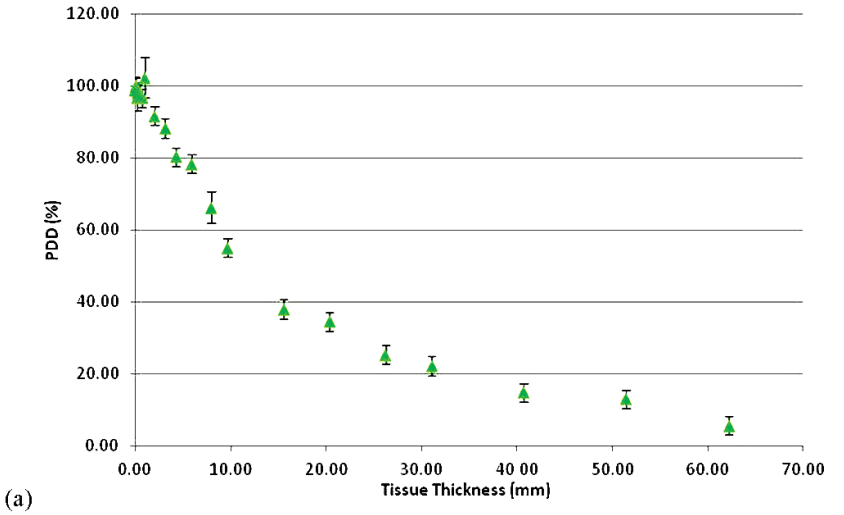

(a)

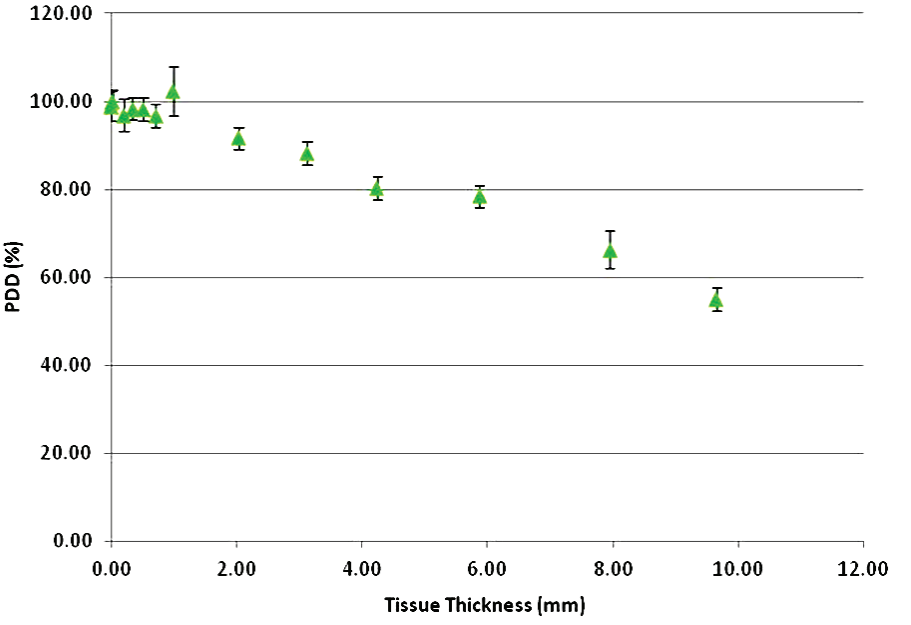

(b)

FIGURE 7.6 Percent depth dose (PDD) for the Rapiscan Secure 1000 anterior unit collected using the PS-033 thin-window (0.5 mg/cm^2) ion chamber at tissue thicknesses (a) up to 6 mm and (b) less than 10 mm.

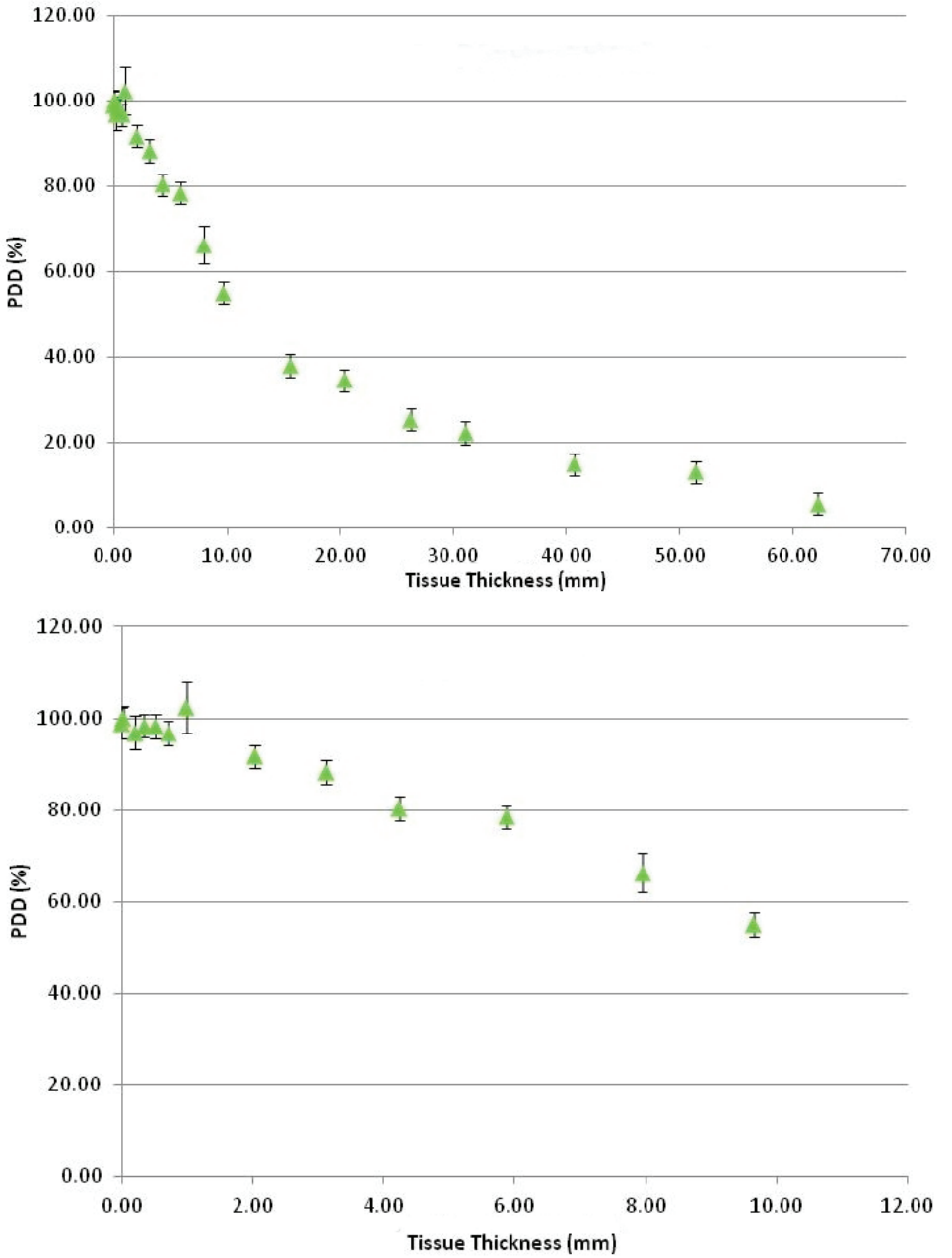

FIGURE 7.7 Percent depth dose (PDD) for the Rapiscan Secure 1000 posterior unit collected using the PS-033 thin-window (0.5 mg/cm^2) ion chamber at tissue thicknesses (a) up to 6 mm and (b) less than 10 mm.

TABLE 7.7 Percent Depth Dose (PDD) for the Rapiscan Secure 1000 Anterior and Posterior Units for Data Collected on the PS-033 0.5 mg/cm^2 and 32 mg/cm^2 Window Chambers

	Anterior		Posterior	
Tissue Depth (mm)	PDD (%) 0.5 mg/cm^2 chamber	PDD (%) 32 mg/cm^2 chamber	PDD (%) 0.5 mg/cm^2 chamber	PDD (%) 32 mg/cm^2 chamber
0.00	98.98	100.00	100.00	100.00
0.02	100.00	—	96.19	—
0.20	96.87	98.17	96.77	97.96
0.34	98.36	97.47	98.62	97.69
0.51	98.30	96.76	94.77	96.48
0.71	96.70	94.49	90.92	95.49
0.99	102.36	92.43	85.79	93.32
2.03	91.69	86.74	81.72	86.25
3.12	88.31	81.47	75.16	80.43
4.24	80.39	76.56	73.94	74.37
5.87	78.45	68.58	69.50	66.98
7.95	66.29	58.45	57.93	59.68
9.65	55.12	56.29	56.99	54.78
15.55	37.99	40.96	36.06	41.12
20.35	34.52	32.58	31.95	31.96
26.25	25.40	24.97	24.38	25.34
31.05	22.23	20.36	20.57	18.68
40.70	14.82	14.15	10.81	12.91
51.40	13.03	9.79	9.65	8.96
62.20	5.67	7.59	9.65	6.45

PDD data were collected using the larger 15 cc parallel-plate ion chamber (32 mg/cm^2 window thickness). The larger sensitive volume of this chamber provided improved signal collection at the low exposures produced by the scanning system. A comparison of the response for these two chambers is reported in Figure 7.8. The comparison demonstrates that consistent data were collected from both chambers except at very small values for tissue depth where the dose peak observed using the thin-window (0.5 mg/cm^2) 4.9 cm^3 chamber was overwhelmed by the thicker (32 mg/cm^2) window of the 15 cc chamber.

Standard deviations for each set of exposure measurements were calculated based on the replicate data set and were typically about 3 percent of the mean value, with the largest being 5.7 percent for the thin-window chamber. For the 15 cc chamber, the standard deviation for each set of exposure measurements averaged less than 1 percent of the mean value, with the largest being 1.5 percent. Uncertainties in the tissue depth are substantially smaller than the size of the symbols in the accompanying figures.

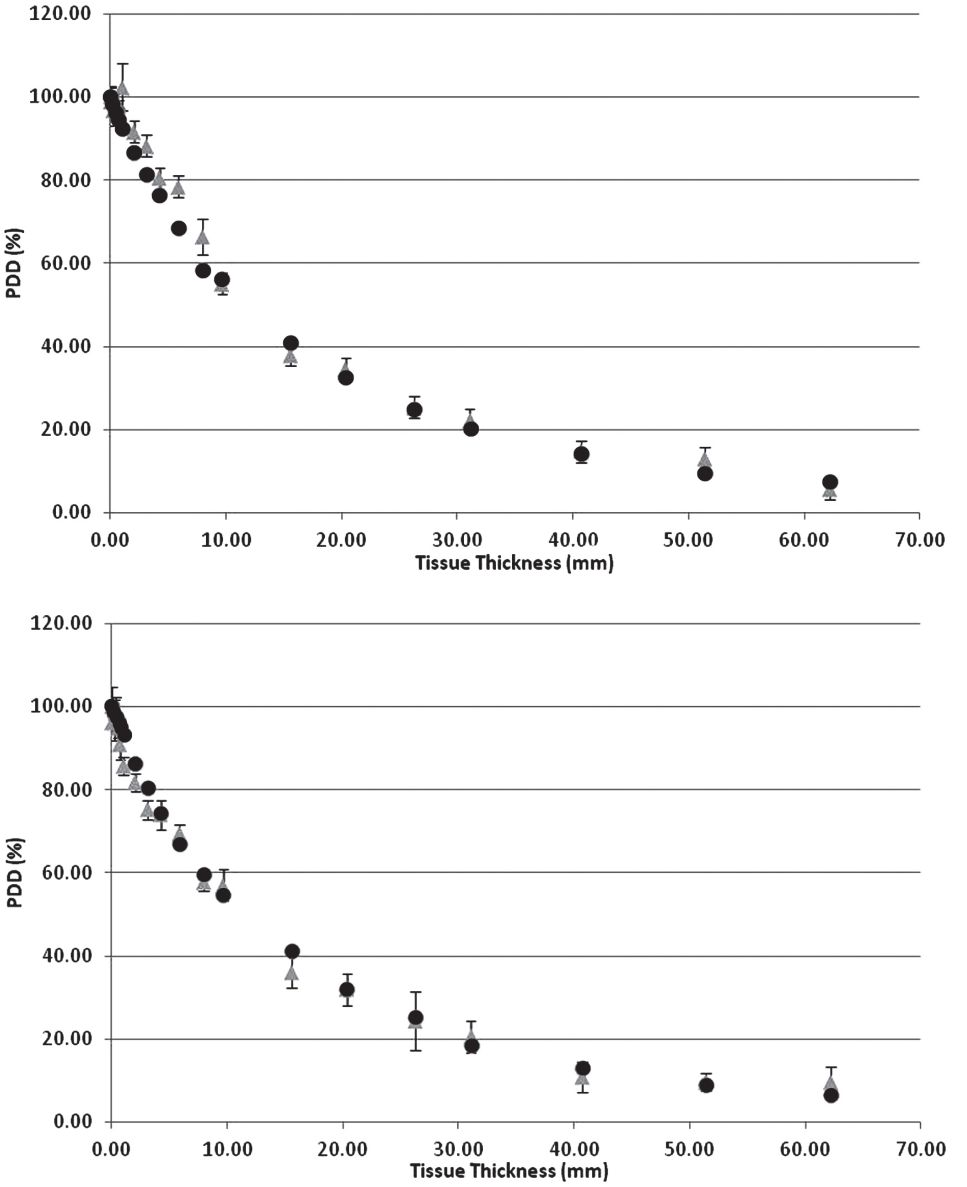

FIGURE 7.8 Comparison of percent depth dose (PDD) data for the Rapiscan Secure 1000 collected using the thin-window (0.5 mg/cm^2) chamber (triangles) and the 32 mg/cm^2 window chamber (circles) for (a) the anterior unit and (b) the posterior unit.

Air Kerma Results

Person Being Screened

Air kerma was measured with the 150 cc parallel-plate ion chamber centered at multiple vertical locations (see Table 7.8) for both the anterior and the posterior unit. The measurement locations were selected to evaluate any variations in beam intensity as the beam scans vertically. Because of the low intensity of the scanning beam, a series of 10 individual measurements were recorded and averaged to provide the air kerma at each vertical location.

Two additional sets of measurements were made at positions x = 25.8 cm, y = 0 cm, z = 82.8 cm, and x = −25.8 cm, y = 0 cm, z = 82.8 cm, which specify locations 30 cm from the front surface of the anterior and posterior units, respectively. This provided a reference air kerma that may be used to demonstrate compliance with the applicable ANSI standard and is also identified in Table 7.8.

A series of 10 individual measurements were made at each measurement location. Each measurement was made with the ion chamber positioned as previously described, and a normal, but single-sided, subject scan was performed. The average and standard deviation for the air kerma at each vertical position are provided in Table 7.8.

TABLE 7.8 Air Kerma Measured Along the Central Axis (x = 0 cm, y = 0 cm) at Several Vertical Positions (z) for the Rapiscan Secure 1000

	Anterior Unit		Posterior Unit	
Vertical Position z (cm)	Air Kerma per Scan (nGy)	Standard Deviation (nGy)	Air Kerma per Scan (nGy)	Standard Deviation (nGy)
26.8	27	2	26	2
48.8	28	2	31	1
82.8	29	2	32	2
122.8	31	2	30	2
138.8	28	2	30	2
161.8	27	2	30	2
184.8	26	1	29	2
184.8	—	—	29	2
194.8	—	—	33	1
At 30 cm from x-surface				
82.8	48	3	56	4

NOTE: The two z = 184.8 cm results represent two separate sets of 10 individual scans performed under the same conditions.

Bystander (Outside the Screening Volume)

Leakage Radiation Geometry

A measurement location on the backside of the posterior unit was selected to evaluate leakage radiation that may be exiting the unit. The 150 cc parallel-plate ion chamber was positioned against the rear exterior of the posterior AIT system assembly at a height of z = 171 cm, with x = −130 cm, and y = 0 cm, centered on the path that the X-ray source travels while vertically scanning.

Scatter Radiation Geometry

In order to represent the geometry that would cause radiation to be scattered outside of the subject scanning area toward bystanders (e.g., passengers not being screened and transportation security officers), an anthropomorphic phantom representative of an adult male was used as described previously.

Results

The low levels of radiation that were expected to result from this set of measurements required continuous integration over a period of approximately 2 minutes. The Fluke 451B was operated in integration mode and never recorded any values above 0 nGy. Results presented are based on the Keithley model 96020C 150 cc parallel-plate ion chamber with the charge collected by the PTW Unidose electrometer. At low exposure levels, the background and electrometer/chamber leakage can produce a significant contribution to the measured result. In order to reduce this contribution, a baseline measure of background electrometer/chamber leakage rate was made. An estimate of this total contribution was made based on the resulting integration time and subtracted from the gross charge accumulated over the period. The net accumulated charge was subsequently converted to air kerma using the appropriate chamber calibration factor and making air temperature and pressure corrections relative to the chamber's calibration conditions. The integrated results were then divided by the number of scans included for each measurement position to provide the average air kerma per scan at each measurement position, illustrated in Table 7.9.

Committee Review of the Rapiscan Secure 1000 System Design

The committee did not have access to Rapiscan personnel or AIT system design documentation during the course of this evaluation because Rapiscan could not participate within the set time frame of the study, but the committee did review

TABLE 7.9 Air Kerma per Scan Outside the Inspection Area of the Rapiscan Secure 1000

Position	Air Kerma per Scan (nGy)	Standard Deviation (nGy)
Leakage—Rear exterior x = 130 cm, y = 0 cm, z = 171 cm	4.0	6.0
Scatter—Center of exit x = 0 cm, y = 72 cm, z = 120 cm	0.0	16
Scatter—Operator side of exit x = −44.8 cm, y = 72 cm, z = 120 cm	7.0	4.0

the public documentation available, from both public sources and TSA, for the Rapiscan Secure 1000. The committee also inspected the Rapiscan Secure 1000 AIT system that was made available to the committee at NIST.

A few of the interlocks, safety, and control requirements in the ANSI standard could not be verified in the field or without reviewing the machine design or fully disassembling a machine. However, the committee assumes that the Rapiscan Secure 1000 machine design and interlocks were (as required) demonstrated by the vendor to meet ANSI/HPS N43.17-2009 or the version of ANSI/HPS N43.17 in force at the time of qualification testing at TSA prior to deployment at airports.

Documentation for Compliance with ANSI Standards

The factory acceptance test (FAT) and the site acceptance test (SAT) and other operating procedures define the procedures prior to deployment and after installation of any backscatter system. The documents used by TSA and equipment producers in previous years, during deployment of the Rapiscan backscatter AIT systems at airports, refers to Form R-0646, "Radiation Emission Measurement for Secure 1000." This form, and the accompanying Form R-0685, defines what is inspected and measured from a radiation-safety perspective during FAT and SAT and in the following situations:

- After system relocation,
- During maintenance, and
- Annually.

Forms R-0646 and R-0685 for all fielded AIT systems have been publicly available on the TSA website for several years,[16] but they are currently unavailable

[16] Transportation Security Administration, "Surveys of Backscatter Imaging Technology Machines," http://www.tsa.gov/research-center/surveys-backscatter-imaging-technology-machines, accessed July 23, 2014.

online; only a list of documents is provided on the website.[17] The forms request the following information pertinent to radiation safety:

- X-ray tube serial number (anterior and posterior unit);
- The result of an emergency stop button test;
- If scan in progress lights were operational;
- If X-ray caution labels were present on the anterior, posterior, and communications units;
- If X-ray warning labels were present on the X-ray generators for the anterior and posterior;
- The outcome of a safety interlock test;
- If the key is removable when the unit is in operation;
- Settings of the generator (voltage and current);
- Length of the scan time, in seconds;
- If the operator instructions are available; and
- General condition of the AIT system.

It is not specified what the exact safety interlock test referred to above is. The committee notes the following points related to existing interlock systems as they are described in the Rapiscan operator manual:

- *Power to the system is controlled by a key switch.* The key switch has three positions "off," "standby," and "on." When the key is placed on "standby," the system waits for commands from the operator console and will time out if commands are not received.
- *A mechanical sensor at the bottom of the door is depressed when the door is closed.* If the door is opened, the sensor is released and the interlock prevents operation of the system. Both anterior and posterior access-panel interlocks must be enabled for a scan to initiate and complete.
- *X-rays will terminate if there is over voltage or over current.*
- *Reference detector signal.* When a detector is placed in the X-ray beam, the X-ray intensity is monitored for radiation levels out of range.
- *Velocity of vertical motion.* A sensor that travels with the X-ray tube will generate electrical impulses to monitor vertical motion. X-rays are terminated if motion stops.
- *Velocity of horizontal motion of the scanned beam.* An optical interrupt sensor located on the assembly is used to monitor that the rotational velocity is maintained. X-rays are terminated if speed is out of tolerance limits.

[17] The links to the documents posted on April 11, 2013, May 24, 2011, and March 16, 2011, no longer work.

- *X-ray tube head temperature.* X-rays will terminate if the X-ray tube is out of range.

Safety-related information that was requested by Form R-0646 included the following:

- Test procedure used (described below),
- Background radiation reading,
- Measurement instrument type (and serial number), and
- Data acquired.

The form indicated that data acquired should include measurements of where a person would stand when being screened—called *in beam radiation exposure measurements*—which consist of total integrated exposure as averaged over 10 measurements using a Fluke 451P meter positioned 304.8 mm (12 inches) from the center of the scan window and 914.4 mm (36 inches) from the floor of both anterior and posterior units.[18] Data acquired should also include *radiation leakage measurements,* which are similar to in beam measurements but located at four positions at the center of the active units' external surface, for both the anterior and the posterior, where a potential bystander could be. The final data acquired should include *inspection zone boundary radiation dose measurements*, done 304.8 mm (12 inches) from the edges of the units scan windows (four measurements), again where a potential bystander could be.

The data on Forms R-0646 and R-0685 were compared to the exposure limits set, and if results were within the administrative integrated exposure limits, the AIT system was considered to meet the ANSI/HPS N43.17-2009 standard with respect to limits for reference effective dose and X-ray leakage. If any value exceeded the limits, that fact would be reported to service program managers prior to placing a system into operation.

Key Finding: Acceptance tests and periodic inspection tests guided by the safety inspection forms previously used during deployment are sufficient to

[18] The Model 451P Ion Chamber Survey Meter is a hand-held, 8 atm pressurized, 230 cc active volume air ionization chamber meter designed to measure gamma and X-ray radiation above 25 keV and beta radiation above 1 MeV. The plastic chamber wall is 200 mg/cm^2 thick. The instrument has a ±10 percent accuracy of reading between 10 and 100 percent of full-scale indication on any range. The typical relative energy response is approximately 0.4 for 20 keV, 0.8 for 40 keV, and 1 for 50 keV (Fluke Biomedical, "451P Pressurized µrad Ion Chamber Radiation Survey Meter," http://www.flukebiomedical.com/biomedical/usen/radiation-safety/Survey-Meters/451P-pressurized-ion-chamber-radiation-detector-survey-meter.htm?PID=54793, accessed July 23, 2014).

meet the indicators, controls, and safety interlocks requirements of the ANSI/HPS N43.17-2009.

Safety Procedures for Maintaining the Rapiscan Secure 1000 During the Course of Its Use

According to the written safety procedures for the Rapiscan Secure 1000, prior to any startup of a unit, there should be verification that service access doors for each AIT system module are closed and locked before powering up the AIT system modules. In order to ensure that the system is working properly, personnel should run a scan at least once a day and inspect the image of a test piece to ensure that needed safety systems were working properly. On a monthly basis, there should be inspection of all external cables for possible wear or damage as well as inspection of the "Scan in Progress" light to ensure that all words are illuminated. On a semiannual basis, there should be inspection of the functionality of the X-ray power supply, the controller, and the internal control computer, as well as for all warning lightbulbs.

The equipment was to be serviced only by qualified and trained service providers. Operators of the equipment were not to open any cabinets. The ultimate responsibility for the radiation safety of the system, the operators, and the general public rests with the owner,[19] which designated individuals responsible for ensuring compliance with the requirements of ANSI/HPS N43.17-2009. The owner was also responsible for ensuring a personnel training program, with refresher training provided at least once every 12 months.

Key Finding: Equipment manufacturers recommend that a test piece be scanned daily to evaluate proper operation of the AIT system because this ensures that many of the needed safety system requirements in ANSI/HPS N43.17-2009 work properly. The committee agrees with this recommendation but was unable to determine if this was being done because of the current lack of X-ray backscatter AITs in the field at commercial airports.

Committee Review of the Interlocks on the Rapiscan Secure 1000 System

The committee considered potential failure mechanisms that could result in X-ray overexposure of the person being screened or bystanders such as the operator. On the Rapiscan Secure 1000 located at NIST, committee members verified that the X-ray source can be activated only with the key in the "on" position with a scan initiated and that the key cannot be removed unless it is in the "off" position.

[19] In this case, the owner would be TSA.

The committee confirmed that the X-ray source turns off at the end of each scan. Scans could not be initiated if any of the panel doors enclosing the X-ray source and other electronics were ajar or if the emergency-off button had been activated. The committee verified that the X-ray source turned off immediately even though the vertical mechanical scan bar completed full travel to the park position at the top or bottom of the AIT system. These investigations are listed, together with previous studies' findings, in Tables 6.5 and 6.6 in Chapter 6 for comparison to other researchers' results and also given in Table 7.10.

The subcontractor's measurements required that the vertical scan bar be locked at a specific height. To enable this configuration, the AIT system was put into engineering mode, which requires a higher-level password than that used for screening but gives greater access to controlling individual functions. This way, the vertical scan motor was turned off and the scan bar was moved by hand. Table 7.10 summarizes the committee's review compared to ANSI/HPS N43.17-2009, Section 7.2, "Indicators, Controls, and Safety Interlocks."

The committee was able to confirm that the Rapiscan Secure 1000 AIT system installed at NIST met 6 of the 14 ANSI/HPS N43.17-2009, Section 7.2.1 requirements for all radiation-emitting devices and 5 of the 6 ANSI/HPS N43.17-2009, Section 7.2.2 requirements for general-use radiation-emitting devices. One requirement (7.2.1 f) is site specific and could not be verified outside of observing an AIT system in operation in an airport, and two of the requirements (7.2.1 g, h) could not be confirmed because they would require the deliberate activation of a potentially destructive fault, which NIST would not allow. Requirements 7.2.1 k and 7.2.2 f do not apply to portals that require the subject being screened to be stationary, such as the Rapiscan Secure 1000. An additional three requirements (7.2.1 j, l and 7.2.2 e) could not be confirmed because the operational AIT system cannot be forced to perform the action, but the committee believes that these faults in the field would distort the image to the extent that the screener could not make a pass/fail determination for that screening, and the screening would not result in overexposure of the person being screened. Once the AIT systems use automatic threat recognition, the operators will not see the image, and this check would no longer apply.

Requirement 7.2.1 m states that no malfunction of the AIT system shall result in an exposure exceeding 250,000 nSv. The committee could identify no failure mechanism that would result in an increase in the X-ray photon emission from the X-ray source (e.g., increasing the X-ray tube voltage or current) so that scanning time is the only malfunction that could result in X-ray exposure exceeding the ANSI standard. In this report, the committee shows that for a standard screening of approximately 6 seconds, the computed effective doses are about an order of magnitude lower than the recommended ANSI standard of 250 nSv/screen. The person being screened would have to stand in the AIT system with the X-ray source

TABLE 7.10 Summary of the Committee's Review of the Rapiscan Secure 1000 Compared to the Requirements in Sections 7.2.1 and 7.2.2 of ANSI/HPS N43.17-2009

Text	Committee Comments
ANSI/HPS Section7.2.1	
a. There shall be at least one indicator, clearly visible from any location from which a scan can be initiated, that indicates when a scan is in progress.	Confirmed on NIST AIT system.
b. There shall be at least one lighted indicator clearly visible from the inspection zone. For portal systems the indicator shall be visible from any approach to the inspection zone to indicate that a scan is in progress.	Confirmed on NIST AIT system.
c. Power to the system shall be controlled by a key switch. The key shall be captured (unable to be removed) whenever it is in a position that allows exposures to be initiated.	Confirmed on NIST AIT system.
d. Each system shall have a means for the operator to initiate the emission of radiation other than the function of an interlock or the main power control.	Operator initiates scan from computer console. Confirmed on NIST AIT system.
e. Each system shall have a means for the operator to terminate the emission of radiation other than the function of an interlock.	"Stop scan" icon included on computer screen. Confirmed on NIST AIT system.
f. Means shall be provided to ensure that operators have a clear view of the scanning area.	Operational requirement that is site specific. Not confirmed on NIST AIT system.
g. A ground fault shall not result in the generation of X rays or activate a scan beam from a sealed radioactive source.	Committee unable to confirm impact of a ground fault.
h. Failure of any single component of the system shall not cause failure of more than one safety interlock.	Committee unable to determine the impact of component failure.
i. A tool or key shall be required to open or remove access panels. Access panels shall have at least one safety interlock.	Confirmed on NIST AIT system.
j. For stationary-subject systems, the scanning motion of the X-ray beam relative to the subject shall be interlocked and the exposure shall terminate when the rate of motion of the beam in any direction falls below a preset minimum speed.	Not confirmed. Committee believes image quality would prevent operation in these conditions when advanced imaging technology is not used.
k. For portal systems, the minimum walking or driving velocity through the inspection zone shall be determined by the manufacturer.	Not applicable to stationary subject AIT systems.
l. Operational interlocks shall terminate the primary beam in the event of any system problem that could result in abnormal or unintended radiation emission.	Not confirmed. Committee believes increased radiation exposure would distort image or cause daily test to fail.

TABLE 7.10 Continued

Text	Committee Comments
m. In the event of a malfunction, the system shall terminate radiation exposure rapidly enough so that no location on the subject's body shall receive an ambient dose equivalent (H*10) exceeding 250 μSv (250,000 nSv), regardless of the size of the exposed area.	In this report it is shown that for a normal scan the computed effective doses are about an order of magnitude lower than the recommended ANSI standard of 250nSv/screen. Comparing the 6 second scan and ~25 nSv/screen versus a 250,000 nSv limit, the exposure would have to last for more than 16 hours.
n. Following interruption of X-ray production or external gamma emission by the functioning of any safety interlock, resetting the interlock shall not result in the production of X rays or emission of gamma radiation.	Confirmed on NIST AIT system.
ANSI/HPS Section 7.2.2	
a. For any X-ray system that normally keeps high voltage applied to the X-ray tube at times other than during a scan, there shall be at least one lighted "X ray on" indicator at the control console where X rays are initiated indicating when X rays are being produced.	Confirmed on NIST AIT system.
b. Technique factors for each mode of operation shall be preset by the manufacturer and shall not be alterable by the system operator.	Confirmed on NIST AIT system that technique factors cannot be changed when AIT system is in operator mode. Verified in discussion with TSA.
c. Each access panel to the X ray source shall have at least one safety interlock to terminate the X-ray production when opened.	Confirmed on NIST AIT system.
d. The following warning label shall be permanently affixed or inscribed on the X-ray system at the location of any controls used to initiate X-ray generation: "CAUTION: X-RAYS PRODUCED WHEN ENERGIZED."	Confirmed on NIST AIT system.
e. X-ray emission shall automatically terminate after a preset time or exposure.	Not confirmed. Assumed to have been demonstrated at the time of qualification.
f. For portal systems, motion sensors shall monitor the speed of pedestrians or vehicles through the inspection zone (in the forward direction) and the radiation exposure shall terminate when the speed drops below the minimum (as determined according to Section 7.2.1k).	Not applicable to stationary subject AIT systems.

operating for approximately 10,000 times longer than a single scan (16 hours) to approach the limit set in Section 7.2.1 m, an obviously long time. The committee considers this requirement to be met because the X-ray source is not capable of producing a higher X-ray energy or flux, and the time a person would have to stand in the AIT system to receive such a dose is unrealistically long.

The overall committee assessment is that the Rapiscan Secure 1000 as designed meets the requirements of ANSI/HPS N43.17-2009.

> **Key Finding:** Based on the committee's review and test of the Rapiscan Secure 1000's interlocks, the committee was unable to identify any circumstances where an accidental failure or a deliberate reconfiguration of the AIT system could result in either a person being screened or the operator receiving an effective dose larger than that from a normal screening.

Because there is no failure mechanism that would give more than a normal screening dose, as stated in the key finding, scanning time is the only factor left. The AIT system would have to operate for more than 16 hours to exceed the dose limit of 250,000 nSv as stated in Table 7.10 (row 7.2.1 m); it is unreasonable to expect that a person being scanned would be exposed for that amount of time.

In addition, it is worth mentioning that the AIT system inspected at NIST cannot be reconfigured remotely because it is not connected, nor can it be connected, to the Internet or by modem to any other device. Reconfiguration can only be done from the AIT system itself.

SUMMARY OF KEY FINDINGS FOR BOTH MEASURED SYSTEMS

The key parameters for the Rapiscan Secure 1000 and the AS&E SmartCheck systems to be used in the dose computations are summarized in Table 7.11.

TABLE 7.11 Summary Measurement Results for the Rapiscan Secure 1000 and the AS&E SmartCheck

	HVL_1 (mm Al)	HVL_2 (mm Al)	50 PDD (mm)	Air Kerma (nGy)	E_{REF} (nSv)
Rapiscan anterior	0.92	1.47	~11	30.6	3.5
Rapiscan posterior	0.85	1.42	~11	29.8	3.2
AS&E	1.1	1.7	~12.5	113	15.5

NOTE: E_{REF}, reference effective dose; HVL_1, first half-value layer; HVL_2, second half-value layer; PDD, percent depth dose .

DOSE COMPUTATIONS

Objectives

The charge to the committee included the task of determining if radiation exposures received during X-ray backscatter AIT screening were in compliance with applicable health and safety standards for the general public and occupationally exposed individuals. It is clear from previous reports (reviewed in Chapter 6) and the measurements that the NRC subcontractor made (see earlier in this chapter), together with the computations below, that the AIT systems evaluated meet the ANSI requirement for E_{REF} below 250 nSv per screening. However, it has been speculated in recent years that it might be possible for some individuals to receive an effective dose, E, during a screening that exceeds the E_{REF} by a large enough margin to result in exposures exceeding ANSI recommendations. Therefore, one of the efforts with this independent study was to go beyond previous evaluations (see studies described in Chapter 6) to include an assessment of absorbed dose and effective dose for adults, children, and pregnant women under routine screening conditions as well as doses that might be received as a result of serious malfunctions.

Introduction

The NRC subcontractor Wesley Bolch, Advanced Laboratory for Radiation Dosimetry Studies, J. Crayton Pruitt Family Department of Biomedical Engineering, University of Florida, applied state-of-the-art computational techniques to assess the organ-absorbed dose and whole-body effective dose received by adults, children, and the developing fetus of pregnant females scanned by a computationally modeled X-ray backscatter AIT system and by variations on that system that include some current and anticipated engineering designs. Passengers were simulated using a suite of hybrid digitized phantoms. The computational phantoms used in this study were obtained from the University of Florida computational hybrid phantom library.[20,21] The phantoms are constructed as a collection of mathematical surfaces based in NURBS (non-uniform rational basis spline) that define the shapes and locations of individual internal organs as well as the body surface contour. From this library, each phantom was adjusted using targeted values for sitting height (i.e., based on the length of the torso, neck, and head) and four body circumferences:

[20] A.M. Geyer, S. O'Reilly, C. Lee, D.J. Long, and W.E. Bolch, The UF/NCI family of hybrid computational phantoms representing the current US population of male and female children, adolescents, and adults—Applications to CT dosimetry, *Physics in Medicine and Biology* 59(18):5225-5242, 2014.

[21] M.R. Maynard, N.S. Long, N.S. Moawad, R.Y. Shifrin, A. Geyer, G. Fong, and W.E. Bolch, The UF family of hybrid phantoms of the pregnant female for computational radiation dosimetry, *Physics in Medicine and Biology* 59:4325-4343, 2014.

waist, buttocks, arm, and thigh. Human morphometric data were obtained from the National Health and Nutrition Examination Survey database, from data collected between 1999 and 2006. The phantom library covers the 5th to 95th height and weight percentiles for children and adolescents (age 2 to 20) and adults (age 20 to 85) in the United States.

This family of hybrid computational phantoms was based on a set of reference phantoms representing ages 1, 5, 10, and 15 and adult males and females. These reference phantoms have heights, weights, and masses for internal organs described in International Commission on Radiological Protection (ICRP) Publication 89.[22] Scaling was then performed to either increase or decrease the torso height together with the volumes, and hence the mass, of all internal organs. The final stage was to add or subtract subcutaneous fat to create phantoms of different weights, thus forming an array of phantoms of differing height and weight combinations. The assigned body mass index (BMI) for each phantom is not unique because a number of different combinations of height/weight can yield an equivalent value of BMI. This process for phantom library creation does not include the possibility that a given phantom will have its assigned weight based on increases or decreases in skeletal muscle or lean body mass. The implicit assumption is that weight changes at a given phantom height are dictated by proportional changes in subcutaneous fat. It does not imply that these phantoms represent the only or true morphology for that value of BMI for all airline passengers.

These computations were not designed to estimate radiation exposure to specific individuals. The methodology was developed to provide estimates of radiation doses received by a population of passengers with a range of morphologies during routine screening. This was complimented with a series of sensitivity studies to investigate additional variations. The combination of these approaches provides information on the global uncertainties inherent in the computational approach.

The committee chose to use a generic mathematical model (or reference model) of an X-ray backscatter AIT system rather than an exact model of an existing system. The idea is that with such a model system it is possible to compare how differences in design and settings affect dose for not only previous systems but also potential future systems. Thus, a Monte Carlo simulation model of a reference X-ray backscatter AIT system was implemented for the computations. This reference system was based on a compilation of information assembled from the following sources:

[22] International Commission on Radiological Protection, *Basic Anatomical and Physiological Data for Use in Radiological Protection Reference Values*, ICRP Publication 89, *Annals of the ICRP* 32(3-4), 2002.

1. Previous reports documenting approximate scanning geometry, including vertical transport of the X-ray source, beam size and divergence, and polar angle of the beam as a function of elevation;
2. Previous reports documenting information on beam intensity (i.e., air kerma) as a function of vertical and horizontal position of the X-ray beam;
3. Data acquired by the committee from measurements of HVL in aluminum;
4. Data acquired by the committee from measurements of PDD in tissue-equivalent material; and
5. The ability to have just an anterior or both an anterior and a posterior system.

The simulated X-ray backscatter AIT system is a reference system composed of information available to the committee at the time it conducted its investigation. The nature of this Monte Carlo approach is such that the results can be scaled to any system with similar geometry and photon energy distribution by multiplying the ratio of the air kerma from any other AIT system to the air kerma of the AIT reference system.

Three populations of air passengers were simulated as follows:

1. Reference adult males and females at 50th percentile height and at five different weight percentiles;
2. Children (male and female) at ~105 cm height and at three different weight percentiles; and
3. The developing fetus of pregnant females at three periods of gestation.

In addition to routine or standardized scanning operations, the following sensitivity studies were performed to evaluate variations that might affect compliance with the radiation protection standards:

1. The effect of variations in the irradiation geometry of the reference system and the presumption of a simplified broad parallel beam of the same energy distribution[23] on organ and effective dose;
2. The effect of variations in organ and effective dose due to changes in the horizontal location of the screened passenger between the anterior and posterior units;

[23] This study was conducted to enable evaluation of and comparisons to AIT systems that may not include angular variations in the vertical and horizontal scan, which is created by tilting the X-ray source as it moves from the bottom to the top of the scanning region and fixed horizontal position of the tube anode. The study also intends to do comparisons with previous computations that made the parallel beam assumption due to modeling limitations of their Monte Carlo approach.

3. Assessment of both organ and effective dose as a function of X-ray tube potential greater than the nominal 50 kV;
4. Assessment of the radiation absorbed dose averaged across the entire skin of an adult passenger (both dermis and epidermis) during one screen as compared to the associated radiation dose to the radiosensitive region of skin at a depth of 50 to 100 μm from the skin surface, also averaged across the total body; and
5. Assessment of the radiation absorbed dose per screen to the adult female breast and lens of the eye and a central region of the skin during a presumed worst-case malfunction where the horizontal and vertical sweep remained stationary for the same duration as that of a normal scan.

X-Ray Source Term

Features of the Reference AIT System

To develop the mathematical model of the reference AIT system, some features reported by NIST were adopted, including (1) the relative geometrical configurations of the anterior and posterior scanning units and their X-ray tubes; (2) the relative values of horizontal and vertical air kerma within the scanning region; and (3) the measured air kerma per scan at a reference point (used to normalize the Monte Carlo organ doses). The geometry of the scanning units is discussed in a later section. Items 2 and 3 were incorporated directly into the construction of the X-ray source term used to irradiate the computational phantoms during virtual screening simulations.

The horizontal (parallel to AIT system face) and vertical exposure maps, shown in Figures 7.9 and 7.10, provided an approximate measure of the relative photon fluence at a plane located a fixed distance from the anterior and posterior units. The figures are normalized to 1.0 at the location in the two-dimensional plane having the maximum value of air kerma (i.e., at a vertical distance of 192 cm from the mat). These distributions of relative exposure were implemented for the reference AIT system and formed the basis for particle sampling functions used in the virtual X-ray source term for both the anterior and the posterior unit.

The results of the Monte Carlo process are initially normalized to the absorbed dose per incident photon.[24] The objective is to obtain the effective dose per scan, which in turn requires the number of incident photons per scan. This "normaliza-

[24] Because Monte Carlo calculations follow the histories of individual photons and average the results over large numbers of photons, the result is the energy deposited (or absorbed dose) per photon. The absorbed dose at a specified location resulting from exposure to a specific number of photons is the sum of the absorbed doses at that specified location produced by each of the protons.

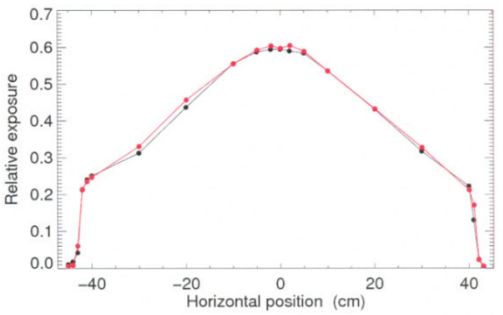

FIGURE 7.9 Horizontal exposure variation of the posterior unit measured at a height of 100 cm from the mat at a distance of 30 cm from the front plane of the AIT system (red, upward scan; black, downward scan). The maximum exposure from the posterior unit was measured at a vertical position of 192 cm and a horizontal position of 0 cm. SOURCE: Figure 10 from NIST Report to DHS, *Assessment of the Rapiscan Secure 1000 Single Pose (ATR version) for Conformance with National Radiological Safety Standards*, Jack L. Glover, Ronaldo Minniti, Lawrence T. Hudson, and Nicholas Paulter, National Institute of Standards and Technology, Gaithersburg, Md., final report related to IAA No. HSHQDC-11-X-00585, April 19, 2012.

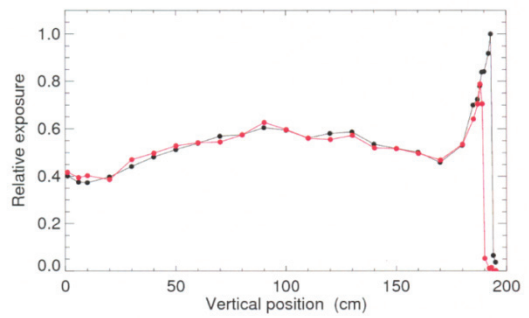

FIGURE 7.10 Vertical exposure variation of the posterior unit along the central axis of the person being scanned at a distance of 30 cm from the front plane of the AIT system. The greatest exposure is seen toward the top of the scan. The downward scan (black) shows a maximum at a height of 192 cm. The upward scan (red) shows its maximum at a height of 188 cm. SOURCE: Figure 11 from NIST Report to DHS, *Assessment of the Rapiscan Secure 1000 Single Pose (ATR version) for Conformance with National Radiological Safety Standards*, Jack L. Glover, Ronaldo Minniti, Lawrence T. Hudson, and Nicholas Paulter, National Institute of Standards and Technology, Gaithersburg, Md., final report related to IAA No. HSHQDC-11-X-00585, April 19, 2012.

tion factor" is obtained from the ratio of measured air kerma per scan to the Monte Carlo-simulated value of air kerma per photon. This yields the number of photons per scan. The results presented in the following sections are normalized to a value of 9.203×10^8 photons per scan, which corresponds to an air kerma of 68 nGy/scan representing a simulated scanning protocol for the reference AIT system. All results relating to organ absorbed dose and effective doses received during passenger screening will scale linearly with the value of air kerma.

Photon Energy Distribution Using HVL and PDD

The energy spectrum of the incident photons is a major component of the input to the Monte Carlo calculations. The MATLAB-based code SPEKTR,[25] based on the methods presented by Turner et al.,[26] was used to generate a candidate spectrum. It generates a candidate "soft" clinical X-ray spectrum based on entering the high (peak) voltage, in kilovolts (kV), and high-voltage ripple.[27] Typically, the user then "hardens" the candidate spectrum by calculating the effect of filtering the spectrum with a selected absorbing material (e.g., aluminum) until the resulting HVLs of this modified spectrum match the measured values. This process yields the representative spectrum emerging from that X-ray tube and inherent filtration.

The first available data from the NRC subcontractor yielded an HVL (HVL_1) of 1.18 mm Al obtained from measurements of an AS&E SmartCheck AIT system. However, the candidate spectrum using 50 kV generated by SPEKTR had an HVL_1 value of approximately 1.45 mm Al. The candidate spectrum was therefore "softened" by iteratively adding low-energy photons using an inverse process of exponential attenuation as a function of photon energy. The eventual result was a suitably softened spectrum with an HVL_1 matching that initially measured for the AS&E SmartCheck. Figure 7.11 visually compares the original candidate spectrum and the softened spectrum matching the AS&E SmartCheck HVL_1 values initially measured.[28]

[25] J.H. Siewerdsen, A.M. Waese, D.J. Moseley, S. Richard, and D.A. Jaffray, Spektr: A computational tool for x-ray spectral analysis and imaging system optimization, *Medical Physics* 31:3057-3067, 2004.

[26] A.C. Turner, D. Zhang, H.J. Kim, J.J. DeMarco, C.H. Cagnon, E. Angel, D.D. Cody, D.M. Stevens, A.N. Primak, C.H. McCollough, and M.F. McNitt-Gray, A method to generate equivalent energy spectra and filtration models based on measurement for multidetector CT Monte Carlo dosimetry simulations, *Medical Physics* 36:2154-64, 2009.

[27] Power supplies of today have very little ripple, and thus the voltage is close to constant and the peak value (Vp) is the same as the average value; in this case, it is enough to report the voltage (V) instead of Vp and the ripple.

[28] The initial measurements were used for designing the generic computation model for dose calculations; later, the measurements were refined and are reflected in the reported values of Table 7.11.

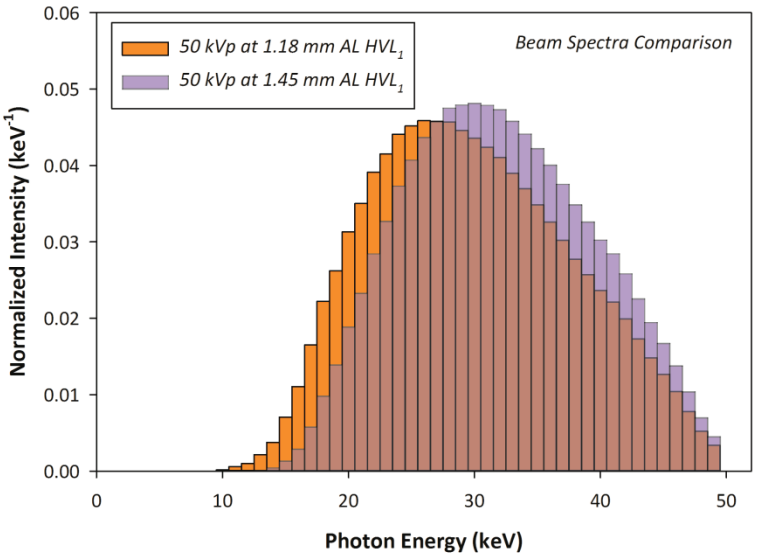

FIGURE 7.11 Comparison of the initial calculated X-ray spectrum at 50 kV yielding a first half-value layer (HVL_1) of 1.45 mm of aluminum (mm Al) and the revised softened spectrum that yields an HVL_1 of 1.18 mm Al. SOURCE: Tom Borak.

Energy Sampling

The softened energy spectrum shown in Figure 7.11 was incorporated into the computational X-ray source term. Standard Monte Carlo methods based on random numbers were used to sample photon energies for the emerging scanning beam with probabilities represented by this distribution.

Simulating the Scanning X-Ray Beam Spot Incident Upon the Passenger

The objectives of this process are both to reproduce the intensity of the X-ray beam at locations in the y-z reference plane and to include the direction or vector of the beam as it intercepts the passenger. This depends on the tilt angle of the beam during vertical translation and on the lateral angle of the beam spot as it scans horizontally.

Vertical and Horizontal Intensities of Scanning Beam

The basis for sampling the origin and direction of the photons used for the X-ray source term of the reference AIT system are given in Figures 7.9 and 7.10. The software PlotReader™ was used to manually capture data points from each figure. NIST reported relative exposures in the reference plane for both upward and downward scanning motions. Upward and downward exposure data were averaged at each point for each figure. The horizontal data (Figure 7.9) were then fitted piece-wise to two Gaussian functions and then normalized. The vertical data (Figure 7.10) were digitized into 1 cm bins using linear interpolation in MATLAB™ and then normalized. The horizontal and vertical data sets now represented the relative distribution of photons (as a function of y and z) that should be expected at a reference plane located 30 cm from and parallel to the front plane of a scanning unit. These relative distributions were assumed for both the anterior and the posterior unit. An implicit assumption in this work is that this X-ray energy distribution was constant across all horizontal angles of the beam sweep.

Photon Starting Position and Direction

Randomly sampling the two probability distributions representing Figures 7.9 and 7.10 described above provides the location of a photon incident upon a reference plane located 30 cm from the front of a scanning unit. The starting position of the photon was determined by linearly mapping (ray tracing[29]) back toward the geometric location of the X-ray source in the reference AIT system, accounting for additional specifications such as vertical translation and tilt angle of the source associated with that vertical position. The ray trace provides a unit vector corresponding to the direction of the emitted photon.

Normalization to Air Kerma

All results provided by the MCNPX code were normalized to the number of starting source photons. The number of starting source photons must be scaled by the total number of X-ray photons per scan to yield doses in absolute units. The user must, therefore, post-process results with some physical quantity (or quantities) to provide an anchoring between simulated and physical dose quantities. All results from a scan simulation obtained in this manner must be multiplied by a "normalization factor" to convert, for example, from dose-to-passenger per starting photon to dose-to-passenger per scan. Once the X-ray source term was constructed

[29] *Ray tracing* is a technique for generating an image by tracing the path of light (or X rays) through the pixels in an image plane and simulating the effects of its encounters with virtual objects such as, in this case, the human phantom or parts of the X-ray backscatter AIT system.

and compiled, the normalization factor was estimated by simulating a virtual air kerma measurement analogous to that made with a physical ion chamber in an earlier report (68 nGy per scan at a known location).[30] A sphere of air with a radius and location equivalent to the Radcal Corporation ion chamber used by NIST was modeled in MCNPX and irradiated using the simulated X-ray source term. The NIST air kerma measurement was divided by the resulting virtual air kerma (nGy per starting photon), yielding an estimate of the total number of photons emitted per scan (9.203×10^8 photons per scan in this study). It was not necessary to model the complex geometry of the NIST ionization chamber because the chamber was calibrated by NIST to provide an air kerma measurement to a similarly sized volume of air as was modeled in MCNPX.

Validation of Monte Carlo Sampling Procedures

The X-ray source term was validated in three ways: (1) by confirming that the simulated virtual scans were generating the desired photon energy fluence and thus the correct HVL; (2) by comparing simulated and analytical normalization factors; and (3) by comparing simulated PDD with measured PDD.

The virtual fluence validation was achieved using the reference plane located 30 cm away from and parallel to the front plane defining the scanning region of the AIT system. The surface was divided into 1-cm bins along the horizontal and vertical directions. Virtual scans were performed using the X-ray source term, and the photon fluence in each of the surface bins was quantified and plotted. As expected, the photon fluence as a function of horizontal and vertical distance (Figure 7.12) mirrors the composite of Figures 7.9 and 7.10, indicating that the distribution of photons produced by the simulated reference AIT system is very similar to that produced by the Rapiscan Secure 1000 AIT system tested at NIST.

The normalization factor derived from MCNPX (9.203×10^8 photons per scan) was validated via comparison to a calculated normalization factor. Using the HVL_1-matched (1.18 mm Al) 50 kV spectrum, mass energy-absorption coefficients for air (a standard NIST table[31]) were used to calculate the number of photons required to deliver 68 nGy to a volume of air equal in size to the detector used for air kerma measurements. Additionally, using MCNPX, the fluence into that volume of air

[30] The value of 68 nGy was selected based on an earlier measurement made by NIST because measurements by the NRC subcontractor of air kerma per scan were not available when it was necessary to begin the Monte Carlo computations. All results relating to organ absorbed dose and effective doses received during passenger screening will scale linearly with the value of air kerma. NIST has since updated its report, and, therefore, 68 nGy is considered a generic value.

[31] P.J. Lamperti and M. O'Brien, *NIST Measurement Services, Calibration of X-Ray and Gamma-Ray Measuring Instruments,* NIST Special Publication 250-58, April 2001, http://www.nist.gov/calibrations/upload/sp250-58.pdf.

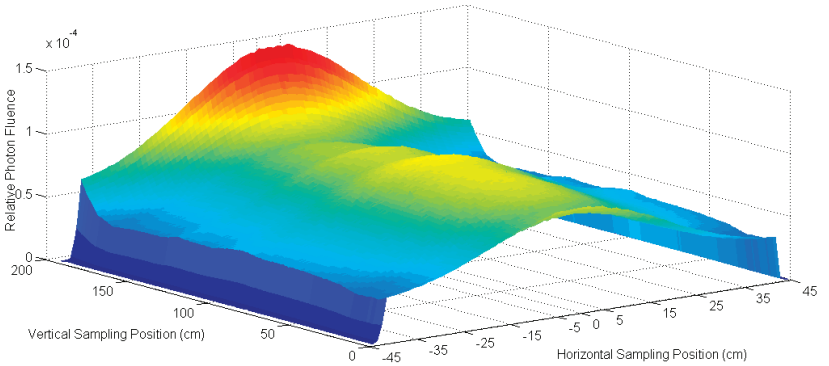

FIGURE 7.12 Composite horizontal and vertical relative photon fluence at plane 30 cm from front plane of a scanning unit as simulated in MCNPX. SOURCE: Tom Borak.

from one complete scan was calculated to make the value relative to one scan. A calculated value (8.00×10^8 photons per scan) based on a first collision approximation was within 15 percent of the normalization factor derived from MCNPX.

The validation using PDD was achieved by virtually simulating the pertinent irradiation geometry adopted by the NRC subcontractor during the physical measurements. The beam was modeled simulating a full horizontal scan with a 3 mm vertical collimation. The virtual simulations incorporated a soft tissue phantom with density and elemental compositions comparable to the physical phantom material used in the physical measurements. The detailed geometry of the parallel-plate ionization chamber did not need to be modeled in the virtual simulations because the software was able to estimate tissue absorbed dose directly. Simulated doses were quantified as a function of depth in the virtual tissue phantom and used to generate a PDD curve. The simulated PDD is compared to the measured PDD in Figure 7.13.

Description of the Passenger Irradiation Geometry

A visual representation of the irradiation geometry used for the reference AIT system is provided in Figure 7.14. The NIST coordinate system was adopted (Figure 7.1), where the x-axis is the direction parallel to the faces of the scanning units, the y-axis is the direction orthogonal to the faces of the scanning units, and the z-axis is the vertical direction. The distances between the AIT system's anterior and posterior surfaces (109 cm) and planes (87 cm) were obtained from the NIST report.[32] The distance from the anterior plane to the source (48 cm) was also ob-

[32] Glover et al., *Assessment of the Rapiscan Secure 1000 Single Pose (ATR version) for Conformance with National Radiological Safety Standards*, 2012.

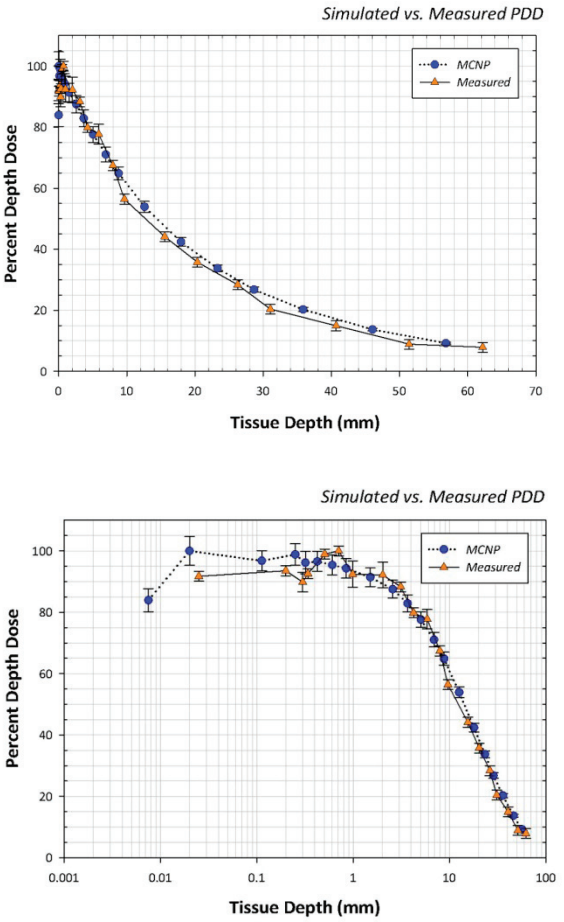

FIGURE 7.13 Comparisons between measured and percent depth dose (PDD) in tissue equivalent material. Blue circles are results from MCNP radiation transport simulation, and orange triangles are measurements by the NRC subcontractor on the AS&E SmartCheck system. Results are shown with (a) linear and (b) logarithmic depth scale. SOURCE: Tom Borak.

tained from the same NIST report. A reference point of 30 cm from the anterior plane was used in the irradiation geometry. The horizontal (x-axis) scan width was approximately 90 cm at this point, according to measurements detailed in the NIST report discussed in this section. Based on visual inspection of a Rapiscan Secure 1000 unit at TSIF, the source vertically traverses (z-axis) approximately 118 cm in one scan and reaches a maximum height of approximately 152 cm. The rotational angle of the source at its most vertical point (+45 degrees) was obtained from the original patent application. This configuration yields a maximum vertical scan height of approximately 230 cm. The rotational angle of the source at its lowest vertical point was estimated to be −26 degrees.

With the exception of the passenger-positioning-sensitivity calculations done

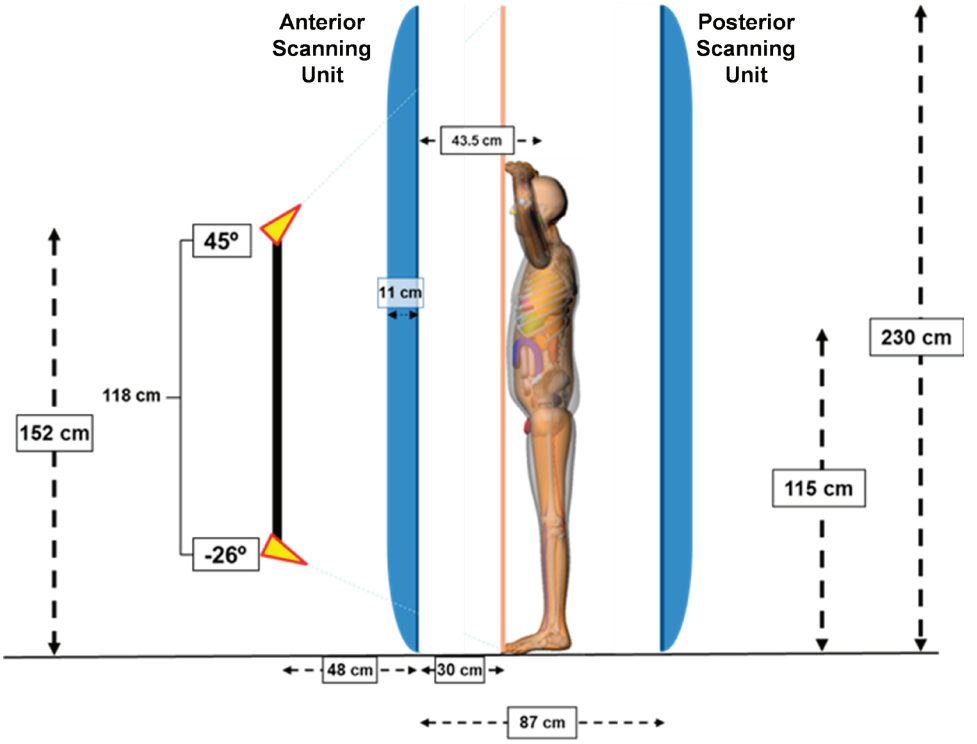

FIGURE 7.14 Dimensional data used to establish the irradiation geometry for the NRC reference X-ray backscatter AIT system used in the Monte Carlo radiation transport simulations. SOURCE: Thomas B. Borak and Wesley E. Bolch, University of Florida.

by the NRC subcontractor, all phantoms were centered as follows: (1) parallel to the faces of the AIT systems (x-axis), facing the anterior unit, and (2) between the anterior and posterior units (center of phantom at a distance of 43.5 cm from the front plane of the AIT system). All phantoms were arranged in a representative scanning position with arms raised (Figure 7.15). It is noted that because the virtual passengers were centered based on their anatomical extent, the locations of the feet were slightly different as the subject's body weight increased among the model series.

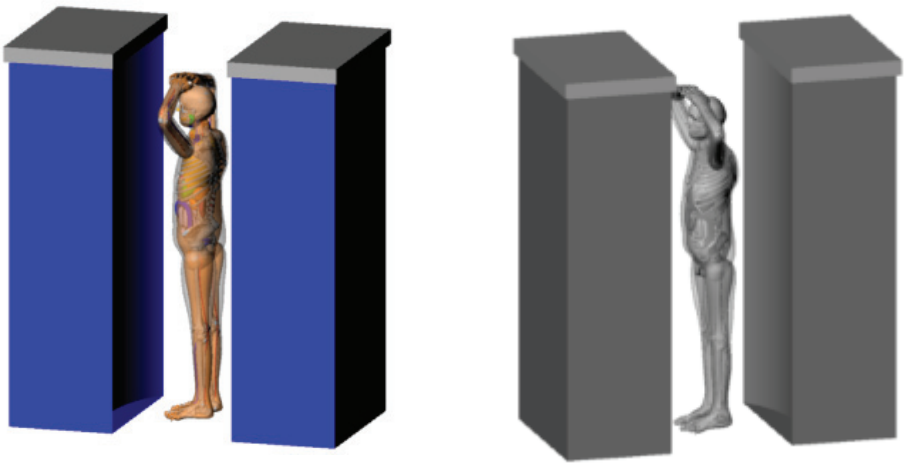

FIGURE 7.15 Graphical images of the computational hybrid phantom, an adult 50th percentile male, with arms raised and positioned within the scanning location between the anterior and posterior units. SOURCE: Wesley E. Bolch, University of Florida.

Adult Reference Phantoms

The adult males and females representing the 5th, 25th, 50th, 75th, and 95th percentiles for weight at their respective 50th percentile for height were utilized. Lateral and anterior-posterior views of the adult male and female phantoms that were used in these simulations are shown in Figures 7.16 and 7.17, respectively. The colored features provide visual distinction of tissues and organs. Gray regions represent variations in additional fat and surface skin. The figures do not include pixilation that quantitatively differentiates skin and subcutaneous fat.

Pediatric Phantoms

Pediatric male and female phantoms were chosen at a height of 105 cm and corresponding to 5th, 50th, and 95th percentiles for weight. The 105 cm height corresponds to an approximate age of a 4.5-year-old child. This height was meant to correspond to the shortest passengers that might be screened. Lateral and anterior-posterior views of the pediatric male and female phantoms that were used for these simulations are shown in Figures 7.18 and 7.19, respectively.

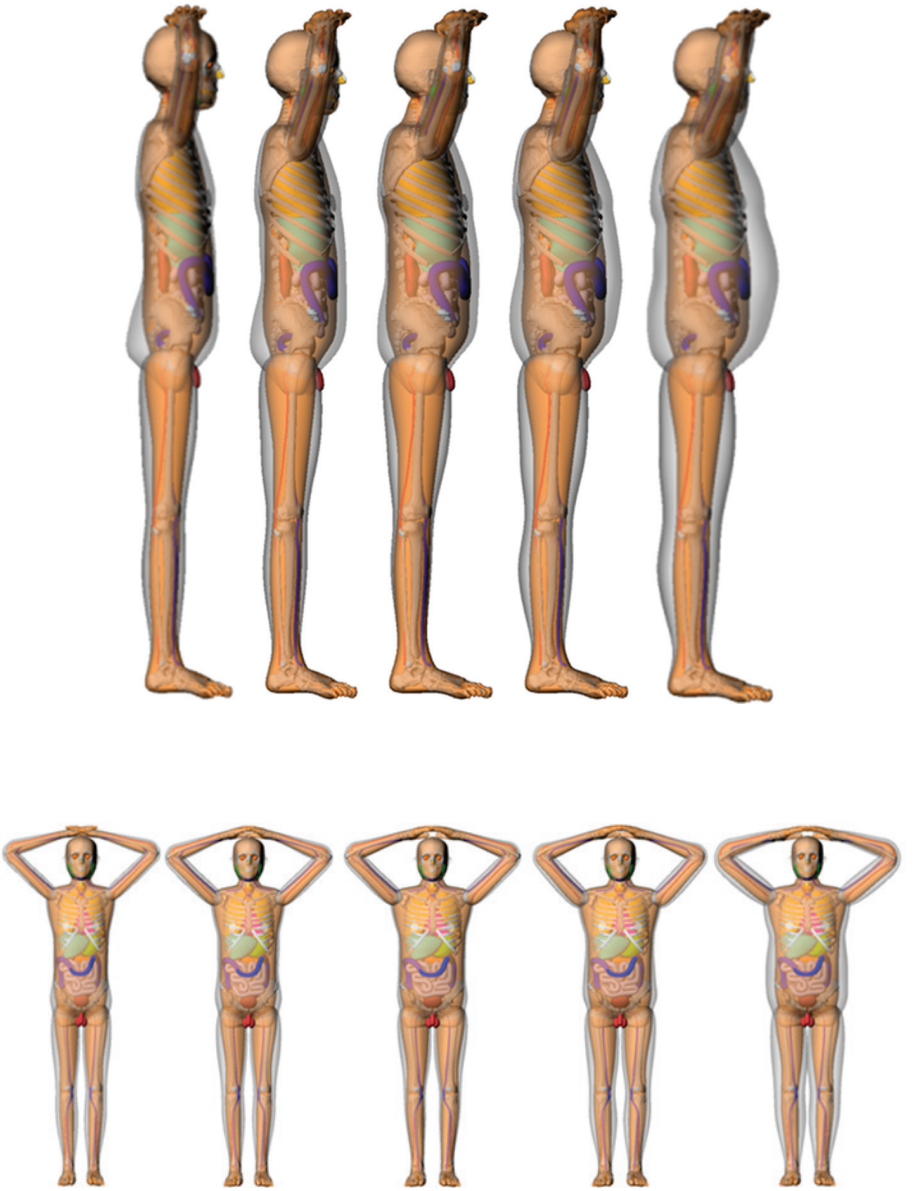

FIGURE 7.16 Left lateral (*top*) and anterior-posterior (*bottom*) views of the adult male phantoms used for the passenger screening simulations set at 50th percentile for height and varied by body mass index: (A) 5th percentile, (B) 25th percentile, (C) 50th percentile, (D) 75th percentile, and (E) 95th percentile. SOURCE: Wesley E. Bolch, University of Florida.

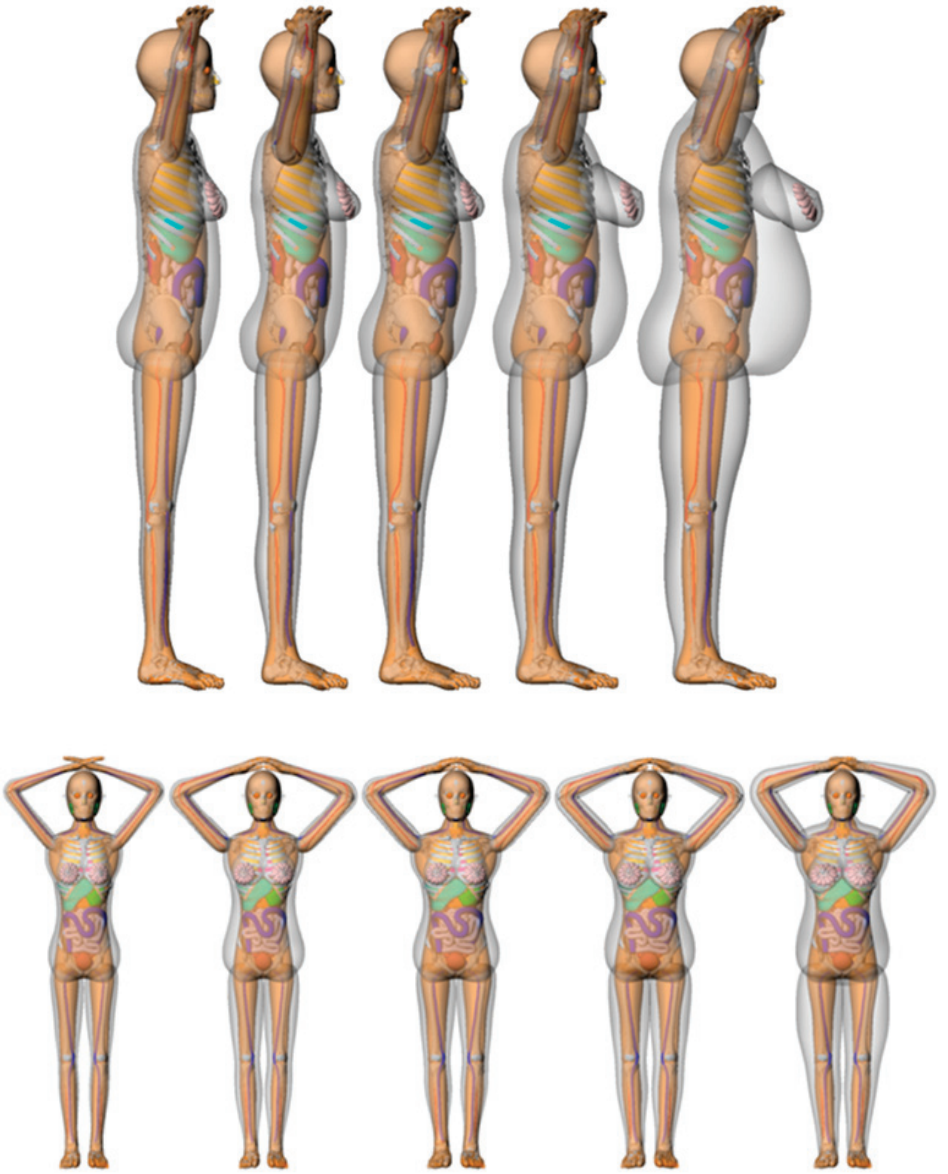

FIGURE 7.17 Lateral (*top*) and anterior-posterior (*bottom*) views of the adult female phantoms used for the passenger screening simulations set at 50th percentile for height and varied by body mass index: (A) 5th percentile, (B) 25th percentile, (C) 50th percentile, (D) 75th percentile, and (E) 95th percentile. SOURCE: Wesley E. Bolch, University of Florida.

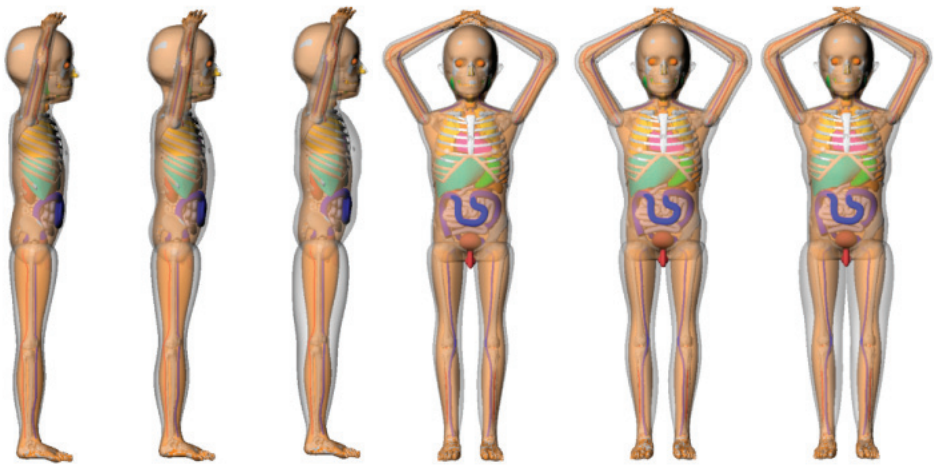

FIGURE 7.18 Left lateral and anterior-posterior views of the pediatric male phantoms used for screening simulations set at 105-cm height and varied by body mass index: (A) 5th percentile, (B) 50th percentile, and (C) 95th percentile. SOURCE: Wesley E. Bolch, University of Florida.

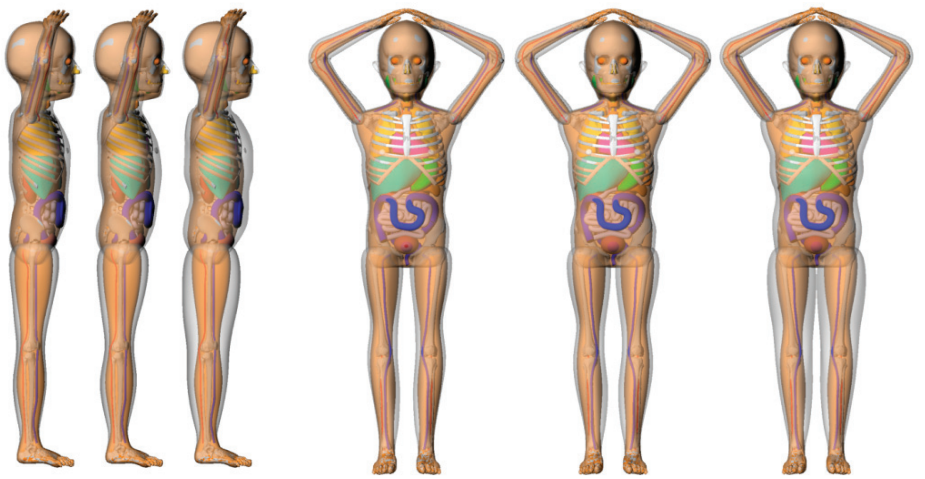

FIGURE 7.19 Left lateral and anterior-posterior views of the pediatric female phantoms used for screening simulations set at 105-cm height and varied by body mass index: (A) 5th percentile, (B) 50th percentile, and (C) 95th percentile. SOURCE: Wesley E. Bolch, University of Florida.

Pregnant Female Phantoms

The pregnant female phantom series provides highly detailed anatomical representation for eight fetal ages spanning an entire pregnancy. Three of these phantoms, representing fetal ages (post-conception) of 15 weeks, 25 weeks, and 38 weeks (Figures 7.20 to 7.22), were virtually screened in MCNPX to estimate fetal doses resulting from the simulated X-ray backscatter AIT system irradiation.

Dosimetry Results for Standard Screening Conditions

All phantom simulations presented in this report were performed in MCNPX v2.7 using the custom X-ray source term described earlier and the passenger positioning described above in Figure 7.14. All simulations were performed on the University of Florida HiPerGator supercomputer using particle history specifications that yielded sufficiently low relative errors (majority <1 percent). Anterior

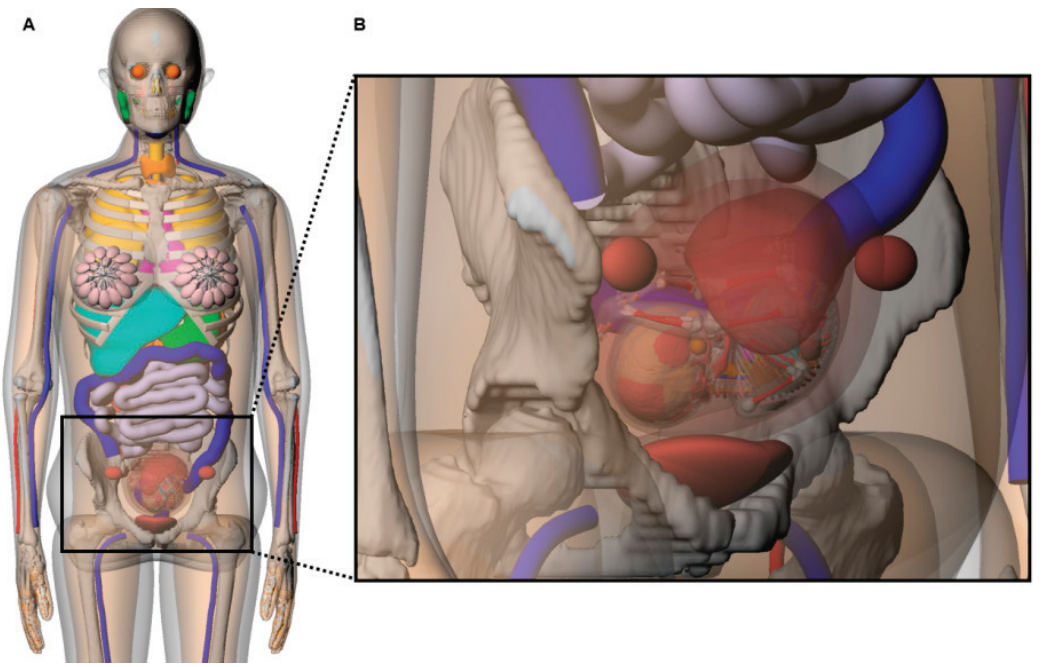

FIGURE 7.20 The 15-week pregnant female phantom: a frontal view (A) and magnified right-oblique view (B). SOURCE: Wesley E. Bolch, University of Florida.

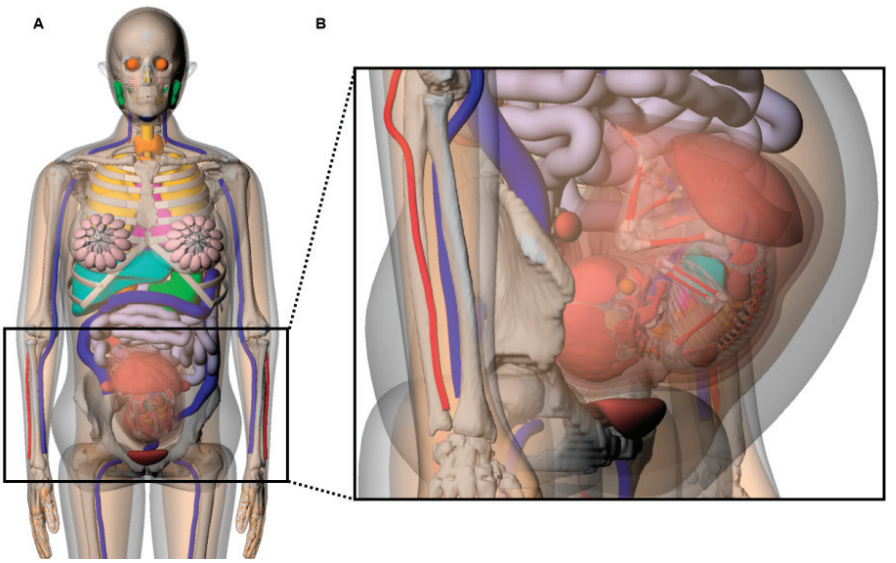

FIGURE 7.21 The 25-week pregnant female phantom: a frontal view (A) and magnified right-oblique view (B). SOURCE: Wesley E. Bolch, University of Florida.

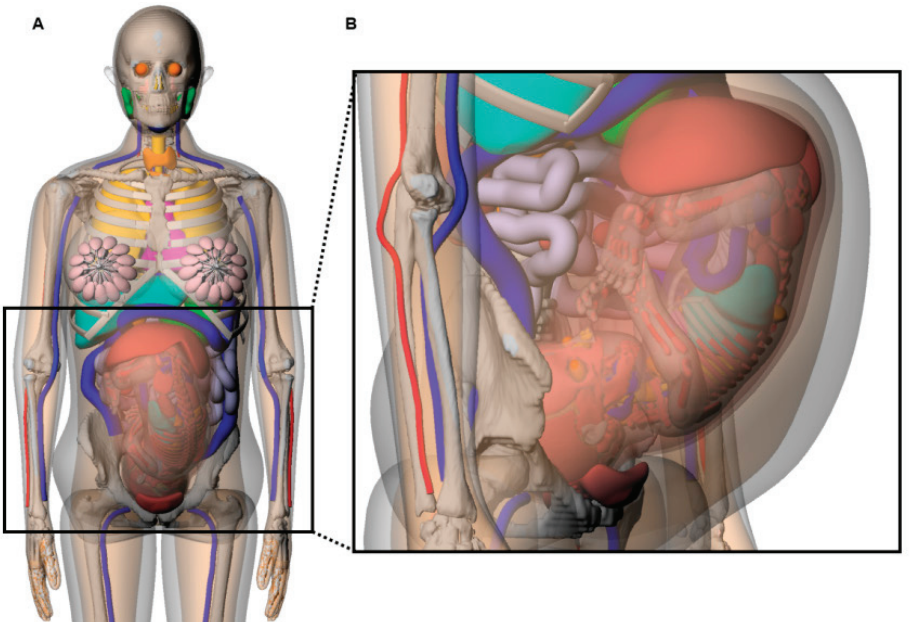

FIGURE 7.22 The 38-week pregnant female phantom: a frontal view (A) and magnified right-oblique view (B). SOURCE: Wesley E. Bolch, University of Florida.

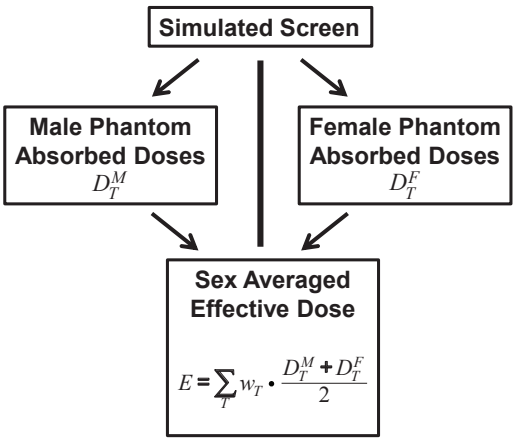

FIGURE 7.23 Diagram showing how the adult male and female phantom data are combined to obtain sex-averaged effective dose results for adult passengers. NOTE: M refers to male, F refers to female, and T refers to a specific tissue or organ. SOURCE: Tom Borak.

and posterior scans were simulated independently and mathematically summed to provide results for a total passenger protocol.

The effective dose is determined by applying tissue-weighting factors to all exposed tissues and organs. However, these weighting factors represent mean values for humans, averaged over both sexes and all ages. In order to facilitate comparisons of these results with the ANSI limit of reference effective dose, the committee combined the results of the male and female phantoms using the process outlined in ICRP Publication 103[33] (see Figure 7.23).

Results of the dosimetry calculations for adult passengers are shown in Table 7.12 (and for pediatric passengers in Table 7.13 and for the developing fetus in Table 7.14). The absorbed dose received per screen to pertinent organs is shown separately for males and females. Complete lists of absorbed doses for all male and female organs are provided in Appendix C. The effective dose is the value obtained by averaging the results from both male and female phantoms.

Sensitivity Analysis

Several sensitivity analyses were conducted to explore possible dose variation under different screening scenarios. These analyses include irradiation geometry, passenger position, skin sensitivity, failure modes, and X-ray energy and spectral shape.

[33] ICRP Publication 103, 2007.

TABLE 7.12 Summary per AIT Screening of Critical Organ Absorbed Dose and Effective Dose to Adult Passengers of 50th Height Percentile at Five Different Weight Percentiles

	Weight Percentiles, U.S. Adults				
	5th	25th	50th	75th	95th
Male absorbed dose per screen (nGy)					
Thyroid	31	27	24	24	16
Skin	44	43	43	42	42
Eye Lens	44	44	42	42	39
Female absorbed dose per screen (nGy)					
Breast	26	23	23	20	18
Thyroid	22	21	17	11	4
Skin	46	45	44	45	46
Eye Lens	46	44	43	37	32
Effective Dose (nSv)					
Per anterior scan	12	10	9	7	4
Per posterior scan	3	3	3	2	2
Per screen	**15**	**13**	**12**	**9**	**6**

NOTE: For comparison, the ANSI reference effective dose for an HVL_1 of 1.18 mm Al and an air kerma of 68 nGy per scan is 20 nSv.

TABLE 7.13 Summary per AIT Screening of Critical Organ Absorbed Dose and Effective Dose to Pediatric Passengers of ~105 cm in Total Height and Three Different Weight Percentiles

	Weight Percentiles, U.S. Children		
	5th	50th	95th
Male absorbed dose per screen (nGy)			
Thyroid	47	45	47
Skin	49	49	48
Eye Lens	60	60	60
Female absorbed dose per screen (nGy)			
Breast	43	39	32
Thyroid	47	44	48
Skin	49	46	48
Eye Lens	60	54	60
Effective Dose (nSv)			
Per anterior scan	20	18	16
Per posterior scan	6	5	5
Per screen	**25**	**23**	**22**

NOTE: For comparison, the ANSI reference effective dose for an HVL_1 of 1.18 mm Al and an air kerma of 68 nGy per scan is 20 nSv.

TABLE 7.14 Absorbed Doses per AIT Screening to the Fetus and Four Fetal Organs, Incurred during Anterior Scan, Posterior Scan, and Total Screen for the U.S. Adult Pregnant Female at 15 Weeks, 25 Weeks, and 38 Weeks Post-Conception

	Absorbed Dose (nGy)								
	15 Weeks Post-Conception			25 Weeks Post-Conception			38 Weeks Post-Conception		
	Anterior	Posterior	Screen	Anterior	Posterior	Screen	Anterior	Posterior	Screen
Whole body	7.2	1.3	**8.5**	3.4	0.6	**4.0**	3.4	0.9	**4.3**
Brain	3.7	2.3	**6.0**	0.8	1.4	**2.2**	0.5	2.7	**3.2**
Lungs	8.3	0.9	**9.2**	5.1	0.2	**5.3**	2.6	0.2	**2.7**
Thyroid	5.8	1.4	**7.2**	2.5	0.4	**2.9**	1.3	0.3	**1.6**
Active bone marrow	14	2.5	**16**	6.4	1.8	**8.1**	8.4	2.7	**11**

Standard Geometry versus Plane Parallel Beams

The effect of beam geometry on passenger dose was investigated in this analysis. Two beam geometries were simulated: a broad, uniform parallel beam, and the geometry of the NRC reference AIT system described above. The uniform parallel beam was modeled using the same X-ray spectrum (Figure 7.11) and air kerma (68 nGy per scan) described earlier. However, the horizontal exposure profile in Figure 7.9 as well as the vertical exposure profile in Figure 7.10 were replaced with uniform distributions. Thus, the two-dimensional beam profile for the reference AIT system in Figure 7.12 is represented as a flat surface. The adult male and adult female phantoms (50th percentile height and weight) were scanned using each geometry, and the resulting doses are summarized in Table 7.15.

Passenger Position Within the Unit

Variations in the dose to organs and effective dose received by the passenger due to position variations between the anterior and posterior units was investigated by placing the adult male phantom closer and further from each scanning unit

TABLE 7.15 Absorbed Doses to Critical Organs for Males and Females and Effective Doses for 50th Percentile of U.S. Adults Using the Beam Geometry Developed for the NRC Reference X-Ray Backscatter AIT System and a Plane Parallel Beam Geometry Incident Upon the Passengers

	Geometry		
	Reference AIT Scanner	Uniform Parallel Beam	Ratio
Male absorbed dose per screen (nGy)			
Thyroid	24	49	2.0
Skin	43	78	1.8
Eye Lens	42	65	1.6
Female absorbed dose per screen (nGy)			
Breast	23	36	1.6
Thyroid	17	40	2.3
Skin	44	80	1.8
Eye Lens	43	68	1.6
Effective Dose (nSv)			
Per anterior scan	9	15	1.7
Per posterior scan	3	4	1.5
Per screen	**12**	**19**	1.7

NOTE: The third column shows the ratio between these two geometries. For comparison, the ANSI reference effective dose for an HVL_1 of 1.18 mm Al and an air kerma of 68 nGy per screen is 20 nSv.

TABLE 7.16 Changes in Organ Absorbed Dose and Effective Dose per Screen with Shifts Toward the Anterior Unit or Toward the Posterior Unit

	Distance Away from Center Scanning Position (cm)						
	Toward Anterior Unit				Toward the Posterior		
	15	10	5	0[a]	5	10	15
Male absorbed dose per screen (nGy)							
Thyroid	30	28	26	24	22	21	20
Skin	43	43	42	43	43	44	45
Eye Lens	53	49	45	42	38	35	33
Female absorbed dose per screen (nGy)							
Breast	30	27	25	23	21	20	18
Thyroid	20	19	18	17	17	16	15
Skin	45	44	44	44	45	46	47
Eye Lens	57	51	46	43	40	36	33
Effective dose (nSv)							
Per anterior scan	12	11	10	9	8	8	7
Per posterior scan	2	2	2	3	3	3	3
Per screen	**14**	**13**	**12**	**12**	**11**	**11**	**11**
Ratio (position to nominal)	1.2	1.1	1.0	1.0	1.0	0.9	0.9

[a] The zero value refers to the nominal and central scanning position between an anterior and a posterior unit.

NOTE: For comparison, the ANSI reference effective dose for an HVL_1 of 1.18 mm Al and an air kerma of 68 nGy per screen is 20 nSv.

in increments of 5 cm. The total translational distance was 30 cm (±15 cm from center). The resulting doses are summarized in Table 7.16.

Variations in X-Ray Tube Voltage

A sensitivity analysis was performed to investigate the effects of varying beam voltage on doses to the adult phantom. Doses resulting from the beam spectrum generated for this report (the beam spectrum used was matched to the HVL_1 measured by the NRC subcontractor) were compared to doses resulting from additional spectra as-generated from the SPEKTR code[34] (i.e., the HVL_1s of these spectra were not modified beyond their inherent values). Each spectrum was incorporated into the AIT system X-ray source term and utilized to virtually screen the adult male and female phantom under the same irradiation geometry described earlier. Table 7.17 provides a summary of the resulting organ absorbed doses and effective dose received by the passenger.

[34] J.H. Siewerdsen, A.M. Waese, D.J. Moseley, S. Richard, and D.A. Jaffray, Spektr: A computational tool for x-ray spectral analysis and imaging system optimization, *Medical Physics* 31:3057-3067, 2004.

TABLE 7.17 Comparison of Reference X-Ray Backscatter AIT System of the Organ Absorbed Dose and Effective Dose as a Function of X-Ray Tube Potential

	Absorbed Dose						
X-Ray Tube Potential (kV)	50[a]	50	60	70	80	90	100
Half-value layer (HVL_1)	1.18	1.45	1.74	2.02	2.30	2.58	2.86
Male absorbed dose per screen (nGy)							
Thyroid	24	27	33	37	41	45	48
Skin	43	45	47	50	52	54	55
Eye Lens	42	44	45	47	48	50	51
Female absorbed dose per screen (nGy)							
Breast	23	26	29	32	35	37	39
Thyroid	17	22	26	31	35	39	42
Skin	44	46	49	52	54	56	57
Eye Lens	43	45	47	49	50	52	53
Effective dose (nSv)							
Per anterior scan	9	11	13	15	17	19	21
Per posterior scan	3	3	5	6	8	10	11
Per screen	12	14	18	22	25	29	32
Ratio (to column 1)	1.0	1.2	1.4	1.7	1.9	2.2	2.3
	ANSI Reference Effective Dose						
	20	25	30	34	39	44	49

[a] Values in the first data column are results from the PDD validated and softened X-ray spectrum at the operational value of 50 kV. All other values are from TASMIP-generated spectra (without HVL_1 matching) and assuming an equivalent reference air kerma of 68 nGy per scan. http://www.ncbi.nlm.nih.gov/pubmed/9394272.

Dose to Radiosensitive Cells in the Skin

The skin is divided into two main regions: the dermis and the epidermis. The biological response in the epidermal region occurs soon after an exposure to ionizing radiation whereas the biological response in the dermal region occurs after a latent period following exposure to ionizing radiation.[35] The biological targets are basal cells in the epidermis and the fibroblasts/vascular endothelial cells in the dermis. Irradiation of the basal cell layer can lead to desquamation, while irradiation of the fibroblasts and vascular endothelial cells can lead to erythema (skin reddening). The ICRP reference value for the thickness of the epidermal layer is 70 μm for adults.[36]

[35] E.J. Hall and A.J. Giaccia, *Radiobiology for the Radiologist*, Lippincott Williams and Wilkins, Philadelphia, Pa., 2006.

[36] ICRP, ICRP Publication 89: Basic Anatomical and Physiological Data for Use in Radiological Protection: Reference Values, *Annals of the ICRP* 32, 2002.

A sensitivity analysis was performed to compare the radiation dose to the entire skin thickness with the dose to just the radiosensitive epidermal skin layer. To conduct this analysis, a stylized elliptical cylinder torso model was created to represent the 50th percentile adult male using three anterior-posterior and three lateral measurement averages (representing the upper, middle, and lower regions of the trunk). The torso model was composed of soft tissue covered by a 0.158 cm skin layer (corresponding to the assumed standard ICRP skin thickness of an adult male).

The model was centered in the AIT system and doses to the 0.158 cm skin depth region and the dose to the sensitive area (50 to 100 μm) skin depths were simulated. The ratio of the dose in the sensitive region to the total skin dose was calculated. Because this ratio is near unity, the dose to the entire skin thickness was considered a reasonable surrogate for dose to the sensitive layer. Using this ratio, the dose to the sensitive skin layer of the adult male hybrid phantom was estimated from the whole skin dose presented earlier. Table 7.18 summarizes the results.

Failure Mode Analysis

Failure mode analysis of two conditions of equipment failure was performed on the adult female phantom in order to examine possible maximum doses to the lens of the eye, breast tissue, and skin. The first failure mode assumed a stationary vertical beam position and a functional chopper wheel resulting in a horizontally broad and vertically narrow (~3 mm) beam. The second failure mode assumed a stationary vertical beam position and a *nonfunctional* chopper wheel resulting in a stationary pencil beam. A circular beam cross section was assumed for the second failure mode with an area equivalent to a 3 mm × 3 mm square beam, the approximate dimensions of the properly collimated scanning beam under normal

TABLE 7.18 Comparison of the Absorbed Dose per Scan to Either the Total Skin Volume (Dermis and Epidermis) and the Presumed Radiosensitive Epidermal Stem Cell Layer (50 to 100 μm) in a Cylindrical Stylized Torso Phantom

	Absorbed Dose per Screen (nGy)	
	Stylized Phantom	Hybrid Phantom
Target - Total skin	37.3	43.5[a]
Target - Radiosensitive layer	37.9	44.2[b]
Ratio (total skin/radiosensitive layer)	1.02	

[a] Sex-averaged dose with adult hybrid phantoms.

[b] Hybrid phantom total skin dose × 1.02.

NOTE: The simulations showed only 2 percent increase in dose. Corresponding doses to skin in the 50th percentile adult male phantom are shown as well.

TABLE 7.19 Reference Geometry AIT Absorbed Doses Under Conditions of a Standard Screening Compared to Those Incurred Under Conditions of Maximum Exposure due to Two Different Modes of Equipment Failure

Tissue	Normal Screen (nGy)	Failure Mode 1[a] (nGy)	Failure Mode 2[b] (nGy)	Tissue Reaction Threshold (nGy)	(Gy)
Lens	43	29,000	1,100,000	500,000,000	0.5
Skin	44	26,000	870,000	2,000,000,000	2
Breast	23	310	7,400		

[a] Failure Mode 1: Beam fixed vertically but not horizontally (chopper wheel operational).
[b] Failure Mode 2: Beam fixed vertically and horizontally (chopper wheel not operational).

operation. The beams of both failure modes were oriented toward the targets of interest and were assumed to emit the same number of photons produced under normal operation for a full body scan. Table 7.19 summarizes the approximate doses to the lens, breast, and skin under these failure modes. For the second failure mode, peak skin dose was calculated assuming a 1×1 cm^2 area on the respective skin region. The maximal skin and lens doses (failure mode 2) of 0.87 mGy (870 μGy or 870,000 nGy) and 1.1 mGy (1,100 μGy or 1,100,000 nGy), respectively, are well below the minimum threshold values for deterministic effects of both skin (2 Gy or 2,000,000,000 nGy)[37] and eye lens (0.5 Gy or 500,000,000 nGy).[38] The skin determines the threshold limit for the breast due to the sensitivity for necrosis of the skin compared with clinical issues involving breast tissue.[39]

Summary

The NRC subcontractors and the committee performed a detailed computational assessment of the doses received during a security screening process involving X-ray backscatter AIT systems. This involved a detailed Monte Carlo

[37] S. Balter, J.W. Hopewell, D.L. Miller, L.K. Wagner, and M.J. Zelefsky, Fluoroscopically guided interventional procedures: A review of radiation effects on patients' skin and hair, *Radiology* 254:326-341, 2010.

[38] F.A. Stewart, A.V. Akleyev, M. Hauer-Jensen, J.H. Hendry, N.J. Kleiman, T.J. MacVittie, B.M. Aleman, A.B. Edgar, K. Mabuchi, C.R. Muirhead, R.E. Shore, and W.H. Wallace, ICRP Publication 118: ICRP Statement on Tissue Reactions and Early and Late Effects of Radiation in Normal Tissues and Organs—Threshold Doses for Tissue Reactions in a Radiation Protection Context, *Annals of the ICRP* 41:1-32, 2012.

[39] F.A. Metler and A.C. Upton, *Medical Effects of Ionizing Radiation*, Third Edition, Saunders, Elsevier, Philadelphia, Pa., 2008.

simulation using a representative source term and state-of-the-art hybridized human phantoms. The model used in the computations is referred to as the reference X-ray backscatter AIT system. The model represents a dual scan–single-pose configuration with an anterior unit providing an anterior image and a posterior unit producing a posterior image. The spatial dimensions were obtained from the previous NIST report evaluating a Rapiscan Secure 1000. This also included the size of the collimated X-ray beam, vertical span of the X-ray source, angular pitch of the X-ray source, and horizontal properties of the scanned beam. These results can be compared with previous studies reviewed in Chapter 6 and summarized in Table 6.4.

X-Ray Source

Typically, the energy distribution of the X-ray photons incident on the person scanned are derived from the operating voltage, anode angle, and measurements of the first HVL (HVL_1) in aluminum. This information serves as input to a standardized computer model that yielded the desired energy distribution. In this case, the information came from NRC subcontractor measurements made on an AS&E SmartCheck and a Rapiscan Secure 1000 AIT system. These measurements also included a central-axis PDD in tissue-equivalent material. The objective was to use the measured PDD as a validation of the Monte Carlo simulation using the computer-generated energy distribution.

Beam Intensity

The beam intensity serves as a scale factor for estimating the absorbed dose to the passenger as well as a calibration of the Monte Carlo computations. The quantity used for this is the air kerma per scan (in nGy) at a reference location between the anterior and posterior units. The Monte Carlo method transports one incident photon at a time. A simulation of the air kerma measurement yielded a normalization factor in terms of the number of photons required to generate 1 nGy of air kerma.

Results

In this section, a screen is considered to be the combination of an anterior and a posterior scan of 50 kV with an HVL of 1.18 mm Al and air kerma of 68 nGy per scan. It should be noted that the results will scale linearly with air kerma if the other conditions remain the same.

- The conventional method for computing the energy distribution of the incidents photons for 50kV X-ray backscatter AIT systems did not adequately predict the data obtained for PDD in tissue.
- The absorbed doses to individual tissues and organs for the reference adult phantoms located midway between the anterior and the posterior were all less than 50 nGy per screen.
- In general, the absorbed doses decreased in the adult phantoms as the BMI increased.
- The sex-averaged effective dose for the adult phantom ranged from 15 nSv at the 5th percentile BMI to 6 nSv for the 95th percentile BMI. (The ANSI E_{REF} for these conditions is 20 nSv.)
- The sex-averaged effective dose for the adult phantom was significantly greater for the anterior scan compared with the posterior scan. This difference in all cases depends on the distance of the organ from the X-ray source and on the organ's location within the individual.
- The absorbed doses to individual tissues and organs for the pediatric phantoms located midway between the anterior and the posterior AIT system units were all less than or equal to 60 nGy per screen.
- The absorbed doses to tissues and organs remained relatively constant in the pediatric phantoms as the BMI increased.
- The sex-averaged effective dose for the pediatric phantoms ranged from 25 nSv at the 5th percentile BMI to 22 nSv for the 95th percentile BMI. (The ANSI E_{REF} for these conditions is 20 nSv.)
- The sex-averaged effective dose for the pediatric phantoms was significantly greater for the anterior scan compared with the posterior scan.
- The absorbed doses to the fetus of a pregnant female located midway between the anterior and the posterior AIT system units were all less than 10 nGy per screen.
- The absorbed doses to the active bone marrow of the developing fetus of a pregnant female located midway between the anterior and the posterior AIT system units ranged from 16 nGy at 15 weeks post-conception to 11 nGy at 38 weeks post-conception.
- The absorbed doses to individual tissues and organs for the reference adult phantoms located midway between the anterior and posterior AIT system units were all greater for a plane-parallel incident-X-ray beam compared with the exposure conditions in an actual AIT system.
- The sex-averaged effective dose for the adult phantoms increased as the phantom was located closer to the anterior unit.
- The absorbed doses to the locations of radiosensitive cells, at depths between 50 μm and 100 μm, were not significantly larger than the dose averaged over the complete layer of skin.

- The localized absorbed doses for a stationary beam in both vertical and horizontal directions and normal scan time duration while centered upon the lens of an eye, a female breast, or central skin of the chest were on the order of 1,000,000 nGy for the lens of the eye and the skin and 7,000 nGy for the breast.
- For a constant air kerma, the sex-averaged effective dose for the adult phantoms ranged from 12 nSv at a tube voltage of 50 kV (HVL = 1.18 mm Al) to 32 nSv at 100 kV (HVL 2.86 mm Al). The ANSI E_{REF} ranged from 20 nSv to 49 nSv under these conditions.

FINDINGS AND RECOMMENDATIONS

Measurements

Key Finding: Using appropriate detectors, the estimated values of the radiation outside the inspection area that might affect a bystander are so low as to be statistically indistinguishable from the background radiation.

System Design

Although the radiation measurements and dose computations were performed for the committee in a detailed manner, the committee was unable to unequivocally determine whether the X-ray backscatter AIT systems studied have adequate operating safety interlocks that will prevent the AIT system from exceeding the ANSI/HPS N43.17-2009 standard under every imaginable situation for the following reasons:

- The committee was not given an opportunity to independently verify how all of the interlocks would perform in different situations, with the exception of simple functions such as termination of operation if a door was opened. Such testing would need engineering support from the manufacturer and require unique testing tools, and it would require dismantling portions of the AIT systems, potentially causing damage to them.
- The committee was not given a demonstration of how interlocks are checked at the manufacturer level from either Rapiscan or AS&E.
- Detailed electrical and mechanical drawings and computer code descriptions and documents describing internal functions at the most fundamental level of the AIT systems are either restricted from public access or were not made available by the manufacturers to either the committee or the sponsor.

However, the committee was able to inspect the interior of both the Rapiscan Secure 1000 and the AS&E AIT system. AS&E representatives also described to the committee how many of the interlocks are intended to perform on their second-generation prototype.

With the above limitations noted, having evaluated as many aspects of the AIT systems as mechanically and electrically as possible, and combining that knowledge with the measurements and computations performed, the committee can make the following statements:

Key Finding: It appears that the X-ray backscatter systems adhere to the recommended safety mechanisms described in the ANSI/HPS N43.17-2009 standard.

Key Finding: Given the results obtained by the committee on radiation measurements and calculations for the X-ray AIT systems investigated, normal screening of an individual would need to extend for more than 60 seconds for an individual to be exposed to radiation that exceeds the ANSI/HPS N43.17-2009 limit. In comparison, a typical screen takes about 6 seconds.

Key Recommendation: Future X-ray advanced imaging technology (AIT) systems should have some independent mechanism to ensure that the AIT system does not screen any person for longer than the time needed to acquire the appropriate image while keeping radiation exposure compliant with the safety principle of as low as (is) reasonably achievable.

Key Recommendation: Any future testing procedures should at a minimum continue to follow the indicators, controls, and safety interlocks requirements of the ANSI/HPS N43.17-2009 standard, or similar testing procedures, and include daily verification of safety parameters by a test piece.

Dose Computations

The committee's approach in examining the dose to the individual being screened differs from that of previous investigations in two ways:

- It made use of sensitive detectors with tissue-equivalent phantoms to verify beam intensity, X-ray quality, and penetration; and
- It performed computations using estimates of beam intensity, scanning geometry, and digitized human phantoms that have realistic dimensions and morphology.

Based on these improved conditions, the committee states that:

Key Finding: Under routine operations, the computed effective doses using realistic computational X-ray sources and scanning geometries, coupled with the digitized hybrid phantoms, are similar to the ANSI reference effective dose and an order of magnitude below the limit of 250 nSv/screen, as set forth in the applicable ANSI standard.

Key Finding: For either the Rapiscan Secure 1000 or the AS&E SmartCheck systems, as determined by the committee for adults and children:

- The effective doses are about the same as those calculated following the simplified formula for the reference exposure dose identified by the ANSI/HPS N43.17-2009 standard;
- The effective doses are lower than those in previous reports using plane-parallel X-ray beams with stylized geometrical (low-fidelity) human phantoms; and
- Sensitivity analysis showed that under a range of different conditions, including passenger position in the AIT system and increases in the energy (i.e., by increasing the tube high voltage) of the X-ray beam, the computed effective dose would not increase by more than a factor of 3 and, even so, it would remain well below the limit specified in the ANSI/HPS N43.17-2009 standard.

Section 6.1.1.1 of ANSI/HPS N43.17-2009 specifies that the exposure limitations is "based on a computational adult model and is not always indicative of the actual effective does, especially for small children." Section 6.1.1.1 also refers to a radiation dose for a full-body scan. The NRC subcontractor's calculations enabled the committee to estimate variations in absorbed dose not captured in the ANSI standard. This included details of absorbed dose distributions in a wide variety of body types, including children and the developing fetus, as well as specific organs in each of those body types. Under standard operating conditions, the committee found that:

Key Finding:

- No person, regardless of age and weight modeled, would exceed the effective dose limit per screen (i.e., 250 nSv/screen), as defined by the ANSI/HPS N43.17-2009 standard;
- The absorbed dose per screen to the developing fetus at any of the three stages post-conception is less than 0.0003 percent of the recommended limit for radiation protection of the fetus during the entire gestation period;

- The absorbed dose to the epithelial layer of radiosensitive cells in the skin is not significantly elevated (~1.6 percent) compared to the average dose to the skin; and
- The dose received by the lens of the eye, skin, or female breast during a stationary beam of X rays for the duration of the scan were at least 2 orders of magnitude below thresholds where tissue injury might occur.

It might be worth mentioning that Mowery et al.[40] indicate that during the worst-case scenario, when all interlocks are defeated by malicious code, the AIT system can be instructed to deliver the whole radiation dose from a scan to a single random point on the body. If this worst-case scenario occurs and the random delivery of the dose actually happens to be in the worst place possible, the eye, the computations presented above indicate that this dose is at least 2 orders of magnitude below the threshold where tissue injury might occur. This fact points out how important the previous recommendation is that there is some independent mechanism to ensure that the AIT does not screen any person for longer than the time needed to acquire the appropriate image.

Key Finding: The agreement between the estimated dose results from the NRC subcontractor and the results from previous studies confirms that the calculations performed in previous studies were adequate to establish compliance with effective dose limits recommended in ANSI/HPS N43.17-2009.

[40] K. Mowery, E. Wustrow, T. Wypych, C. Singleton, C. Comfort, E. Rescorla, S. Checkoway, J.A. Halderman, and H. Shacham, Security analysis of a full-body scanner, *Proceedings of the 23rd USENIX Security Symposium*, 2014, https://www.usenix.org/conference/usenixsecurity14/technical-sessions/presentation/mowery.

Appendixes

A

Statement of Task

An ad hoc committee will review previous studies as well as current processes used by the Department of Homeland Security (DHS) and equipment manufacturers to estimate radiation exposures resulting from backscatter x-ray advanced imaging technology (AIT) system use in screening air travelers, and provide a report with findings and recommendations on:

1. Whether exposures comply with applicable health and safety standards for public and occupational exposures to ionizing radiation, and
2. Whether system design (e.g., safety interlocks), operating procedures, and maintenance procedures are appropriate to prevent over exposures of travelers and operators to ionizing radiation.

This study will not address legal, cultural or privacy implications of this technology.

NOTE: The committee's work plan further stipulated that as part of this study, the Academies will subcontract with an appropriate independent testing organization or qualified consultants to conduct field studies measuring the radiation dosage emitted by the machines as they are used.

B

Glossary, Acronyms, and Abbreviations

AAPM	American Association of Physicists in Medicine
absorbed dose	The amount of energy from ionizing radiation deposited at a given point. Absorbed dose is measured in Gray.
advanced imaging technology (AIT)	Technology is intended to screen passengers at airports or other secure facilities (such as prisons) that allow for visual detection of both metallic and non-metallic threat items, including weapons, explosives, and other concealed objects on passengers. These items would not be detected by walk-through metal detectors.
air kerma	Radiation quantity often used to express the radiation concentration delivered to a point, such as the entrance surface of the body. It is measured in joules/kilogram (J/kg).
ALARA	as low as (is) reasonably achievable
ANSI	American National Standards Institute
AS&E	American Science and Engineering, Inc.
ATR	automatic target recognition

backscatter	The reflection of waves or signals back to the direction from which they came.
BMI	body mass index
bystanders	Persons—for example, operators or persons waiting in line to be scanned—not being scanned but who may receive dose from the operation of the backscatter X-ray machine because of their proximity to the inspection area.
CDC	Centers for Disease Control and Prevention
CPE	charged particle equilibrium
DDE	deep dose equivalent
DHS	Department of Homeland Security
effective dose	Effective dose is a dose parameter that takes into consideration the type of radiation and the sensitivity of the body parts exposed. Effective dose is expressed in sieverts (Sv).
EMO	emergency-off (button)
FAT	factory acceptance test
FDA	Food and Drug Administration
HPS	Health Physics Society
HVL	half-value layer
ICRP	International Commission on Radiological Protection
ICRU	International Commission on Radiation Units and Measurements
interlocks	Systems (devices or processes) used to prevent failure of a machine. Interlocks can be electrical, mechanical, or software.

JHU/APL	Johns Hopkins University/Applied Physics Laboratory
KERMA	kinetic energy released in matter (known as kerma)
Linear-nonthreshold (LNT) dose reponse model of radiation effects	Model used for radiation protection purposes to estimate risks at low radiation doses where there is not sufficient epidemiological or biological evidence to draw direct conclusions about risks. The linear nonthreshold model assumes that there is a linear relationship between dose and effect and therefore allows for extrapolation from the outcomes observed at higher radiation doses to lower doses.
NCRP	National Council on Radiation Protection and Measurements
NIST	National Institute of Standards and Technology
NRC	National Research Council
NURBS	Non-Uniform Rational Basis Spline
organ dose	The absorbed dose averaged over an organ. Organ dose is measured in Gray.
OSHA	Occupational Safety and Health Administration
OSL	optically stimulated luminescence
PDD	percent depth dose
primary and secondary screening	Primary screening is screening that all passengers are subject to. Secondary screening is additional screening that may be used based on the response to the primary screening, randomization, or other metrics that suggest that further information is needed about a passenger (e.g., to possibly resolve an alarm during primary screening).

radiation	The energy that comes from a source and travels through some matter or through space. There are two types of radiation: ionizing and nonionizing. Ionizing radiation, which includes X-rays, is considerably more energetic compared to nonionizing radiation such as that found in microwaves. Ionizing radiation is more harmful to living organisms per unit of energy deposited than is nonionizing radiation as it has the potential to cause DNA damage and, consequently, cancer. Currently, there is no convincing evidence that nonionizing radiation can cause cancer, with few exceptions; for example, ultraviolet and skin cancer.
RFP	request for proposals
SAT	site acceptance test
scan	The operation necessary to produce one image (e.g., front view) from one radiation source. One radiation source simultaneously producing multiple images also constitutes one scan. Two sources simultaneously producing two images constitute two scans. In some cases several scans may be required for a single screening of the subject.
screening	The sum of radiation exposures or scans necessary to image objects concealed on all sides of the body as intended by the system design under normal conditions. Examples: (1) for backscatter systems a screening typically consists of four scans, one from each side; (2) for transmission systems a screening typically consists of one scan.
SDE	shallow dose equivalent
Sievert (Sv)	The international (SI) name for the unit of dose equivalent radiation measured in J/kg, calculated by multiplying the absorbed dose (in Gy) with a weighting factor.
SP	single pose
SSD	source-skin distance

TMR	tissue-maximum ratio
TSA	Transportation Security Administration
TSIF	Transportation Systems Integration Facility
uncertainty	Lack of sureness or confidence in predictions of models or results of measurements (NCRP Report No. 158).
USAPHC	U.S. Army Public Health Command

C

Organ Absorbed Doses

Results of some dosimetry calculations for adult passengers are shown in Table 7.13 (and for pediatric passengers in Table 7.14 and for the developing fetus in Table 7.15). This appendix contains the complete lists of absorbed doses for all male and female organs for adults and children (Tables C.1 to C.3).

TABLE C.1 Organ Absorbed Doses to U.S. Adult Males at 50th Height and Various Weight Percentiles (nGy per scan)

	Absorbed Dose (nGy) for U.S. Adult Males at 50th Height					
	5th Weight Percentile			25th Weight Percentile		
	Dose per Scan		Dose per Screen	Dose per Scan		Dose per Screen
	A	*P*	*(A + P)*	*A*	*P*	*(A+P)*
Breast	36	1	36	30	0	31
Colon	21	2	22	13	1	15
Lung	7	7	13	5	6	11
Stomach	10	3	12	6	2	8
Testes	31	5	35	30	5	34
Bladder	7	1	8	5	1	7
Esophagus	3	2	5	2	2	4
Liver	10	4	13	6	3	8
Thyroid	30	1	31	26	1	27
Brain	1	1	2	1	1	2
Salivary Glands	10	6	17	10	6	17
Skin	22	22	44	21	22	43
Adrenals	2	6	8	1	4	6
Extrathoracic Region	18	1	19	17	1	18
Gall Bladder	7	2	9	3	2	5
Heart Wall	8	2	10	6	2	8
Kidneys	2	11	13	1	9	10
Lymphatic Nodes	2	11	13	1	9	10
Muscle	9	10	19	8	9	17
Oral Mucosa	4	1	4	3	1	4
Pancreas	5	3	8	3	3	6
Prostate	4	3	8	4	4	8
Small Intestine	11	1	12	7	1	8
Spleen	2	12	14	1	10	11
Thymus	7	1	8	5	1	6
Lens	44	0	44	43	0	44
Active Marrow	2	3	5	1	3	4
Shallow Marrow	3	4	7	2	4	6

NOTE: A, anterior; P, posterior.

50th Weight Percentile			75th Weight Percentile			95th Weight Percentile		
Dose per Scan		Dose per Screen	Dose per Scan		Dose per Screen	Dose per Scan		Dose per Screen
A	*P*	*(A+P)*	*A*	*P*	*(A+P)*	*A*	*P*	*(A+P)*
31	0	31	18	0	19	10	0	10
12	1	13	8	1	9	4	0	4
4	6	10	3	5	8	2	4	6
5	1	7	4	1	5	2	1	3
27	4	31	27	4	30	25	3	28
5	2	7	5	1	6	3	1	4
2	1	3	1	2	3	1	1	2
5	3	7	3	2	6	2	2	3
23	1	24	23	1	24	15	1	16
1	2	2	1	2	2	1	2	2
10	6	16	10	6	16	10	6	16
20	23	43	20	23	42	19	24	42
1	4	5	1	4	5	0	2	3
15	1	16	15	1	15	12	1	12
3	1	4	2	1	3	1	1	2
5	1	7	4	1	5	2	1	3
1	8	9	1	6	7	0	5	5
1	8	9	1	6	7	0	5	5
7	9	17	6	8	15	5	6	11
3	1	4	3	1	4	3	1	4
2	2	4	2	2	3	1	1	2
3	4	7	3	4	7	3	3	6
7	1	7	5	1	5	3	1	3
1	10	11	1	10	10	0	6	6
4	1	5	3	1	4	2	1	3
42	0	42	41	0	42	39	0	39
1	2	4	1	2	3	1	2	3
2	4	6	2	3	5	1	3	4

TABLE C.2 Organ Absorbed Doses to U.S. Adult Females at 50th Height and Various Weight Percentiles (nGy per scan)

	Absorbed Dose (nGy) for U.S. Adult Females at 50th Height					
	5th Weight Percentile			25th Weight Percentile		
	Dose per Scan		Dose per Screen	Dose per Scan		Dose per Screen
	A	*P*	*A+P*	*A*	*P*	*A+P*
Breast	25	0	26	23	0	23
Colon	10	2	12	9	2	11
Lung	6	6	12	4	5	9
Stomach	7	2	9	6	2	8
Ovaries	5	1	6	4	1	6
Bladder	9	1	11	9	1	10
Esophagus	3	3	6	2	3	5
Liver	6	4	10	5	3	8
Thyroid	20	2	22	20	1	21
Brain	1	3	4	1	3	4
Salivary Glands	8	7	15	7	7	14
Skin	23	23	46	21	24	45
Adrenals	1	9	10	1	7	8
Extrathoracic Region	14	1	16	14	1	15
Gall Bladder	4	3	6	3	2	5
Heart Wall	7	2	9	5	2	6
Kidneys	1	19	20	1	18	19
Lymphatic Nodes	9	9	18	8	9	16
Muscle	9	9	18	8	9	16
Oral Mucosa	3	1	4	2	1	4
Pancreas	2	5	7	2	5	6
Uterus/Cervix	3	2	5	3	2	5
Small Intestine	6	2	8	6	2	8
Spleen	2	12	13	2	9	11
Thymus	7	2	9	6	1	7
Lens	46	0	46	44	0	44
Active Marrow	2	3	5	2	3	5
Shallow Marrow	3	4	8	3	4	7

NOTE: A, anterior; P, posterior.

50th Weight Percentile			75th Weight Percentile			95th Weight Percentile		
Dose per Scan		Dose per Screen	Dose per Scan		Dose per Screen	Dose per Scan		Dose per Screen
A	*P*	*A+P*	*A*	*P*	*A+P*	*A*	*P*	*A+P*
23	0	23	20	0	20	18	0	18
7	1	9	4	1	4	1	1	2
4	5	9	2	4	6	1	4	4
5	2	7	3	1	5	1	1	2
4	1	4	2	1	2	0	0	1
7	1	8	3	1	4	1	1	1
2	2	4	1	2	3	0	2	2
4	3	7	3	3	5	1	3	3
16	1	17	10	1	11	3	1	4
1	3	4	1	3	4	1	4	5
8	7	14	6	7	14	5	6	11
21	24	44	18	27	45	16	30	46
1	7	8	0	6	6	0	6	6
13	1	15	10	1	11	4	1	5
3	2	4	1	2	3	0	1	2
5	2	6	2	1	3	1	1	2
1	18	19	0	14	14	0	12	12
7	8	15	5	7	12	3	6	9
7	8	15	5	7	12	3	6	9
2	1	4	2	1	3	2	1	3
1	4	5	1	3	4	0	3	3
2	2	4	1	2	2	0	1	1
4	2	6	2	1	3	1	1	2
1	10	11	1	8	8	0	7	7
5	1	6	3	1	4	1	1	2
43	0	43	37	0	37	32	1	32
1	3	4	1	2	3	0	2	2
2	4	6	2	3	5	1	3	4

TABLE C.3 Organ Absorbed Doses to U.S. Pediatric Males and Females at ~100 cm Height and Various Weight Percentiles (nGy per scan)

	Absorbed Dose (nGy) for U.S. Pediatric Males at ~100 cm Height								
	5th-Percentile Weight			50th-Percentile Weight			95th-Percentile Weight		
	Dose per Scan		Dose per Screen	Dose per Scan		Dose per Screen	Dose per Scan		Dose per Screen
	A	*P*	*A+P*	*A*	*P*	*A+P*	*A*	*P*	*A+P*
Breast	40	1	41	39	1	40	29	1	30
Colon	27	3	31	24	3	27	23	3	26
Lung	15	11	26	15	10	25	11	10	21
Stomach	15	5	19	12	4	16	12	4	16
Testes	34	8	42	35	8	43	35	8	43
Bladder	15	6	22	13	6	19	13	5	19
Esophagus	10	5	15	10	5	15	9	5	14
Liver	13	6	19	11	5	16	10	5	15
Thyroid	42	4	47	41	4	45	43	4	47
Brain	4	5	9	4	5	9	4	5	10
Salivary Glands	9	9	18	9	9	18	9	9	18
Skin	28	21	49	28	21	49	27	20	48
Adrenals	3	14	16	2	13	15	2	11	13
Extrathoracic Region	21	3	24	21	3	24	21	3	24
Gall Bladder	10	4	15	9	4	13	8	4	12
Heart Wall	18	4	22	16	4	20	13	4	17
Kidneys	4	13	17	4	13	16	4	12	16
Lymphatic Nodes	14	13	26	13	12	25	12	11	22
Muscle	14	13	26	13	12	25	12	11	22
Oral Mucosa	8	2	10	8	2	11	9	2	11
Pancreas	8	7	14	6	6	13	6	6	12
Prostate	22	6	29	22	6	27	23	6	29
Small Intestine	17	4	21	15	3	19	14	3	17
Spleen	5	14	19	4	13	17	4	12	16
Thymus	23	3	26	22	3	25	17	3	20
Lens	59	1	60	59	1	60	59	1	60
Active Marrow	5	5	10	5	5	9	4	4	9
Shallow Marrow	6	7	13	6	7	12	5	6	12

NOTE: A, anterior; P, posterior.

Absorbed Dose (nGy) for U.S. Pediatric Females at ~100 cm Height								
5th-Percentile Weight			50th-Percentile Weight			95th-Percentile Weight		
Dose per Scan		Dose per Screen	Dose per Scan		Dose per Screen	Dose per Scan		Dose per Screen
A	*P*	*A+P*	*A*	*P*	*A+P*	*A*	*P*	*A+P*
42	1	43	38	1	39	31	1	32
28	3	31	24	3	27	23	3	27
16	11	27	14	10	24	12	10	22
15	5	20	13	5	18	12	4	16
10	5	15	8	4	12	8	4	12
26	4	30	18	3	22	23	4	26
10	5	15	10	5	14	9	5	14
13	6	19	10	5	14	10	5	15
43	4	47	40	4	44	44	4	48
4	5	9	4	5	9	4	5	10
9	9	18	9	8	18	9	9	18
28	21	49	26	20	46	27	21	48
3	14	16	2	12	15	2	11	14
21	3	24	19	3	22	21	3	24
11	5	15	8	4	12	9	4	13
18	4	21	16	4	20	14	4	17
4	13	18	3	12	16	4	12	16
14	13	27	12	12	24	12	11	23
14	13	27	12	12	24	12	11	23
9	2	11	8	2	10	8	2	10
8	7	14	7	7	14	7	6	13
8	5	13	7	4	11	7	4	11
17	3	21	15	3	18	15	3	18
5	14	19	5	15	20	4	12	16
23	3	26	22	3	25	18	3	21
59	1	60	54	1	54	59	1	60
5	5	10	4	5	9	4	5	9
6	7	13	6	6	12	5	6	12

D

Summary of Statistics from Previous Studies

The results of some of the measurements described in previous reports and outlined in Chapter 6 are summarized in Tables D.1 through D.3. The measured kerma was reported by three groups, Johns Hopkins University/Applied Physics Laboratory (JHU/APL),[1] National Institute of Standards and Technology (NIST),[2] and American Association of Physicists in Medicine (AAPM),[3] as described in Table D.1. Aluminum half-value layers were reported by the same three groups, as described in Table D.2. Effective dose was estimated by the same three groups using the reference effective dose formula and by the U.S. Army Public Health Command (USAPHC)[4] using the deep dose equivalent from optically stimulated luminescence (OSL) dosimeter readings, as described in Table D.3.

[1] JHU/APL, *Radiation Safety Engineering Assessment Report for the Rapiscan Secure 1000 in Single Pose Configuration*, NSTD-09-1085, Version 2, Laurel, Md., August 2010; hereinafter referred to as the JHU/APL report.

[2] J.L. Glover, R. Minniti, L.T. Hudson, and N. Paulter, *Assessment of the Rapiscan Secure 1000 Single Pose (ATR version) for Conformance with National Radiological Safety Standards*, NIST report for the TSA, inter-agency agreement HSHQDC-11-X-00585, April 19, 2012; hereinafter referred to as the NIST report.

[3] AAPM, *Radiation Dose from Airport Scanners: Report of AAPM Task Group 217*, College Park, Md., 2013; hereinafter referred to as the AAPM report.

[4] USAPHC, *Radiation Protection Consultation No. 26-MF-0E7K-11*, Rapiscan Secure 1000 Single Pose Dosimetry Study, Aberdeen Proving Ground, Md., 2012.

TABLE D.1 Measured Kerma

Report	K_{Std} (nGy) per Scan	K_{max} (nGy) per Scan
JHU/APL	41 ± 1	
NIST	47 ± 1[a]	95 ± 6
AAPM	46 ± 3	

[a] The value 47 ± 1 is from the updated September 28, 2012, NIST report; however, the committee initially had access to a preliminary report, dated April 19, 2012, where the value was 48.6 ± 1.

TABLE D.2 Measured Aluminum Half-Value Layers

Report	HVL_1 (mm of Al)
JHU/APL	1.18
	1.63
NIST	1.09
AAPM	0.93
Mean	1.2 ±0.3

NOTE: JHU/APL dual values are for a primary and secondary unit.

TABLE D.3 Estimated Effective Dose per Screening

Report	E_{REF} (nSv)/Screen
JHU/APL	14.7
NIST	15.5
AAPM	10.7
USAPHC	38-49

THE PRIMARY RESULTS OF THE THREE RAPISCAN STUDIES: A STATISTICAL OVERVIEW

The results about exposure in the JHU/APL, NIST, and AAPM reports are summarized as in Table D.1. This summary accurately describes what the studies say, but the studies are cryptic in discussing how they reached margins of error for their estimates of average exposure. At a minimum, all the studies deviate from standard statistical methods for describing the uncertainty in key parameters. Here, the committee elaborates on this point one study at a time and then considers how one might synthesize the results of the three studies in the spirit of meta-analysis.

The AAPM Report

Having obtained data about nine Rapiscan machines (six of them deployed at the Los Angeles International Airport), the authors report on page 9 that

> The energy-corrected measurements at reference point averaged for all tested units was 0.046 μGy with a standard deviation of 0.003 μGy and a range of 0.04 μGy to 0.052 μGy.

To generalize from the study, a statistician would typically make the tacit assumption that the nine units tested are a random sample of all Rapiscan units used at airports and would use the observed results to obtain both a point estimate of average exposure and a 95 percent confidence interval for average exposure. This confidence interval would be construed as the *range of plausible values* for average exposure over all Rapsican machines and would have a 95 percent probability of including the all-Rapiscan average. The statement quoted above, however, does not provide the 95 percent confidence interval; nor is it obvious how to construct that interval from the information the report provides.

Much of the problem relates to ambiguity over whether the authors are reporting a *standard deviation* (the phrase they use) or instead a *standard error*. The standard deviation is a familiar measure of spread among the original measurements, in this case nine. By contrast, the standard error reflects the uncertainty in using the average of the original measurements as a proxy for the overall mean. As the sample size increases, the standard deviation among the measurements would not be expected to change because the early pattern of spread would tend to be replicated among later measurements; however, the standard error would decrease because bigger samples produce more accurate results. Indeed, the standard deviation (SD) and the standard error (SE) are related by the formula:

$$SE = SD/\sqrt{n}$$

where n is the sample size.

To find the 95 percent confidence interval for the mean, based on nine observations, the usual formula would be:

$$\overline{X} \pm 2.306 * SE$$

where $\overline{X}$ is the sample mean (here 0.046) and

$$\text{SE} = \begin{cases} .003 \text{ if the authors actually reported the SE} \\ .001 \text{ if the authors actually reported the SD} \end{cases}$$

This factor-of-three difference arises because $n = 9$ in the SE versus SD formula above. The factor 2.306 arises from use of the t-probability distribution with eight degrees of freedom, which is the usual distribution applied to a random sample of size nine.

Depending on which of the two values is used for the SE, we reach a 95 percent confidence interval of either (.0391, .0529) with SE = .003 or (.0437, .0483) with SE = .001.

The best guess, given what the authors said, is that they were reporting the standard deviation, because they state that the range from the smallest to largest observations extended from .04 μGy to .052 μGy. For that reason, (.0437, .0483) is the more plausible 95 percent confidence interval, which implies that the point estimate of .046 suffers a "margin of error" of .0023. Expressed in nGy, the interval is (43.7, 48.3).

The NIST Report

The NIST report statistic that is comparable to that from the AAPM report is "47 ± 1 nGy." However, interpreting the uncertainty range ±0.8 nGy is very difficult given what is reported. The authors do not tell us the size of the sample; rather, they report on page 21 that

> The air kerma was measured on several occasions and in each case the ion chamber was repositioned multiple times in order to provide an estimate of the uncertainty associated with positioning the chamber.

Needless to say, one cannot apply sampling formulas to vague formulations like "several occasions" or "multiple times." It is conceivable that the authors correctly present the 95 percent confidence interval for mean exposure, which extends from 47 – 1 to 47 + 1, or from 46 to 48. But they offer no reason to be confident that they have done so.

In any case, the authors report that "only one system was tested." Thus, while their results say something about *within-machine* variability for a particular unit, they say nothing about *cross-machine* variability in mean exposure. Yet the AAPM results suggest that cross-machine variation might be considerably greater than cross-scan variations for a single machine. The appearance of greater precision for the NIST measurement might be illusory, even if its confidence interval for mean exposure is narrower than that of AAPM, because NIST had only one data point as compared to nine for AAPM.

The JHU/APL Report

The JHU/APL report is more specific than the other two are in that it offers the original results in Tables 8-1 and 8-2. It appears that only one machine was tested, with five scans performed for both the secondary unit and the primary unit. There was very little variability across the five scans: the coefficient of variation among the five scans was on the order of 1 percent, meaning that the standard deviation SD was only 1 percent of the mean. For that reason, $\text{SE}=\frac{SD}{\sqrt{5}}$ was only about ½ of 1 percent. With n = 5, the 95 percent confidence interval for the overall mean would follow:

$$\overline{X} \pm 2.78 \text{ SE}$$

Given an $\overline{X}$ of 41 nGy and an SE of .005 $\overline{X} \approx 205$, the confidence interval would extend from 40.43 to 41.57.

Again, however, the results offer no indication of cross-machine variability, a key consideration in making inferences about mean exposure for all Rapiscan machines.

SYNTHESIZING THE RESULTS

It appears that the AAPM report results are statistically consistent with those from the JHU/APL report. After all, AAPM got a mean exposure of 41 nGy for one machine, which fell within the range of 40 nGy to 52 nGy that AAPM observed over nine machines.

However, without knowing more about the measurement procedures, there is no way to combine the results of the three studies that is manifestly correct. One approach might assume each of the three studies yielded an average exposure that differs from μ, the true average exposure for all Rapiscan machines, by an amount that follows a zero-mean bell-shaped normal curve, with the standard deviation σ of all three curves being the same. That assumption implies that, a priori, all three studies are equally accurate in estimating μ.

Under that assumption, combining the results is mathematically tractable. Given that the three studies yielded mean exposures of 46, 41, and 47, the point estimate of average exposure based on "one study, one vote" would be (46 + 41 + 47)/3 ≈ 45 nGy. The common standard deviation σ for the measurement error affecting each study's result would be approximated as 3 for these three observations. A

95 percent confidence interval for μ would extend from 38 to 50. If that interval seems large, it is because the estimate of σ based on the three key numbers is highly unstable: when one of the three results exceeds another by 6 (i.e., 47 − 41), then the true standard deviation σ could be larger than 3. The confidence interval takes account of worst-case possibilities as well as more typical ones.

Another approach would follow the principle of "one machine, one vote," and would combine results for the 11 machines tested, nine of them by AAPM. The sample mean for these 11 data points would be $(9 \times 46 + 41 + 47)/11 \approx 46$ nGy, while their standard deviation would be approximately one and a half. Working from there to the standard error of the estimate 46 nGy and applying the appropriate t-distribution formula yields a 95 percent confidence interval for μ that extends from 42 to 49 nGy. That this interval is narrower than 38 to 50 reflects the fact that random samples of size 11 are considered almost an order of magnitude more reliable than random samples of size 3. Of course, this method effectively gives 9/11 = 82 percent of the weight to the AAPM study, which would be unwarranted if the procedures followed in that study were less reliable than were those in the others. Judging the relative plausibility of the studies cannot be accomplished without examining the methodologies used to measure the radiation emitted from the AIT systems and calculating the doses to the persons being screened and others.

E

Biographies of Committee Members and Contractors

COMMITTEE

HARRY E. MARTZ, JR., *Chair*, is the director of the Nondestructive Characterization Center at Lawrence Livermore National Laboratory (LLNL). Dr. Martz received a B.S. degree from Siena College and M.S. and Ph.D. degrees from Florida State University. For 6 years, he led the computed tomography project at LLNL, applying computed tomography and X-ray and proton radiography to material characterization and gamma-ray gauge techniques to treaty verification activities. As center director, his projects included the use of nonintrusive X-ray and gamma-ray computed tomography techniques as three-dimensional imaging tools to understand material properties and analyze radioactive waste forms. Dr. Martz has applied these techniques to the inspection of automobile and aircraft parts, reactor fuel tubes, high explosives, and shape charges. Recent research includes use of X rays to find explosives in luggage and special nuclear materials in cargo containers. The research and development at the center includes the design and construction of scanners and preprocessing, image reconstruction, and analysis algorithms. Dr. Martz served on the National Research Council (NRC) Committee on Commercial Aviation Security and the Panel on Airport Passenger Screening.

BARBARA J. McNEIL, *Vice Chair*, is the Ridley Watts Professor and was appointed the founding head of the Department of Health Care Policy at Harvard Medical School in 1988. She is also a professor of radiology at Harvard Medical School and at Brigham and Women's Hospital (BWH). She continues to practice nuclear

medicine one day a week at BWH. She was interim dean of Harvard Medical School in summer 2007. Dr. McNeil received her A.B. degree from Emmanuel College, her M.D. degree from Harvard Medical School, and her Ph.D. degree from Harvard University. She is a member of the Institute of Medicine (IOM) and of the American Academy of Arts and Sciences. Dr. McNeil is also a member of the Blue Cross Technology Evaluation Commission; she formerly chaired the Medicare Evidence Development Coverage Advisory Committee and is now a member of that committee. She is currently a member of the NRC's Nuclear and Radiation Studies Board and its vice chair. She serves as an advisor for several other federal and private organizations. Dr. McNeil formerly served on the Publications Committee of the *New England Journal of Medicine* as well as on the Prospective Payment Assessment Commission. Her early career involved research in decision analysis and cost-effective analysis. More recently, her work has focused on quality of care and technology assessment. Dr. McNeil's research involves relationships with payers, providers, and the federal government. Her largest ongoing study compares quality of care in the Veterans Administration system with that in the private setting for patients with cancer. For several years, Dr. McNeil coordinated several large studies comparing the value of alternative imaging modalities for patients with cancer.

SALLY A. AMUNDSON is an associate professor of radiation oncology in the Center for Radiological Research at the Columbia University Medical Center in New York. Dr. Amundson's research uses functional genomics approaches to study low-dose radiation and bystander effects, unique effects of space radiation, and the development of gene expression approaches for radiation biodosimetry. She is co-director of the Center for High-Throughput Minimally-Invasive Radiation Biodosimetry. She has served on the National Council for Radiation Protection and Measurements (NCRP) since 2004 and is currently co-chairing an NCRP committee tasked with producing a commentary on a "multiplatform national approach for providing guidance on integrating basic science and epidemiological studies on low-dose radiation biological and health effects." Since 2009, Dr. Amundson has served on the Science Advisory Committee of the Radiation Effects Research Foundation (RERF) in Hiroshima, Japan, chairing the RERF scientific review for 2012. She is also an associate editor of *Radiation Research*, a member of the Radiation Research Society (RRS) Council, and a recipient of the Michael Fry Research Award from the RRS.

DAVID E. ASPNES is a Distinguished University Professor and member of the Department of Physics at North Carolina State University. Formal education includes B.S. and M.S. degrees in electrical engineering from the University of Wisconsin, Madison, and a Ph.D. degree in physics from the University of Illinois, Urbana-Champaign. He joined the North Carolina State University Physics Department

in 1992 as a full professor and was made a Distinguished University Professor in 1999. He was elected as a member of the National Academy of Sciences (NAS) in 1998. Principal research interests have been in the areas of optical spectroscopy and semiconductor and surface physics. Contributions include the discovery, elucidation, and development of low-field electroreflectance for high-resolution spectroscopy of semiconductors and the determination of their band structures; the development and application of spectroscopic ellipsometry to surfaces, interfaces, thin films, and bulk materials; and the development and application of reflectance-difference spectroscopy to real-time analysis of epitaxial growth. Current research activities are directed toward nondestructive analysis of surfaces and interfaces and, in particular, the real-time diagnostics and control of semiconductor epitaxy by organometallic chemical vapor deposition. Dr. Aspnes has published more than 400 papers and has been granted 23 patents.

ARNOLD BARNETT is the George Eastman Professor of Management Science and Professor of Statistics at the Massachusetts Institute of Technology (MIT) Sloan School of Management. He holds a B.A. in physics from Columbia University and a Ph.D. in mathematics from MIT. Dr. Barnett's research specialty is applied statistical analysis generally focused on problems of health and safety. Aviation safety is among his prime areas of application: he was described as "the nation's leading expert" on aviation safety by *NBC News*, and he received the President's Citation in 2002 from the Flight Safety Foundation for "truly outstanding contributions on behalf of safety." He has worked for 16 airlines, six airports, the Federal Aviation Administration, and the Transportation Security Administration. Dr. Barnett has received the President's Award for "outstanding contributions to the betterment of society" by the Institute for Operations Research and the Management Sciences (INFORMS); he also received the 2001 Expository Writing Award from INFORMS and is a fellow of that organization. A popular instructor, he has been honored 12 times for outstanding teaching at MIT.

THOMAS B. BORAK is a professor in the Department of Environmental and Radiological Health Sciences at Colorado State University. He received a B.S. in physics from St. John's University (Minnesota) and a Ph.D. in physics from Vanderbilt University. His research interests are in radiation physics and dosimetry, which currently includes "Early Stage Innovations for the NASA Office of Space Technology Research and the Impacts of Dose Received from External Radiation and Risk Perception on Psychological Sequelae in Ukrainians following the Chornobyl Accident," funded by the National Science Foundation. He has had scientific staff appointments at Fermilab, CERN, and Argonne National Laboratory. He has been a consultant to the Governor of Colorado concerning issues relating to low-level radioactive waste management and nuclear criticality safety.

Dr. Borak was a member of the NRC Committees on Risk Assessment of Exposure to Radon in Drinking Water (1999) and the Assessment of the Scientific Information for the Radiation Exposure Screening and Education Program (2005). He is a distinguished emeritus member of the NCRP and recently served on the Radiation Advisory Committee for the Science Advisory Board of the Environmental Protection Agency. Dr. Borak is certified by the American Board of Health Physics.

LESLIE A. BRABY is a research professor and senior lecturer in nuclear engineering at Texas A&M University, College Station. He received his B.A. in physics from Linfield College and Ph.D. in radiological physics from Oregon State University. He joined General Electric, later Pacific Northwest National Laboratory at Hanford, Washington, initially conducting research on detectors and instruments for measuring absorbed dose. Motivated by the need to understand the biological effectiveness of different radiations, he proceeded to study the interaction of ionizing radiation with biological material and the resulting changes in biological systems. One aspect of this is the study of the probability density of energy deposition in cell nuclei and other small volumes, now known as microdosimetry. His experience in microdosimetry research led him to develop the tissue-equivalent proportional counter systems currently used for radiation dosimetry on the International Space Station. In order to study the biological changes that occur at low doses, he developed the first single particle microbeam irradiation system, as well as other specialized irradiation equipment, and continues to work with biologists to study dose and dose rate effects as well as the bystander effect. He moved to Texas A&M University in 1996 and continues his research in radiation dosimetry while teaching radiation physics, dosimetry, and microdosimetry at the graduate level. He has served on a number of NCRP and International Commission on Radiation Units and Measurements (ICRU) committees dealing with dosimetry, microdosimetry, and radiation safety in space. He chaired NCRP committees leading to Commentaries 17 and 20 dealing with radiation protection issues associated with neutron and high energy X-ray based cargo scanning systems. He also chaired the ICRU committee which developed Report 86, which recommends use of charged particle fluence rather than absorbed dose to quantify heterogeneous exposures such as those resulting from low-dose or microbeam irradiation.

MATS P.E. HEIMDAHL is the director of the University of Minnesota Software Engineering Center at the University of Minnesota, Minneapolis. Dr. Heimdahl's research interests are in software engineering, safety critical systems, software safety, testing, requirements engineering, formal specification languages, and automated analysis of specifications. He is also currently pursuing the following areas: static analysis of system and software requirements (e.g., through model checking and theorem proving); how dynamic methods (e.g., simulation and testing) can be

used to validate requirements specifications; model based software development; automated test case generation; and software certification.

SANDRA L. HYLAND is a consultant. Prior to this she was a senior principal engineer at BAE systems. Dr. Hyland has 25 years of experience in program management in both for- and nonprofit organizations. She was a senior semiconductor engineer at BAE systems. Prior to that, she served in various positions at Tokyo Electron. She has also served as a staff officer at the NRC's National Materials Advisory Board and an advisory engineer at IBM. Dr. Hyland has a Ph.D. in materials science and engineering from Cornell University, an M.S. in electrical engineering from Rutgers University, and a B.S. in electrical engineering from Rensselaer Polytechnic Institute. Dr. Hyland is a member of the American Vacuum Society, the Electrochemical Society, and the Institute of Electrical and Electronics Engineers (IEEE). She is a fellow of the Society of Women Engineers and previously served as chair of the NRC Committee on Engineering Aviation Security Environments-False Positives from Explosive Detection Systems.

SHELDON H. JACOBSON is a professor and director of the Simulation and Optimization Laboratory in the Department of Computer Science at the University of Illinois, Urbana-Champaign. Dr. Jacobson works in the field of operations research, a discipline that embodies the application of analytical tools to analyze and understand complex and complicated systems. His methodological research addresses problems related to stochastic sequential assignment when there is uncertainty in the model inputs, and the design of novel exact algorithms for hard discrete optimization problems based on the cross-fertilization of traditional search methods like branch and bound with memory. Dr. Jacobson's areas of application include aviation security system design and analysis (optimal allocation and use of security assets, and understanding the impact of new technologies on security system performance), problems within the general area of public health (pediatric vaccine formulary design and pricing, pediatric vaccine stockpiling, the relationship between obesity and transportation, and the impact of cell phone use on automobile accident rates). The author of more than 200 journal research articles, book chapters, conference proceeding papers, and professional and editorial papers, Dr. Jacobson has been recognized with several national and international awards, including the Award for Technical Innovation in Industrial Engineering from the Institute of Industrial Engineers and a Guggenheim Fellowship from the John Simon Guggenheim Memorial Foundation.

JAY S. LOEFFLER is the chair of radiation oncology, Massachusetts General Hospital, Boston, and the Herman and Joan Suit Professor, Department of Radiation Oncology, Harvard Medical School. Dr. Loeffler is an honors graduate of Williams

College and Brown University School of Medicine. He completed his radiology/oncology training at the Harvard Joint Center for Radiation Therapy and a year of post-doctoral fellowship at Harvard School of Public Health Radiobiology Laboratory. He was recruited to Massachusetts General Hospital in 1996 as director of the NE Proton Therapy Center. He is an authority on the treatment of benign and malignant brain tumors and is a member of the IOM. He is an author of more than 200 peer-reviewed publications, 180 book chapters and review articles, and is co-editor of 9 textbooks. He has served as principal investigator on a large program project grant from the NCI concerning proton therapy. He serves on the editorial boards of eight journals.

C. KUMAR N. PATEL is the founder, president, and chief executive officer of Pranalytica, Inc., a Santa Monica-based company that is the leader in quantum cascade laser technology for defense and homeland security applications. He is also professor of physics and astronomy, electrical engineering, and chemistry at the University of California, Los Angeles (UCLA). He served as vice chancellor for research at UCLA from 1993-1999. Prior to joining UCLA, he was the executive director of the Research, Materials Science, Engineering and Academic Affairs Division at AT&T Bell Laboratories, where he began his career by carrying out research in the field of gas lasers. He is the inventor of the carbon dioxide and many other molecular gas lasers that ushered in the era of high-power sources of coherent optical radiation. Dr. Patel was awarded the National Medal of Science for his invention of the carbon dioxide laser. His other awards include the Ballantine Medal of the Franklin Institute, the Zworykin Award of the National Academy of Engineering (NAE), the Lamme Medal of the IEEE, the Texas Instruments Foundation Founders Prize, and many more. Dr. Patel holds a B.E. in telecommunications from the College of Engineering in Poona, India, and received his M.S. and Ph.D. in electrical engineering from Stanford University. He is a member of the NAS and the NAE.

MAURO SARDELA is the director of research facilities at the Frederick Seitz Materials Research Laboratory at the University of Illinois, Urbana-Champaign. Dr. Sardela has a Ph.D. in materials science and was the manager of the X-ray analytical facilities and a senior research scientist at the Frederick Seitz Materials Research Laboratory from 1998 to November 2014. He is author of many highly regarded scientific publications in the fields of materials science and chemistry with focus on novel electronic materials. In addition to his research, Dr. Sardela is responsible for the training and supervision of scientists from various institutions that use the facilities at the University of Illinois. He has been involved in the installation, testing, and development of several commercial X-ray analytical instruments. Dr. Sardela has hands-on experience in several aspects of safety, calibration, and maintenance of advanced X-ray tools. He works closely with several vendors of X-ray instru-

ments in the development of new optics, systems, and metrology in the field. Previously to his current position, Dr. Sardela worked in the semiconductor industry in the California Bay area. As a senior research scientist, Dr. Sardela also holds two positions regarding safety policies and supervision. He is currently a co-chair of the Safety Committee at the Materials Research Laboratory in charge of overseeing and determining safety policies of all scientific work in the entire department, involving X-rays and laser radiation in addition to chemical and biological materials. Dr. Sardela has also been nominated by the vice chancellor of research as a member of the University of Illinois Radiation Safety Committee, which is the most prominent entity at the university in charge of overseeing safety procedures and regulations in the entire campus involving X rays, lasers, and radiological materials.

ZHI-MIN YUAN is professor of radiation biology and director of the John B. Little Center at the Harvard School of Public Health. He received his medical degree from the Jiangxi Medical College in China and his Ph.D. in biomedical chemistry from the University of Maryland. Afterward, he served at different scientific positions at Harvard School of Public Health. Dr. Yan's research is funded primarily by the Department of Energy (DOE) and the National Institutes of Health (NIH) and focuses on elucidation of signaling mechanisms that regulate cellular stress in response to radiation and other stimuli and on examining how stress signals affect cell behaviors in the context of cancer. One of his current studies involves investigating the mechanisms underlying low-dose radiation-induced adaptive response.

CONTRACTORS

WESLEY E. BOLCH is professor of biomedical engineering and medical physics in the J. Crayton Pruitt Family Department of Biomedical Engineering at the University of Florida (UF). He serves as director of ALRADS (the Advanced Laboratory for Radiation Dosimetry Studies) at UF. Dr. Bolch earned his B.S.E. degree in environmental engineering and his M.E. and Ph.D. degrees in radiological physics from the University of Florida. He has been certified by the American Board of Health Physics since 1994 and licensed in Radiological Health Engineering by the Texas Board of Professional Engineers since 1992. In 2011, Dr. Bolch was elected fellow of both the Health Physics Society (HPS) and the American Association of Physicists in Medicine (AAPM). He has been a member of the Society of Nuclear Medicine's Medical Internal Radiation Dose (MIRD) Committee since 1993, a member of NCRP since 2005, and a member of Committee 2 of ICRP since 2005. Within the latter, he serves as C2 Secretary and Leader of the ICRP Task Group on Dose Calculations (DOCAL). He has published more than 160 peer-reviewed journal articles, co-authored/edited 14 books/book chapters, and served as author on two NCRP reports, two ICRP publications, and two MIRD monographs. Dr. Bolch has man-

aged a broad research program including (1) NIH- and DOE-funded projects to construct high-resolution models of the skeleton to support dose-response studies in radionuclide therapy and radiation epidemiology; (2) NIH-funded projects to develop scalable NURBS-based and voxel-based computational phantoms of adult and pediatric patients and associated software for organ dose assessment in nuclear medicine, computed tomography, interventional fluoroscopy, and radiotherapy; (3) private company-funded projects to develop stereotactic kilovoltage X-ray treatments for age-related macular degeneration and glaucoma; and (4) Centers for Disease Control and Prevention-funded projects in stochastic modeling of worker inhalation and gamma-ray exposures following radiological accidents and potential terrorist events. He is the recipient of the 2014 Distinguish Scientific Achievement Award by the Health Physics Society acknowledging outstanding contributions to the science and technology of radiation safety.

DAVID E. HINTENLANG is an associate professor of biomedical engineering and medical physics in the J. Crayton Pruitt Family Department of Biomedical Engineering at the University of Florida (UF). He is the program director for the Graduate Medical Physics Program and the graduate coordinator for the Department of Biomedical Engineering, and he contributes to the clinical training of medical physicists in the UF Department of Radiology's Diagnostic Imaging in Medical Physics Residency Program. Dr. Hintenlang is board certified by the American Board of Radiology in diagnostic radiological physics, licensed in the State of Florida to provide clinical services to health care facilities, and is certified by the Food and Drug Administration to provide medical physics services under the Mammography Quality Standards Act. Dr. Hintenlang is vice president of the Gainesville Medical Physics Group, Inc., and he manages accreditation programs under the auspices of the American College of Radiology and the joint commission for multiple facilities and medical imaging modalities, including mammography, computed tomography, magnetic resonance imaging, nuclear medicine, and ultrasound. His research interests revolve around the empirical evaluation and modeling of clinical applications of radiation imaging and dosimetry where he has more than 90 peer-reviewed publications. Recent publications are directed toward the development of novel measurement devices, systems and techniques to accurately quantify and minimize patient doses from computed tomography, and mammography while simultaneously optimizing image quality. Dr. Hintenlang received his B.S. in physics from Bucknell University and his M.S. and Ph.D. degrees in physics from Brown University. He has been elected a fellow of the American College of Medical Physics and is a recipient of the AAPM Distinguished Service Award and the Health Physics Society Elda E. Anderson Award.